The role of the actin-binding protein Arp2/3 in growth cone actin dynamics and guidance

DISSERTATION

SUBMITTED TO THE FACULTY OF THE GRADUATE SCHOOL OF THE UNIVERSITY OF MINNESOTA

BY

Jose Enrique San Miguel-Ruiz

IN PARTIAL FULFILLMENT OF THE REQUIREMENTS FOR THE DEGREE OF

DOCTOR OF PHILOSOPHY

Paul C. Letourneau, Adviser

May, 2014

Acknowledgements

I want to thank my advisor Paul Letourneau for providing me the opportunity to work in his lab. During this time, his support and mentoring encouraged my professional and personal development. His legacy to the field of growth cone guidance and development will always be a personal source of inspiration and drive to keep pushing forward.

I would also like to thank Lihsia Chen, Steve McLoon, and David Odde for being terrific committee members. Their observations and suggestions throughout the years enriched my project and the way I think and engage scientific problems. I am particularly thankful to Steve for always asking tough questions, for telling me when I was wrong, for pushing me to be a better student and think more critically, for exciting scientific discussions, and for all his support and guidance.

Additionally, I want to thank previous members of Paul's lab. Bonnie Marsick and Coco Roche were a constant and valuable source of knowledge and patience, both, initially, when I joined the lab and, later, when I was working on the experiments for my thesis. I would also like to thank Josh Farley for his friendship, along with the support and good times that came with it.

I would also like to thank my friend and fellow graduate student Carlos Ayala. He has been supportive and a great science colleague, but also an excellent companion when I needed a distraction from work.

And finally my mother, whose love, abnegation, and encouragement forged a better person.

Abstract of Thesis

Neuronal growth cones are responsible for wiring the immature nervous system. They rely on guidance cues present in the extracellular environment to guide axons to their targets. Guidance cues achieve effective changes in directionality by modulating the growth cone cytoskeleton. Particularly important for this process are the changes in actin dynamics at the leading edge of the growth cone. However, which and how actin-binding protein (ABP) regulate actin dynamics to achieve correct guidance is not clear. This thesis shows evidence on the role of two ABP's during growth cone guidance.

The first chapter, *The role of the Arp2/3 complex in actin dynamics and growth cone guidance is substrate dependent*, characterizes the role of the actin nucleator Arp2/3 in growth cone actin dynamics and guidance. Arp2/3 has been shown to be important in leading edge actin dynamics in non-neuronal cells, but little was known about its role in neuronal growth cones. Because during development growth cones migrate in association with diverse adhesive substrates during development, we probed the hypothesis that the functional significance of Arp2/3 is substrate dependent. We report that Arp2/3 inhibition led to a reduction in the number of filopodia and F-actin content on laminin and L1. However, we found substrate-dependent differences in growth cone motility, actin retrograde flow, and guidance after Arp2/3 inhibition, suggesting that its role, and perhaps that of other ABP's, in growth cone motility is substrate-dependent.

The next chapter, *Ezrin/radixin/moesin family proteins mediate actin filament dynamics in attractive growth cone guidance to nerve growth factor*, describes the role

that the ezrin/radixin/moesin (ERM) family of membrane-cytoskeletal linker proteins have during attractive growth cone guidance. This family of proteins have been shown to link actin filaments to the cell membrane when activated. We found that endogenous guidance cues for dorsal root ganglion and retinal ganglion cell neurons can activate ERM proteins. Moreover, the increase in filamentous actin normally triggered by the stimulation of these attractive guidance cues was abolished when ERM protein function was disrupted. Additionally, we found that ERM activity is closely associated with correct placement of substrate adhesions in growth cones. Finally, we found that disruption of ERM protein function abolishes attractive growth cone guidance and causes mislocalization of ADF/cofilin, an active binding protein previously shown by our group to be required for correct guidance. These results suggest that the correct organization of filamentous actin and adhesions in growth cones by ERM proteins are necessary for correct growth cone guidance.

The final chapter, *The role of Arp2/3 during in-vivo axon guidance in the chick embryo*, deals with the role of the Arp2/3 complex during growth cone guidance in-vivo. For this purpose studied the role of Arp2/3 during the development of chick retinotectal projections and that of the sensory-motor innervation of the hindlimb. We found that Arp2/3-inhibited neurons had no deficiencies during the development of the retinotectal projections. However, we did find that Arp2/3 was required for normal sensory-motor innervation of the hindlimb during development. Thus, suggesting that Arp2/3 is required during developmental axon guidance in some tissues.

Table of Contents

List of Tables

List of Figures

<u>Chapter III:</u> Ezrin/radixin/moesin family proteins mediate actin filament dynamics in attractive growth cone guidance to nerve growth factor

Summary of Publications

San Miguel-Ruiz JE and Letourneau PC (2014) **The role of Arp2/3 in growth cone actin dynamics and guidance is substrate dependent**. *Journal of Neuroscience,* 34(17): 5895-5908

*Modified and presented in Chapter II

Marsick BM, San Miguel-Ruiz JE, Letourneau PC (2012) **Activation of ezrin/radixin/moesin mediates attractive growth cone guidance through regulation of growth cone actin and adhesion receptors**. *Journal of Neuroscience*, 32:282-296.

*Modified and presented in Chapter III

Chapter I: Introduction and Rationale

Neurodevelopment

Neurons are the fundamental working unit of the nervous system. Soon after these cells are generated from neuronal stem cells, they migrate in a stereotyped fashion to populate the developing nervous system (Evsyukova et al., 2013). Upon reaching their niche, neurons put out dendritic and axonal processes to establish connections with other cells in order to survive and function properly (Waites et al., 2005). These connections allow neurons to receive and transmit information to other cells, which in turn permits processing of sensory information, organ function regulation, movement control, and higher functions like memory, thought, and self-awareness. Therefore, correct wiring of the developing nervous system is essential for proper function during adulthood (Engle, 2010).

The growth cone is entrusted with the function of wiring the immature nervous sytem (Gomez and Letourneau, 2013). This specialized motile organelle is present at the tip of every dendrite and axon that embryonic neurons form. Growth cones use dynamic filamentous actin (F-actin) protrusions -filopodia and veils- to guide neuronal processes to their targets (Gomez and Letourneau, 1994). These protrusions attach to the substrate via adhesion molecules on their plasmalemma and with the aid of myosin II contractile activity allow growth cones to gain traction on the substrate and advance (Heidemann et al., 1990; Bridgman et al., 2001; Ketschek et al., 2007; Chan and Odde, 2008). At every choice point along their path, growth cones will rely on adhesive substrates and guidance cues present in the extracellular environment to correctly guide them to their synaptic target (Lowery and Van Vactor, 2009). These guidance cues can have attractive or repulsive effects on growth cones, thus leading them towards or away from their source.

At any given time, growth cones are exposed to multiple guidance cues and the history of previously encountered guidance cues will also affect their responsiveness to subsequent ones. Therefore, growth cones have to integrate sensory information from the substrate and the different guidance cues presented to them at any given time to correctly steer axons to their target (Dontchev and Letourneau, 2002, 2003).

Guidance cues steer neuronal processes to their targets by modulating the cytoskeleton within the growth cone (Gallo and Letourneau, 2004; Kalil and Dent, 2005). These molecular cues are capable of activating specific transmembrane receptors on the growth cone plasmalemma. In turn, these receptors activate signaling cascades that involve kinases, phosphatases, Rho GTPases, Ca^{2+} spikes, and cyclic nucleotides to modulate the cytoskeleton within the growth cone, particularly F-actin dynamics (Gallo and Letourneau, 1998b; Gomez et al., 2001; Huber et al., 2003). Growth cones encountering attractive guidance cues will respond with increased actin polymerization and a motile response towards the chemoattractant source (Marsick et al., 2010; Marsick and Letourneau, 2011; Gomez and Letourneau, 2013). On the other hand, growth cones encountering repulsive guidance cues will reduce actin polymerization and F-actin content close to the source, leading to a motile response away from the source (Marsick et al., 2012b). Consequently, by integrating sensory information from guidance cues, growth cones can remodel their cytoskeletons to put forward a motile response that allows axons to reach their synaptic partners during development.

As an axon migrates and reaches its target cell, the growth cone at its tip will evolve to give rise to a pre-synaptic nerve terminal. This change is believed to be caused by neurotrophins, cell adhesion molecules, and neurotransmitters released by the synaptic

partners (Ernst et al., 1998; Ernst et al., 2000; Waites et al., 2005). These events lead to an increase in the area, volume, and number of synaptic vesicles in the pre-synaptic partner, and a clustering of neurotransmitter receptors in the postsynaptic terminal (Sanes and Lichtman, 1999; Waites et al., 2005). These newly formed synapses will mature in an activity-dependent manner, where the stronger synapses are maintained past embryonic development and the weaker ones pruned and eliminated (Ernst et al., 1999; Sanes and Lichtman, 1999; Waites et al., 2005). This process maximizes efficient communication between nervous system cells and their targets.

Growth cone structure and function

Growth cones are dynamic actin-rich structures at the tip of growing axons. Traditionally, this organelle has been subdivided into two main regions: the central domain (C-domain) and the peripheral domain (P-domain). The C-domain is mostly occupied by microtubules extending from the axon shaft and other cellular organelles like mitochondria, endoplasmic reticulum, and vesicles. The P-domain is mostly composed of F-actin with two different supramolecular arrangements, but with their barbed ends pointing towards the leading edge: filopodia, which are finger-like projections composed of bundled parallel actin filaments and veils, which are the two-dimensional branched actin structures flanked by filopodial protrusions (Lowery and Van Vactor, 2009). Filopodia are thought of as energetically cheap cellular antennae spread around the growth cone perimeter to increase its ability to explore the surrounding environment for guidance cues (Davenport et al., 1993). This idea is supported by the fact that growth

cone filopodial tips are enriched for cell adhesion molecules and guidance cue receptors that would allow it to explore and respond to guidance cues or permissive substrates (Grabham and Goldberg, 1997; Steketee and Tosney, 2002; Marsick et al., 2012a). Moreover, it has been demonstrated that filopodial contact with guidance cues can reorient its trajectory (Hammarback and Letourneau, 1986; O'Connor et al., 1990; Gomez and Letourneau, 1994). Growth cone veils have not been studied in as much detail as filopodia. However, they have been shown to alternate between phases of protrusion and retraction and are proposed to be involved in axon growth. Specifically, a protruded veil would be invaded by microtubules and other organelles upon encountering an attractive guidance cue, thus allowing advance of the C-domain and the growth cone (Goldberg and Burmeister, 1986; Goldberg, 1988). Furthermore, growth cone filopodia have been proposed to serve as stable boundary rails for the growth of veils and, hence, directed growth of an axon (Goldberg and Burmeister, 1986; Steketee and Tosney, 2002).

Actin dynamics during leading edge protrusion and motility

Actin dynamics underlie growth cone leading edge protrusion and motility (Gallo et al., 2002). Essential for these two processes is the actin retrograde flow and actin treadmilling in the growth cone P-domain, both of which are controlled by actin binding proteins (ABP's) (Lowery and Van Vactor, 2009; Gomez and Letourneau, 2013). The actin retrograde flow refers to the backwards flow of the F-actin network away from the growth cone leading edge and into the C-domain. This process is driven by the contractile activity of myosin II pulling on the pointed-end of actin filaments in the P-domain, and

by the push exerted on the membrane by the incorporation of new actin monomers into the barbed-ends of actin filaments abutted against the growth cone leading edge (Medeiros et al., 2006). Barbed end availability is partly dependent on actin nucleators that create new actin filament seeds capable of polymerizing actin monomers. Among the most commonly studied nucleators are the ABP's Arp2/3 and formins, although recently several other have been described, such as Spire, JMY, and Cordon Bleu (Baum and Kunda, 2005; Campellone and Welch, 2010). Arp2/3 binds to the side of a pre-existing actin filament to nucleate a new filamentous actin branch; consequently it is involved in the formation of branched actin structures (Goley and Welch, 2006). As actin nucleators, formins can nucleate unbranched actin filaments de-novo and, then, assist in the continued addition of monomers to the filament as it grows (Zigmond, 2004). Additionally, incorporation of new actin monomers into barbed-ends is also regulated by capping proteins, which limit the number of barbed ends that can polymerize actin monomers, and by anti-capping proteins, like ENA/VASP proteins, that counter the effect of capping proteins (Dent et al., 2011).

Because growth cones have a finite number of actin monomers available for polymerization, proteins like ADF/cofilin and myosin II help to sever actin filaments and remove actin monomers from their pointed ends close to the C-domain (Meberg, 2000; Medeiros et al., 2006; Marsick et al., 2010). These ADP-actin monomers are then translocated to the growth cone leading edge and their cyclic nucleotides exchanged by profilin, so as to provide a steady ATP-actin monomer pool ready for polymerization (Pollard et al., 2000). This process is called actin treadmilling and it ensures an adequate supply of actin monomers to polymerize into the barbed ends of actin filaments and fuel

the retrograde flow of actin (Bugyi and Carlier, 2010). As long as the process of actin polymerization at the leading edge is offset and balanced by the retrograde flow of actin, leading edge protrusion and, hence, motility remains idle.

Growth cone leading edge protrusion and motility require the rate of actin polymerization at the leading edge to overcome the rate of the actin retrograde flow (Lowery and Van Vactor, 2009). This allows the incorporation of actin monomers into barbed ends to lengthen actin filaments under the growth cone leading edge, causing membrane protrusion. Growth cones use substrate adhesions to slow down the overlying retrograde flow of actin filaments and cause leading edge protrusion. The model was first proposed by Mitchison and Kirschner and coined the "clutch hypothesis" (Mitchison and Kirschner, 1988). Their model proposes that interactions between growth cone transmembrane adhesive receptors and the extracellular environment would lead to the formation of an intracellular molecular clutch. This clutch would then couple transmembrane adhesive receptors to the overlying flow of actin filaments to slow down their retrograde rate. In turn, allowing actin filaments over substrate adhesions to remain in a relatively fixed position, except for occasional slips on the clutch grip (Suter et al., 1998; Chan and Odde, 2008; Lee and Suter, 2008), which would allow actin polymerization at barbed ends to push the leading edge forward. We now know details of some of the players that form this molecular clutch. It is known that when integrins engage adhesive substrates, such as laminin or fibronectin, they recruit proteins like talin and vinculin to their intracellular domain (Zhang et al., 2008; Thievessen et al., 2013), in turn, these engage the overlying retrograde flow of actin filaments to slow it down. Similarly, ERM, shootin, and ankyrin proteins couple L1 to the actin cytoskeleton

(Nishimura et al., 2003; Shimada et al., 2008; Marsick et al., 2012a), as do catenins with N-cadherin (Bard et al., 2008). Once these substrate adhesions engage the "clutch", the same myosin II contractile activity that was partially powering the retrograde flow of actin will now provide the traction to pull and move the growth cone C-domain closer to the leading edge membrane. Traction on the growth cone, and by it, has been shown to lead to axon lengthening (Fass and Odde, 2003; Betz et al., 2011). Therefore, substrate adhesions slow down the retrograde flow of actin to allow leading edge protrusion and myosin II-drive growth cone advance.

Leading edge membrane protrusion is the first step for growth cone advance (Lowery and Van Vactor, 2009). It has been shown that axon growth takes place by invasion of microtubules and organelles, both commonly restricted to the C-domain, into a newly expanded growth cone veil in the P-domain (Goldberg and Burmeister, 1986; Goldberg, 1988; Suter and Forscher, 2000). Interestingly, this mechanism has also been shown to occur when growth cones come across an adhesive substrate and make a new adhesion (Suter and Forscher, 2001; Lee and Suter, 2008). In this case, soon thereafter adhesion formation the retrograde flow around the adhesion slowed down and growth cone protrusion followed. Also, the F-actin between the newly formed adhesion and the C-domain disappeared, which allowed the advance of microtubules and organelles to engorge the P-domain, and eventually the advance of the C-domain (Suter et al., 1998; Lee and Suter, 2008). Eventually, consolidation of what used to be the proximal part of the growth cone around the new axon shaft completes the cycle of axon growth. This process repeats constantly over and over during a growth cone's journey to its target. Accordingly, attractive guidance cues can lead to adhesion formation (Carlstrom et al.,

2011; Myers and Gomez, 2011), leading edge protrusion (Marsick et al., 2010), and growth cone motility (de la Torre et al., 1997; Liu et al., 2002). On the contrary, repulsive guidance cues can remove substrate adhesions (Woo and Gomez, 2006; Hines et al., 2010; Carlstrom et al., 2011), stop leading edge protrusion (Marsick et al., 2012b), and slow down/retract growth cone advance (Jurney et al., 2002; Carlstrom et al., 2011).

Arp2/3

Growth cones are actin-rich organelles at the distal tips of axons. Monomeric actin has the capacity to self assemble into F-actin (Pollard, 1986), which can promote growth cone motility and guidance. However, the initial formation of an actin filament, known as nucleation, posses an energetic hurdle for growth cones (Cooper et al., 1983; Mullins et al., 1998), which serves as a control point for actin polymerization. During this period, growth cones rely on ABP's called nucleators that bind and stabilize a trimeric complex of actin monomers, that would otherwise bind weakly and unstably to exist on its own (Pollard, 2007; Campellone and Welch, 2010). Stabilization of this intermediate complex by actin nucleators permits the stable and continued self assembly of subsequent actin monomers into the growing filament. Without nucleators, actin polymerization would be too slow and inefficient to allow a well-organized growth cone response during motility and encounters with guidance cues.

One of the most thoroughly studied actin nucleators is the Arp2/3 complex (Goley and Welch, 2006). This is a seven sub-unit protein complex with very little nucleation activity on its own. The actin nucleation activity of Arp2/3 can be increased by its interaction with nucleation promoting factors (NPF), such as the members of the

WASP/WAVE family of proteins (Kurisu and Takenawa, 2009). When engaged by NPF's, Arp2/3 will bind to the side of a pre-existing actin filament and nucleate a new daughter branch at a particular 70° angle (Amann and Pollard, 2001; Fujiwara et al., 2002). As a result, Arp2/3 is involved in the formation of a branched actin network with accepted roles in a multitude of cellular processes.

The importance of the actin nucleator Arp2/3 is evidenced by the fact that its lack of activity in organisms, ranging from the unicellular to the multicellular, is lethal (Harborth et al., 2001; Fujiwara et al., 2002; Zallen et al., 2002; Dahl et al., 2003; Sawa et al., 2003). Specific roles attributed to the Arp2/3 complex in non-neuronal cells include: lamellipodial protrusion and directed migration (Suraneni et al., 2012; Dang et al., 2013), haptotaxis (Wu et al., 2012), filopodia formation (Svitkina et al., 2003; Biyasheva et al., 2004), adhesions maturation and organization (DeMali et al., 2002; Wu et al., 2012), membrane trafficking (Rozelle et al., 2000; Taunton et al., 2000), and endocytosis (Moreau et al., 1997; Merrifield et al., 2004). Similar comprehensive studies have not been carried out in neuronal growth cones to evaluate the role of Arp2/3 during actin dynamics and guidance. There is only a handful of studies that address the role of Arp2/3 in growth cones and these often report contradictory findings.

Initially, in-vitro studies reported that neuronal growth cones had little branched actin in their P-domain and that Arp2/3 inhibition had no effect on F-actin content, lamellipodia protrusion, or filopodia formation (Strasser et al., 2004). Additionally, Arp2/3-inhibited neurons were found to have longer axons, which, along with the finding that Arp2/3 subunits were enriched in the growth cone C-domain, led the authors to speculate that Arp2/3 functions as a negative regulator of axon elongation by limiting the

advance of microtubules from the C- to the P-domain. Later, it was reported by Korobova and Svitkina that neurons did have a branched actin network close to the leading edge and that it was dependent on Arp2/3 function (2008). Moreover, they reported that Arp2/3 inhibition reduced lamellipodial protrusion, filopodia formation, neuritogenesis, and the rate of the actin retrograde flow. Yang et al. later confirmed that the actin nucleation activity of Arp2/3 was localized to the leading edge of growth cones and that its inhibition led to an increase in the rate of the actin retrograde flow (2012). Unfortunately, from the in-vitro findings provided by these reports, at times contradictory, it is impossible to ascertain a concrete role for Arp2/3 in neuronal growth cones.

In-vivo experiments in *Drosophila* embryos determined that elimination of SCAR, the mammalian orthologue of Scar/WAVE and Arp2/3 activator, led to axon depletion and displacement from their tracts, along with reduced axon fasciculation (Zallen et al., 2002). On the other hand, individual neuronal clones in the *Drosophila* mushroom body (MB) deficient for SCAR, WASp, or the Arp2/3 subunit Arpc1 do not have axon guidance deficits (Ng and Luo, 2004). It has been fairly suggested that the guidance deficits reported by Zallen et al. could be secondary to the general embryonic tissue disruption caused by elimination of SCAR throughout the developing embryos (Dent et al., 2011). However, the creation of mosaic clones in the *Drosophila* MB by Ng and Luo could also obscure the correct interpretation of Arp2/3 function by not differentiating between axon guidance and simple fasciculation of mutant axons along tracts previously established by pioneering axons (2004). Consistent with the findings of Zallen et al., it has been shown in *Caenorhabditis elegans* embryos that disruption of Arp2/3, or its activators WAVE and WASp, leads to clear axon guidance deficits (Shakir et al., 2008;

Norris et al., 2009). Thus, these experiments suggest that Arp2/3 does play a role in axon guidance in-vivo. However, the exact mechanisms by which Arp2/3 inhibition cause axon guidance deficits remains largely unknown.

Guidance cues

Growth cones use guidance cues to correctly steer axons to their target through the developing embryo. These molecular cues can be soluble or membrane bound, and can lead growth cones to their targets by means of chemoattraction or chemorepulsion (Dickson, 2002). Some commonly studied guidance cues are NGF, Netrin, and ephrin A2. Growth cones have transmembrane receptors on their plasmalemma for these guidance molecules, which turn their protrusions into exquisite sensory organelles capable of responding to the presence of these cues. Growth cones can receive guidance instructions from a broad range of molecules that include: neurotransmitters, morphogens, secreted transcription factors, or neurotrophic factors (Huber et al., 2003). Receptors for these molecular cues will respond by relaying guidance information intracellularly by means of kinases, phosphatases, small GTPases, and calcium and cyclic nucleotides fluxes (Gallo and Letourneau, 1998b; Kholmanskikh et al., 2003; Gehler et al., 2004; Chen et al., 2006). In turn, these will produce changes in the cytoskeletal machinery inside the growth cone, particularly the actin cytoskeleton, to produce the mechanical response needed to advance, retract, branch, or turn at choice points (Gallo and Letourneau, 2000). However, the particular response a growth cone has to a given molecular cue is not inherent to the cue's identity, but is the outcome of a growth cone's substrate (Snow and Letourneau, 1992;

Hopker et al., 1999), developmental stage (Shirasaki et al., 1998; Shewan et al., 2002), intracellular signaling (Ming et al., 1997; Hopker et al., 1999), receptors on its plasmalemma (Rajagopalan et al., 2000; Sabatier et al., 2004), and the growth cone's previous encounters with molecular cues (Sabatier et al., 2004; Parra and Zou, 2010).

During an encounter with one of these chemoattractive molecules, growth cones will increase actin polymerization, promote adhesion formation, allow microtubule advance, and allocate more membrane surface and receptors to the plasmalemma through exocytosis. On the other hand, if a growth cone encounters chemorepulsive guidance cues it will respond by reducing actin polymerization and F-actin content, dismantling substrate adhesions, and removing surface membrane from the plasmalemma.

NGF: this is a homodimeric molecule discovered in the 1950s and the first member of the neurotrophin family. In-vivo, NGF has been shown to promote neuronal survival, apoptosis, to regulate development and maintenance of neuronal phenotypes, and promote dendritic arborization (Levi-Montalcini and Booker, 1960; Campenot, 1977; Snider, 1988; Andrews and Cowen, 1994; Crowley et al., 1994; Conover and Yancopoulos, 1997; Frade and Barde, 1998; Sofroniew et al., 2001). Additionally, NGF signaling has been shown to be involved in guiding and promoting branching of sensory axons into the skin epidermis and sympathetic nervous system organs (Rice et al., 1998; Patel et al., 2000; Glebova and Ginty, 2004); consistent with this, its overexpression in the skin epidermis lead to hypertrophic innervation by sensory neurons (Albers et al., 1994). NGF is also a potent stimulator of actin polymerization and functions as a

chemoattractant for dorsal root ganglion (DRG) neurons in-vitro (Gundersen and Barrett, 1979; Gallo et al., 1997; Gallo and Letourneau, 1998a).

NGF signal through two different receptors to mediate its pro-survival and pro-apoptotic effects: the high affinity tropomyosin-receptor kinase A (TrkA) and the low affinity p75 neurotrophin receptor (p75), respectively. Upon binding to the TrkA receptor, NGF induces TrkA dimerization and autophosphorylation. This leads to the recruitment of scaffolding proteins and subsequent activation of downstream signaling pathways like: MAPK/ERK, AKT, phospholipase-C, and members of the Rho family of GTPases Rac and Cdc42, but not RhoA (Bibel and Barde, 2000). In turn, these signaling pathways can modulate the cytoskeleton within the growth cone to steer axons to their targets, as has been shown before (Marsick et al., 2010; Marsick et al., 2012a). However, a comprehensive picture of the ABP's that NGF uses to steer growth cone to their targets is far from complete.

Netrin-1: belongs to the Netrin family of secreted proteins with conserved amino acid sequence to the ECM protein laminin (Huber et al., 2003). Described functions for Netrin-1 in the nervous sytem include regulation of cell migration, cell-cell and cell-substrate adhesion, cell survival, cellular differentiation, and axon extension and guidance (Lai Wing Sun et al., 2011). In-vivo, spinal cord floor plate cells have been shown to generate a gradient of Netrin-1 that serves as a chemoattractant for commissural axons descending into the developing ventral spinal cord (Kennedy et al., 1994; Kennedy et al., 2006). Furthermore, mice lacking Netrin-1 have multiple CNS abnormalities at birth, including failure to develop ventral spinal commissures, corpus callosum, anterior

commissures, and hippocampal commissures (Serafini et al., 1996). In-vitro, Netrin-1 has also been shown to be a potent chemoattractant for RGC neurons (Marsick et al., 2010), and this response is dependent on the Netrin-1 receptor deleted in colorectal cancer (DCC) receptor (de la Torre et al., 1997). In-vivo, Netrin-1 is expressed around the optic nerve head in chick embryos, which lead to the idea that it is as a chemoattractant for RGC axons to exit the retina. However, Netrin-1- and DCC-deficient axons can reach the optic nerve head, but will not get past it, leading to optic nerve hypoplasia (Deiner et al., 1997). Additionally, Netrin-1 and its homologues have been shown to promote filopodial protrusions, axon branching, and synaptogenesis (Kolodziej et al., 1996; Mitchell et al., 1996; Wang and Wadsworth, 2002; Dent et al., 2004). Interestingly, Netrin-1 and its *C. elegans* homologue UNC-40 are capable of inducing chemorepulsion in growth cones that express the alternate Netrin-1 receptor UNC5 (Hamelin et al., 1993; Colavita and Culotti, 1998; Hong et al., 1999).

During chemoattraction, Netrin-1 has been shown to activate multiple signaling pathways that regulate cytoskeletal dynamics and axon growth (Huber et al., 2003). Netrin-1 activation of DCC leads to the recruitment and phosphorylation of focal adhesion kinase (FAK), a critical protein for the development of integrin-dependent substrate adhesions (Ren et al., 2004). DCC activation by Netrin-1 also recruits and activates FYN, which in turn phosphorylates DCC to activate Rac and Cdc42, but not RhoA (Li et al., 2002; Meriane et al., 2004; Shekarabi et al., 2005). Activation of Rho GTPases has been shown to be a crucial regulator of actin dynamics, however, the particular ABP's activated during growth cone chemoattraction to Netrin-1 are still unclear, except for a few exceptions (Lebrand et al., 2004; Marsick et al., 2010; Antoine-

Bertrand et al., 2011; Marsick et al., 2012a). Netrin has also been shown to be a direct activator of the neuronal Wiskott-Aldrich syndrome protein (N-WASP), which can directly modulate the actin nucleator Arp2/3 (Shekarabi et al., 2005). However, direct involvement of Arp2/3 during Netrin chemoattraction has not yet been established.

ephrin A2: is a glycosyl-phosphatidyl-inositol (GPI) membrane-bound chemorepellent cue that plays an important role in maintaining topography during the development of retinotectal projections (Mey and Thanos, 1992). During development, the retinotectal system achieves a stereotypical arrangement of connection, where RGC axons from the temporal and nasal retina project to the anterior and posterior tectum, while the dorsal and ventral axons innervate the ventral and dorsal tectum, respectively (Mey and Thanos, 1992). In part, this connectivity arrangement is achieved by the increasing antero-posterior gradient of ephrin A2 (repulsive to temporal RGC axons) in the tectum, and the complementary high-to-low expression of its receptor EphA3 from the temporal to the nasal side of the retina (Cheng et al., 1995; Monschau et al., 1997; Yamada et al., 2001). This complementary expression of ligand and receptor keeps temporal retina axons (with high EphA3 receptor expression) away from the posterior tectum (with high ephrin A2 ligand expression). This chemorepellent effect of ephrin A2 on temporal retina axons can be successfully recapitulated in-vitro, which allows dissecting the signaling pathways and ABP's required for efficient guidance (Walter et al., 1987; Yamada et al., 2001).

EphA3 is a receptor tyrosine kinase capable of autophosphorylation upon interaction with ephrin A2. How exactly Eph receptors control the growth cone cytoskeleton is not completely understood. Not surprisingly, it has been shown that Eph

receptors downregulate Rho GTPases Rac and Cdc42 activity, and activates RhoA and its effector ROCK to cause neurite retraction (Wahl et al., 2000; Shamah et al., 2001; Jurney et al., 2002). Eph receptors can also inactivate the Ras and MAPK signaling pathway and cause neurite retraction (Elowe et al., 2001; Miao et al., 2001). Additionally, activation Eph receptor activation negatively regulates integrin adhesions (Miao et al., 2000). These results provide a partial mechanistic model as to how ephrin ligands can lead to growth cone repulsion. However, there are very few studies that address the role of ABP's during ephrin A2-mediated growth cone chemorepulsion (Marsick et al., 2012b).

Substrate effect on growth cones

The growing substrate of a neuron is a proven modulator of growth cone motility and behavior (Hammarback and Letourneau, 1986; McLoon and McLoon, 1988; Snow and Letourneau, 1992; Burden-Gulley et al., 1995; Flanagan et al., 2002). As growth cones guide axons to their target tissues they will migrate over different CAM's, such as L1, NCAM, and cadherins (Lemmon and McLoon, 1986; Ranscht, 2000; Maness and Schachner, 2007) and extracellular matrix proteins (ECM), like laminin and heparan sulfate proteoglycans (McLoon et al., 1988; Lee and Chien, 2004). These molecules serve an instructive role by providing a permissive substrate that promotes growth cone passage, or an inhibitory environment that will repel its migration, thus enabling the correct wiring of the nervous sytem. However, their presence is likely to mediate a more proactive role in growth cone guidance, as they have been shown to influence growth cone size and shape (Payne et al., 1992), distribution of cytoskeletal elements (Burden-Gulley and

Lemmon, 1996), concentration of cyclic nucleotides and Ca^{+2} fluxes (Hopker et al., 1999; Ooashi et al., 2005; Tojima et al., 2009), and responses to guidance cues (Hopker et al., 1999; Liu et al., 2002; Weinl et al., 2003; Suh et al., 2004). Similar changes have been observed along a growth cone's journey through different regions of the embryo, which presumably provide different substrates, suggesting that the in-vitro findings are not artifacts of a minimal system (Bovolenta and Mason, 1987; Halloran and Kalil, 1994; Kaethner and Stuermer, 1994; Mason and Wang, 1997; Mason and Erskine, 2000). The fact that substrate molecules can influence the signaling environment within the growth cone provides them a direct link to manipulate its cytoskeleton. ABP's are direct downstream targets of multiple signaling pathways in the growth cone, raising the possibility that substrates can influence their activity. Indeed, it has been shown that different ABP's come into play during exocytosis and neuritogenesis, depending on the substrate on which the neuron grows (Dent et al., 2007; Gupton and Gertler, 2010). Similar studies have no yet been carried out for Arp2/3 during guidance on different substrates.

L1: is a CAM that belongs to the immunoglobulin superfamily of proteins capable of homophillic and heterophilic interactions. It has been shown to be involved in cell adhesion (Rathjen and Schachner, 1984), fasciculation (Wiencken-Barger et al., 2004), neurite growth (Schmid et al., 2000), as a co-receptor for guidance cues (Castellani et al., 2000; Wang et al., 2008), and axon guidance (Kamiguchi and Lemmon, 1997; Wang et al., 2005; Wang et al., 2008). Not surprisingly, mutations to the L1 molecule cause a severe neurological syndrome in humans known as CRASH (Fransen et al., 1995; Chen

and Zhou, 2010). L1 is a single-pass transmembrane protein with a small intracellular domain, which initially perplexed researchers as to how it could signal intracellularly. It has been shown that *trans* interaction with another L1 molecule, causes the recruitment of fibroblast growth factor receptor (FGFR), to form a multimeric complex capable of relaying information intracellularly (Doherty and Walsh, 1996). FGFR-mediated L1 signaling leads to activation of phospholipase C (PLC) with subsequent elevations in Ca^{2+}. In neurons, L1 also activates the MAPK pathway in a Rac- and PI3K-dependent manner to promote axon growth (Schmid et al., 2000). Additionally, it has been shown that growth cones on L1 maintain a higher level of RhoA activation and cAMP, than on laminin (Liu et al., 2002; Ooashi et al., 2005).

laminin: is an ECM protein shown to be present in the developing nervous system (Rogers et al., 1986; McLoon et al., 1988) and required for cell attachment, migration, neuritogenesis, and axon growth (Reichardt and Tomaselli, 1991). Growth cones use integrin adhesive receptors to bind laminin, which triggers a change in conformation in the integrin receptor. This change in conformation leads to the recruitment of scaffolding and signaling proteins to the intracellular domain of the integrin receptor, leading to the activation of multiple cellular signaling pathways within the growth cone (Clegg et al., 2003). These signaling pathways are almost all dependent on focal adhesion kinase (FAK) activity and shown to include paxillin-dependent activation of Rac1, and Src-dependent activation of RhoA. The effect that laminin has, as a substrate, on growth cone signaling is apparent from the fact that RGC neurons on laminin will not respond to Netrin as a chemoattractant, whereas they do on L1. This was later shown to be the result

of high intracellular levels of growth cone cAMP on L1, but comparably lower levels on laminin. Similar effects have been shown with EphB stimulation causing growth cone collapse on laminin, but not on L1 (Suh et al., 2004).

Growth cone signaling during guidance

As growth cones migrate through the developing embryo to steer axons to their targets, they use filopodia to search for directions along the way (Davenport et al., 1993). The long and slender nature of these F-actin protrusions allows them to examine crevices in the ECM and around cells for guidance cues. The tips of filopodia are equipped with membrane receptors that make them exquisite sensory devices capable of picking up, integrating, and relaying signals intracellularly from multiple gradients of such molecules (Robles et al., 2003; Marsick et al., 2012a). The particular effect that a guidance cue has on a growth cone is dependent on membrane receptor complexes, the signaling milieu inside the growth cone, and crosstalk between different signaling pathways (Huber et al., 2003). Generally, attractive guidance cues promote actin polymerization, adhesion formation, and membrane vesicle delivery to the surface, whereas repulsive guidance cues enact opposite effects (Gomez and Letourneau, 2013). These cytoskeletal rearrangements provide the growth cone with motility, directionality, and the necessary traction to steer growth cones to their targets.

Like symphony conductors, Rho GTPases have been shown to orchestrate seamlessly these different processes (Gallo and Letourneau, 1998b; Dickson, 2001; Kim et al., 2003; Sit and Manser, 2011). This family of proteins oscillates between an active

GTP-bound state and an inactive GDP-bound one. During their GTP-bound state, Rho GTPases interact with and activate downstream effector proteins to promote cytoskeletal rearrangements. Therefore, activation of membrane receptors by guidance cues bring about cytoskeletal rearrangements in the growth cone by changing the type of nucleotide inside Rho GTPases. They do so by recruiting adaptor proteins to their intracellular signaling domains, which in turn interact and activate guanine nucleotide exchange factors (GEF's) and/or GTPase activating proteins (GAP's). There is a large number of GEF's and GAP's in growth cones and it is believed that their specificity derives from spatio-temporal restrictions in their expression patterns (Huber et al., 2003). However, they all seem to share a common mechanism of action: GEF's proteins promote the exchange of GDP for GTP, whereas GAP's promote the cleavage of GTP into GDP in Rho GTPases.

Actin polymerization: It is established that attractive guidance cues promote actin polymerization in the leading edge of growth cones and that this process is essential for adequate motility and correct guidance (Lowery and Van Vactor, 2009; Marsick et al., 2010). Rho GTPases have been shown to regulate, directly or indirectly, various actin binding proteins that are involved in growth cone actin polymerization (Sit and Manser, 2011). One of the best studied examples so far is that of N-WASP (Rohatgi et al., 2000), a key regulator of Arp2/3 in the nervous system (Wegner et al., 2008). Normally, N-WASP exists in an auto-inhibited conformation, which is relieved by binding of activated Cdc42 and PIP_2. Active N-WASP has been shown to increase the actin nucleation rate of Arp2/3 by 70-fold (Zalevsky et al., 2001), clearly demonstrating the powerful and direct

role of Rho GTPases during actin polymerization. The auto-inhibited conformation of the family of actin nucleator formins has also been shown to be relieved by the direct binding of Cdc42 or RhoA (Rose et al., 2005; Madrid et al., 2010). The recently discovered actin nucleator Spire has also been shown to bind Rac, RhoA, and Cdc42, but despite the direct association there is no indication for regulation of Spire's nucleation activity (Wellington et al., 1999). Interestingly, Spire has been shown to cooperate with formins during actin nucleation, and the authors have data to suggest that they form one functional unit (Pfender et al., 2011) during this process. Then, it is possible to speculate, that Spires could make GTPases accessible to formin, which do require active Cdc42 or RhoA for its activity.

Actin depolymerization: Axon growth requires actin treadmilling to maintain a constant pool of ATP-actin monomers capable of maintaining polymerization at the barbed end of actin filaments close to the leading edge (Gallo et al., 2002; Gomez and Letourneau, 2013). This process involves removal of ADP-actin monomers from the pointed end of actin filaments. The ABP ADF/cofilin has been shown to accomplish this by speeding the removal of individual actin monomers from pointed ends (Yonezawa et al., 1985; Carlier et al., 1997; Bamburg, 1999), although other groups have found that it can also sever F-actin filaments (Carlier et al., 1999; Ichetovkin et al., 2000; Andrianantoandro and Pollard, 2006). ADF/cofilin activity is negatively regulated through phosphorylation by LIM kinase, which in turn is activated by Rho GTPases effectors p21-activated kinase (PAK) and Rho kinase (ROCK). Therefore, activation of PAK by Rac and Cdc42, and of ROCK by RhoA lead to the inactivation of ADF/cofilin, showing how Rho GTPases can

control F-actin depolymerization. Additionally, myosin II contractile activity has been shown to lead to severing of F-actin close to their pointed ends in growth cones. Again, myosin II activity is positively regulated by RhoA and negatively regulated by Rac and Cdc42 GTPases (signaling details to follow in the next section).

Control of Myosin II activity: Rho GTPases can control actin dynamics by influencing the balance between actin polymerization and depolymerization, but also by regulating the contractile activity of myosin II. It has been shown that myosin II activity can directly control the rate of the F-actin retrograde flow, which can have direct effects on growth cone leading edge protrusion and retraction (Lin et al., 1996). The contractile activity of myosin II has been shown to be positively regulated by ROCK or myosin light chain kinase (MLCK) phosphorylation (Bresnick, 1999). ROCK is a direct downstream target of RhoA, and MLCK activity can be downregulated by the Rac and Cdc42 effector, PAK. Therefore, activation of the Rho GTPases Rac and Cdc42 can attenuate the F-actin retrograde flow, whereas RhoA activation increases it (Huber et al., 2003).

Substrate adhesions: Proper regulation of substrate adhesions is essential for growth cone motility and correct responses to guidance cues (Hines et al., 2010; Carlstrom et al., 2011; Myers and Gomez, 2011; Santiago-Medina et al., 2013). Even though the general mechanism of adhesion formation and removal in growth cones has been largely understudied, there are a few reports showing how Rho GTPases play a central role during these events. Woo and Gomez showed that the initial formation of integrin-based adhesions in growth cones is dependent on Rac activation and that stabilization of such

adhesions required the activation of RhoA, along with concomitant dowregulation of Rac activity (2006). Additionally, members of the PAK family of proteins, which are direct effectors of Rho GTPases, have been shown to colocalize to integrin-based adhesions and influence their stability (Santiago-Medina et al., 2013). Interestingly, the relationship between Rho GTPases and integrin-based adhesions is not unidirectional, as focal adhesion kinase activity was shown to be upstream of Cdc42 activation, and that its activity was required for leading edge protrusion or retraction in response to attractive or repulsive cues by growth cones (Myers et al., 2012).

In addition to the formation of substrate adhesions, Rho GTPases Cdc42 and RhoA have been shown to be involved in the activation of ezrin, radixin, and moesin (ERM) proteins (Oshiro et al., 1998; Nakamura et al., 2000; Antoine-Bertrand et al., 2011), required to form the molecular clutch to link the actin cytoskeleton with transmembrane adhesion proteins (Marsick et al., 2012a). Therefore, the activity of Rho GTPases is necessary for substrate adhesion formation, stabilization, linkage to the actin cytoskeleton, and their subsequent elimination.

Summary

Proper actin dynamics at the leading edge of the growth cone are essential for correct growth cone guidance. The dynamics of the actin cytoskeleton are controlled by ABP's, however their particular roles during guidance are mostly unknown. In the first part of this thesis we present data on the role of the Arp2/3 complex during actin dynamics and guidance. Very little is known about Arp2/3 in growth cones, additionally

reports in the literature are inconsistent. What is known about Arp2/3 in growth cones comes from experiments using different types of neuronal cells, under different culture conditions and modes of Arp2/3 inhibition. To reconcile the different findings in the literature about Arp2/3 and growth cones, we decided to probe the idea that dependency on Arp2/3 is substrate dependent. To this end we decided to investigate growth cone actin dynamics and guidance on the ECM protein laminin and the CAM L1. We found that Arp2/3 inhibition reduced filopodia and F-actin content in growth cones on laminin and L1. However, there were substrate-dependent deficiencies in growth cone motility, actin retrograde flow, and guidance after Arp2/3 inhibition. These results suggest that the role of Arp2/3 in growth cones is substrate-dependent, suggesting that substrate-mediated signals can influence Arp2/3 activity.

On the second part of this thesis, we show how the family of ezrin/radixin/moesin (ERM) proteins help to organize filamentous actin in the growth cone and substrate adhesions to promote efficient growth cone guidance. Taken together, our finding suggest that the dependency of growth cones on the actin nucleation activity of Arp2/3 during motility and guidance are substrate dependent. Additionally, that ERM proteins are required to link and organize, both, filamentous actin and substrate adhesions in growth cones to promote efficient growth cone guidance.

Finally, we address the role of Arp2/3 during in-vivo guidance using the chick retinotectal projections and sensory-motor innervation of the hindlimb. We found Arp2/3 was not required for correct development of the retinotectal projections, but it was necessary for correct sensory-motor innervation of the hindlimb. Thus showing that the actin nucleator Arp2/3 is required for correct axon guidance in some tissues.

Chapter II: The role of Arp2/3 in growth cone actin dynamics and guidance is substrate dependent

This chapter was modified from the original paper published by:

Jose E San Miguel-Ruiz and Paul C. Letourneau

The role of Arp2/3 in growth cone actin dynamics and guidance is substrate dependent.

Journal of Neuroscience (2014), 34(17): 5895-5908

Introduction

Developing axons are lead by their terminal growth cones to the sites where they establish synaptic connections. Extrinsic guidance cues regulate the cytoskeletal machinery, particularly actin filaments, of growth cones to direct them towards their targets. Consequently, proper growth cone actin dynamics are crucial to correctly wire the nervous system (Bentley and Toroian-Raymond, 1986; Lanier et al., 1999; Kwiatkowski et al., 2007; Gomez and Letourneau, 2013).

Arp2/3 is a frequently studied ABP and regulator of actin dynamics (Goley and Welch, 2006; Pollard, 2007). This multi-protein complex binds to the side of a pre-existing actin filament and nucleates an actin branch (Mullins et al., 1997). This branched actin network has been implicated in numerous processes in non-neuronal cells (Goley and Welch, 2006), most commonly associated with lamellipodial formation and protrusion (Suraneni et al., 2012; Wu et al., 2012), though not all reports agree (Di Nardo et al., 2005). Arp2/3 is also required for haptotaxis in fibroblasts, but not chemotaxis (Wu et al., 2012); although, other groups have shown it is required for chemotaxis (Mukai et al., 2005; Suraneni et al., 2012). Additionally, Arp2/3 appears to influence filopodial numbers in cells (Machesky and Insall, 1998; Svitkina et al., 2003), but not always (Sigal et al., 2007). Furthermore, it is linked to endocytosis and vesicular trafficking (Merrifield et al., 2004; Duleh and Welch, 2010). Lastly, Arp2/3 interacts with vinculin and FAK (DeMali et al., 2002; Serrels et al., 2007), influences integrin-based adhesions in fibroblasts (Wu et al., 2012), and promotes efficient cell adhesion between immune system cells (Butler and Cooper, 2009).

The role of Arp2/3 in growth cone actin dynamics and guidance is unclear. Initially, Arp2/3 was considered unnecessary for filopodia numbers, actin organization in veils and in veil protrusion, and as a negative regulator of axon elongation, although guidance defects were reported when Arp2/3 was inhibited (Strasser et al., 2004). Later, Arp2/3 was reported to regulate filamentous actin (F-actin) content, veil protrusion and stability, and filopodium formation in growth cones (Korobova and Svitkina, 2008; Spillane et al., 2011; Yang et al., 2012). Additionally, Arp2/3 inhibition in *Caenorhabditis elegans* causes deficient axon guidance (Shakir et al., 2008; Norris et al., 2009). From these reports, Arp2/3 role in growth cone migration is still uncertain. We believe these discrepancies reflect different neuronal systems and *in vitro* conditions.

Growth cone morphology, behavior, and intracellular processes are influenced by the underlying substrate (Burden-Gulley et al., 1995; Liu et al., 2002). We used two naturally occurring substrates that have profound effects on growth cone morphology and behavior, the extracellular matrix (ECM) protein laminin and the cell adhesion molecule (CAM) L1. On laminin, axons extend with compact filopodial growth cones, while on L1 growth cones are broad and lamellar. These differences could reflect influences that substrates have on ABP's in growth cones. Adhesion molecules are capable of signaling intracellularly and, therefore, influencing the activity of ABP's (Kamiguchi and Lemmon, 1997; Giancotti and Ruoslahti, 1999). Consequently, growth cone dependency on any given ABP could be determined by the substrate. We report here that Arp2/3 inhibition led to a reduction in the number of filopodium and F-actin content on laminin and L1. However, we found substrate-dependent differences in growth cone motility, retrograde

actin flow, and guidance after Arp2/3 inhibition, suggesting that its role, and perhaps that of other ABP's, in growth cone motility is substrate-dependent.

Material and Methods

Materials F-12 medium (21700-075), B27 (17504044), Glutamax (35050061), sodium pyruvate (11360-070), Antibiotic-Antimycotic (15240-062), Alexa Fluor 488- and 568-phalloidin, and Alexa Fluor 488 and 568 secondary antibodies were purchased from Life Technologies. NGF (256-GF-100/CF), Netrin (128-N1-025), ephrin-A2 (603-A2-200), and L1 (777-NC-100) were purchased from R & D Systems. Chariot™ (30025) was purchased from Active Motif. CK666 (ALX-270-506) and Cytochalasin-D (BML-T109) were purchased from Enzo Life Sciences. Chicken neuron transfection kit was purchased from Lonza (VPG-1002). Fertilized White Leghorn chicken eggs were purchased from Hy-Line North America, LLC. Anti-ephrin A2 (sc-912), anti-Arp3 (sc15390), and anti-β3-Tubulin (sc-58888) antibodies were purchased form Santa Cruz Biotechnologies, Inc. Anti-p34 antibody was purchased from Millipore (07-227). Anti-8D9 (L1) antibody was purchased from the Developmental Studies Hybridoma Bank, University of Iowa. Anti-acetylated tubulin (32-2700) antibody was purchased from Life Technologies. All other reagents were acquired from Sigma-Aldrich, unless otherwise stated.

Neuronal culture Coverslips were treated with 0.1% poly-L-lysine for 2 hrs, washed three times in H_2O^{dd}, dried, and coated with 5% nitrocellulose dissolved in amyl acetate. Coverslips with dried nitrocellulose were coated overnight with either 20 ug/mL laminin

or 4 ug/mL L1. Video dishes were assembled by gluing coverslips to petri dishes with a 13mm diameter hole on the bottom, UV sterilized overnight, then coated as above. Embryonic day 7 (E7) lumbar dorsal root ganglia (DRG) or retinal ganglion cell (RGC) neurons were cultured overnight as tissue explants or dissociated cells, in a humidified incubator at 40°C, in accordance with the University of Minnesota Institutional Animal Care and Use Committee. Culture media was composed of F12H supplemented with 1x B27, 2mM glutamine, 1mM sodium pyruvate, 8 mM glucose, and 10mM HEPES.

Neuronal transfection A detailed protocol is described elsewhere (Marsick et al., 2010; Marsick et al., 2012a). Approximately, $5x10^6$ DRG or retinal ganglion cell (RGC) neurons were transfected with either 2 μg of the EGFP or 2 μg of EGFP-CA (construct prevents Arp2/3 activation by NWASP; kindly provided by Dr Lorene Lanier, University of Minnesota, Minneapolis, MN). For retrograde flow measurements, 2μg mCherry-actin (kindly provided by Dr. James R. Bamburg, Colorado State University, Fort Collins, CO) was co-transfected with either EGFP or EGFP-CA. For study of integrin adhesions in growth cones, E7 DRG neurons were transfected with 2 μg paxillin-GFP purchased from Addgene (plasmid 15233). We transfected cells using a Lonza Nucleofector and the G13 program. Transfected cells were grown overnight with 0.5 ng/mL NGF.

Immunocytochemistry A detailed protocol for fixation and blocking of neurons is described elsewhere (Marsick et al., 2010; Marsick et al., 2012a). Antibodies were diluted in PBS with 10% goat serum and 0.2% Triton X-100. Anti-p34 (1:100), anti-Arp3 (1:100), anti-8D9 (L1) (1:100) anti-ephrin (1:200), anti-acetylated tubulin (1:300) or anti-

β3-tubulin (1:500) were diluted in blocking media and applied for 4 hrs. Coverslips were then washed three times in PBS and the corresponding secondary antibodies used, either Alexa Fluor 568 goat anti-rabbit, Alexa Fluor 488 goat anti-mouse, or both were applied at a 1:500 dilution for 1 hr. If fluorescent phalloidin was used, it was applied with the secondary antibodies at a concentration of 2.5 μl for every100 μl of blocking/antibody solution, either for the Alexa Fluor 488 or 568 phalloidin. Coverslips were washed three times in PBS and mounted with *SlowFade* (Invitrogen) and sealed.

Time-lapse microscopy, fluorescent quantification, and morphometric analysis Image acquisition settings were held constant for the different groups within a particular experiment, and images were obtained in one session. All images were obtained using an Olympus XC-70 inverted microscope equipped with a Capital Q camera controlled by MetaMorph software (Molecular Devices), unless otherwise noted. Quantification of fluorescent intensity was done by measuring the integrated signal in the distal 40 μm of the growth cone. Growth cone areas were obtained by thresholding phalloidin-stained images and tracing growth cones outlines. Filopodia numbers were obtained from phalloidin-labeled growth cones, and the number of filopodia per growth cone counted and divided by the growth cone perimeter length. This number was then expressed as the number of filopodium per 100μm of growth cone perimeter. Paxillin-GFP images were obtained using a Zeiss Observer Z1 TIRF microscope (University Imaging Centers) equipped with a QuantEM CCD.

Statistical analyses Data were assessed for normality and variance and analyzed accordingly with an unpaired Student's t test, Mann-Whitney U test, ANOVA, or Kruskal-Wallis, based on the number of groups to be compared. Data is reported as mean +/- standard error of the mean.

Pharmacological inhibitors 50μM CK666 was added to cultures for 4 hrs previous to any manipulation (e.g. NGF stimulation or turning assays). Cytochalasin D was used at 2μM. Control groups received the same volume of DMSO that was used to deliver the drug treatment, without ever exceeding a 5 μl/mL concentration.

Retrograde flow measurements To monitor the retrograde flow of actin in growth cones we transfected neurons with mCherry-actin. Arp2/3 inhibition was achieved pharmacologically with 50μM CK666, or by transfection of EGFP-CA, control groups received DMSO or EGFP transfection, respectively. Retrograde flow time lapses were acquired with a Zeiss Cell Observer Spinning Disk Confocal (University Imaging Centers) equipped with a QuantEM CCD with images obtained every 3 s for 3 min. Kymographs were obtained and analyzed in MATLAB, using a previously published algorithm developed in David Odde's Laboratory (Chan and Odde, 2008).

Barbed-end labeling This protocol has been described in detail before (Marsick et al., 2010).

Growth cone turning assay This method has been described previously (Marsick et al., 2010; Marsick et al., 2012a). Briefly, glass micropipettes were coated with 5% nitrocellulose in amyl acetate. These were then dipped in 1μg/mL NGF in PBS for 3 min. The coated micropipette was lowered into a video dish with a micromanipulator and placed approximately 80μm away from the central domain of a growth cone at a 45° angle, relative to the neurite axis. Growth cones were imaged every 30 seconds. Turning responses were measured as the change in direction in growth cone migration after 45 minutes of presenting the NGF-coated micropipette.

Protein loading The WASP VCA domain peptide was acquired from Cytoskeleton, Inc. (VCG03-A) and reconstituted according to manufacturer's specifications. The VCA peptide was complexed with the Chariot™ reagent from Active Motif, based on manufacturer's specifications. After trying several ratios of the two components, we found that for our experiments the best concentrations were 4μg Chariot™+ 3μ VCA-GST incubated at room temperature for 30 min. The complex was then delivered into growth cones from an immobilized nitrocellulose-coated pipette, as described in the growth cone turning assay.

Stripe assay Coverslips were dipped in a 0.5% 3-aminopropyl-trimethoxysilane solution in H_2O^{dd} for half hour, washed three times for five minutes in H_2O^{dd}, then air-dried in a laminar flow hood, and coated with 5% nitrocellulose in amyl acetate. Silicon molds for the stripes were attached to the coverslips. The solution that passed through the channels was composed of 20 μg/mL ephrin A2-Fc and 10 μg/mL goat anti-Fc, diluted in either 20

μg/mL laminin or 4 μg/mL L1. A total volume of 250 μL of solution was passed though each silicon matrix over a period of 1 hr. At this point 50 μL of PBS were passed through the channels to remove any unbound protein and the matrices were removed from the coverslips. Laminin (20 μg/mL in PBS for 20 min) or L1 (4 μg/mL in PBS for 1 hr) were then applied to the entire coverslip. E7 temporal retina stripes were then plated over the stripes and grown for 16 hrs. Next morning, 50% of the media was replaced and either DMSO or 50 μM CK666 was added to the cultures and allowed to grow for another 24 hrs. At this point, the cultures were fixed, blocked, stained with anti-ephrin A2 and anti-β3 tubulin antibody, and imaged.

L1 Results

L1 as a substrate

The glycoprotein L1 is a homophillic binding CAM important for neurite growth, axon fasciculation and guidance, and synapse formation (Nakamura et al., 2010). As an *in vitro* substrate it promotes the formation of broad lamellar growth cones in E7 DRG or RGC neurons (Fig. 1a,f,h). These growth cones have broad peripheral domains (P-domain) that are periodically subdivided by filopodia, these subdivisions are known as lamellipodial veils and are dependent on Arp2/3 function (Korobova and Svitkina, 2008).

Arp2/3 at the leading edge

To understand its role in actin dynamics and guidance, we first asked where is Arp2/3 localized in our growth cones. We performed immunostaining against two

subunits of the Arp2/3 complex: p34 and Arp3. Consistent with previous reports, wide field microscopy showed the p34 subunit to be localized at the central domain (C-domain) and at leading edge of growth cones (Fig. 1a-b). However, using total internal reflection fluorescence (TIRF) microscopy to image the cytoplasm near the substrate eliminated most of the C-domain staining, but not the leading edge (Fig. 1a-e). Imaging of the Arp3 subunit through wide field and TIRF microscopy revealed a homogeneous staining pattern along the P-domain and leading edge of growth cones (Fig. 1f-g), without enrichment in the C-domain. These results suggest that Arp2/3 is closely associated with the substrate at the leading edge, where we also found L1 to be enriched in the plasmalemma by TIRF microscopy (Fig. 1h-j). Interestingly, Arp2/3 was shown to bind focal adhesion kinase (FAK) and vinculin, and be recruited to nascent integrin adhesions to couple actin polymerization to adhesion formation (DeMali et al., 2002; Serrels et al., 2007). It is unknown if Arp2/3 is also recruited to L1 adhesions, but the localization makes it well suited to mediate actin polymerization at the leading edge and promote its protrusion.

Arp2/3 influences leading edge protrusion, motility, and axon elongation

Actin polymerization is essential for driving growth cone leading edge protrusion (Marsick et al., 2010; Gomez and Letourneau, 2013). Therefore, we sought to investigate the role of Arp2/3 during leading edge protrusion on L1 in response to nerve growth factor (NGF) stimulation. NGF is an attractive guidance cue for DRG neurons during development and a potent stimulator of actin polymerization *in vitro*. We made time-lapse videos of DRG growth cones during NGF stimulation to analyze leading edge

behavior with kymographs, either using 50μM CK666 to inhibit Arp2/3 or DMSO as a vehicle control (Nolen et al., 2009). We found that CK666 significantly reduced the average leading edge protrusion after NGF stimulation for 5 min. (Fig. 2a-i). Yet, more revealing than the reduction in protrusion during Arp2/3 inhibition was the dynamic leading edge behavior. Shortly after initial NGF stimulation, the leading edge of CK666-treated growth cones would protrude but, arbitrarily, individual lamellipodial veils would collapse and retract towards the C-domain of the growth cone (Fig.2g-h, yellow arrows). Yang et al. reported similar observations (2012). At this point, the veil would remain collapsed or start protruding after a brief pause. A plausible explanation for veil collapse during Arp2/3 inhibition is the reduced number of actin branches at the leading edge, thus leaving a weakened actin network to abut against and resist the rearward membrane tension at individual veils. It has also been reported that retracting veils have a lower density of actin branches that protruding veils (Mongiu et al., 2007). Therefore, this experiment suggests that Arp2/3 is necessary for the protrusion and stability of the growth cone leading edge after NGF stimulation on L1.

Leading edge protrusion is associated with growth cone motility and axon elongation. Because Arp2/3 inhibition reduced leading edge protrusion on L1, we asked whether it would affect growth cone motility. We did time-lapse microscopy of growth cones treated either with DMSO or CK666. We found that CK666-treated growth cones had a 30% reduction in their migration velocity over a 1-hour period, compared to DMSO-treated growth cones (Table 1). Consistent with this result, overnight inhibition of Arp2/3 led to axon lengths that were 60-75% those of control axons, either with CK666 or by expression of the dominant-negative construct EGFP-CA (Table 1). This construct

codes for the CA peptide, which has been shown to prevent Arp2/3 activation by WASP/Scar proteins (Hufner et al., 2001; Strasser et al., 2004). These results suggest that Arp2/3 inhibition caused a motility deficit, which predictably led to shorter axons on L1.

Arp2/3, barbed ends, actin polymerization, and filopodium numbers

Leading edge protrusion is driven by monomeric actin incorporation onto free F-actin barbed ends. We wanted to know what effect would Arp2/3 inhibition have on the formation and availability of free barbed ends in growth cones on L1. To this end, we employed a barbed-end quantification assay, using DMSO or CK666 (Marsick et al., 2010; Marsick and Letourneau, 2011). Briefly, growth cones were pre-treated with DMSO or CK666 for 4 hrs, stimulated with NGF for 4 min, permeabilized, bathed in a Rhodamine-actin solution, washed, fixed, and Rhodamine-actin incorporation was quantified. We found that in DMSO-treated growth cones NGF led to a large increase in Rhodamine-actin incorporation at the leading edge, and that the Rhodamine-actin label would colocalize with Alexa-488 phalloidin staining (Fig. 2j-n); thus suggesting that the labeled actin had been incorporated into actin filaments. Similar results were published recently (Yang et al., 2012). On the other hand, NGF stimulation caused very little Rhodamine-actin incorporation into CK666-treated growth cones (Fig. 2j,m,n). This experiment shows that most barbed ends created after NGF stimulation on L1 are located at the leading edge and are dependent on Arp2/3.

Given that Arp2/3 inhibition substantially reduced barbed end numbers on L1, we investigated the effect it would have on total F-actin after NGF or Netrin stimulation. Netrin is a potent stimulator of actin polymerization and a chemoattractant (de la Torre et

al., 1997; Marsick et al., 2010) in the guidance of RGC axons from the retina into the optic nerve head (Deiner et al., 1997). We inhibited Arp2/3 in DRG or retina explants with CK666 for 4 hours before experiments or by overnight expression of the dominant-negative construct EGFP-CA. We applied global stimulation of NGF (DRG), Netrin (RGC), or media as a control to growth cones for 15 minutes, fixed, stained with Alexa-568 phalloidin, and quantified phalloidin fluorescent intensity. We found that in control conditions NGF or Netrin stimulation caused a large increase in the total F-actin content in growth cones (Fig. 3a-b, e-g). These growth cones also increased their surface area and acquired a lamellar morphology with an intense fringe of F-actin close to the leading edge (Fig. 3a-b, h). On the other hand, Arp2/3-inhibited growth cones had a small increase in F-actin content and surface area after NGF or Netrin treatment (Fig. 3c-h). Moreover, they no longer had a lamellar morphology. These results further reinforce our findings that Arp2/3 is an important mediator of actin polymerization in growth cones on L1. Moreover, Arp2/3 activation promotes the protrusion and expansion of the leading edge.

Arp2/3 has been linked to filopodium formation in non-neuronal cells and growth cones (Machesky and Insall, 1998; Korobova and Svitkina, 2008). The mechanism was coined the convergent elongation model and proposes that actin filaments in filopodia can originate from the branched actin network dependent on Arp2/3 activity (Svitkina et al., 2003). We asked whether Arp2/3 influences filopodium numbers in growth cones on L1. Thus, we counted filopodium numbers in DRG growth cones treated with DMSO or CK666, with and without NGF stimulation. We found that Arp2/3 inhibition reduced the extent to which NGF stimulation increased filopodial numbers in growth cones (Fig. 3i).

This finding suggests that Arp 2/3 activity contributes to the stimulus-dependent increase in filopodium numbers in growth cones after NGF stimulation.

Arp2/3 and actin retrograde flow

Actin retrograde flow is controlled by three main factors: a) myosin II activity pulling F-actin back from the leading edge (Lin et al., 1996; Medeiros et al., 2006), b) elongating actin filaments that push on the membrane at the leading edge, resulting in increased membrane tension, which pushes back on the growing filaments, adding to the retrograde flow of the actin network (Henson et al., 1999; Medeiros et al., 2006; Craig et al., 2012), and finally c) linkage of actin filaments to substrate adhesions that restrict their backward flow relative to the substrate (Suter et al., 1998; Shimada et al., 2008; Marsick et al., 2012a). Since Arp2/3 inhibition substantially reduced barbed ends numbers and total F-actin, we investigated what effect it would have on the retrograde flow of actin in growth cones on L1. To this end, we made kymographs from time-lapse videos of DRG and RGC growth cones transfected with mCherry-actin and EGFP-CA, or mCherry-actin and treated with DMSO or CK666 4 hrs prior to imaging. We found that compared to controls, Arp2/3 inhibition led to a 15-30% reduction in the actin retrograde flow along veils, but no change in retrograde flow along filopodia (Fig. 4a-n). We hypothesize that the reduction in the actin retrograde flow after Arp2/3 inhibition is due to the reduced number of barbed ends capable of actin polymerization, which in turn generate less push against the leading edge membrane and the actin network towards the C-domain of the growth cone. We tested this idea using cytochalasin D to block monomeric actin

incorporation into barbed ends and found a significant reduction in the actin retrograde flow rate, suggesting that monomeric actin incorporation into barbed ends can influence the actin retrograde flow (Fig. 4m). As a further control, we measured through immunostaining the activity of phospho-myosin light chain 2 (Ser19), the active form of the regulatory subunit for myosin II and a downstream target of ROCK, and found no difference in staining intensity between control and Arp2/3-inhibited growth cones (Fig. 4o-r). This suggest that Arp2/3-dependent actin polymerization at the leading edge is a significant component in the driving force of the actin retrograde flow in growth cones.

Arp2/3 role in guidance

Chemoattraction depends on asymmetric leading edge protrusion on the side of the growth cone closest to the attractant source (Marsick et al., 2010; Dent et al., 2011). In turn, leading edge protrusion depends on the fine balance between actin polymerization and its retrograde flow at the leading edge. Since Arp2/3 inhibition caused a reduction in both leading edge protrusion and the actin retrograde flow, we asked what effect would Arp2/3 inhibition have during growth cone chemoattraction. NGF (DRG) or Netrin (RGC) was applied to one side of growth cones and their turning response measured. We found that Arp2/3 inhibition led to a 75-85% percent reduction in growth cone turning angle towards NGF or Netrin (Fig. 5a-f). Arp2/3-inhibited growth cones would generate protrusions towards the chemoattractant source, but often these protrusions would collapse, as with the global NGF stimulation experiments (Fig. 2g-h, and 5d`). This experiment shows that the actin nucleator Arp2/3 is required for optimal DRG and RGC growth cone chemotaxis towards NGF and Netrin, respectively, on L1.

This finding led us to ask whether localized activation of Arp2/3 on its own would be sufficient to trigger growth cone turning on L1. During chemotaxis, NGF and Netrin activate multiple signaling pathways that manipulate a variety of cellular processes in the growth cone (multiple ABP's, other cytoskeletal components, vesicular trafficking, calcium signals, etc), all of which contribute to an optimal turning response. However, we wanted to isolate the effect of asymmetric Arp2/3 activation. We performed the same guidance assay mentioned above with modifications. We used the Chariot™ reagent to shuttle the VCA-GST peptide, which is capable of activating Arp2/3 (Hufner et al., 2001; van der Gucht et al., 2005), into growth cones. We have used this approach previously to deliver active ABP's into growth cones and study their effects during chemotaxis (Marsick et al., 2010). We applied Chariot™+VCA-GST or Chariot™+β-Galactosidase as a control, and studied growth cone responses. We found that the Chariot™+VCA-GST combination was capable of steering growth cones toward its source at angles significantly larger than the Chariot™+β-Galactosidase combination (Fig. 5g). More importantly, turning towards the Chariot™+VCA-GST source was abolished in the presence of the Arp2/3 inhibitor CK666, indicating that Arp2/3 mediates the turning response elicited by Chariot™+VCA-GST. Regarding the smaller turning angles triggered by Chariot™+VCA-GST in comparison to NGF or Netrin, it is reasonable to suggest they are the result of the missing parallel signaling pathways that are normally activated by these chemoattractants, besides Arp2/3-mediated actin polymerization. These results establish that asymmetrical activation of the Arp2/3 complex is sufficient to trigger growth cone turning on L1.

We determined that Arp2/3 is required to follow a soluble chemoattractant gradient on L1. Unable to establish a soluble chemorepellent assay that would consistently repel growth cones away from the source, we opted for a membrane-bound chemorepellent assay with alternating stripes of substrate-bound L1 and L1 + ephrin A2. E7 temporal retina stripes were laid perpendicular to the stripes and allowed to grow for 40 hrs; the final 24 hrs were under the effect of DMSO or CK666 (Fig. 5h). This approach allowed explants to initiate and grow neurites before Arp2/3 inhibition; thus, eliminating any possible defect Arp2/3 inhibition might cause during neuritogenesis and allowing us to study guidance only. Explants were fixed, and axon trajectories were revealed by immunolabeling with anti-β3 tubulin, while staining with anti-ephrin A2 assessed the integrity of the ephrin A2 lanes. We found that explants treated with DMSO had axons that consistently remained within the L1 lanes, thus avoiding the L1 + ephrin A2 lanes (Fig. 5i-k). Interestingly, treatment with CK666 led to a range of guidance deficits that ranged from: a) growth cones ignoring ephrin A2 and crossing the boundaries, b) continued migration over the ephrin A2-containing lanes, and c) axonal branching over the ephrin A2-containing lanes (Fig. 5l-p). These results suggest that Arp2/3-dependent actin polymerization is necessary for an effective avoidance response to the membrane-bound chemorepulsive cue ephrin A2 on L1.

Laminin Results

Laminin as a substrate

In culture, L1 promotes the formation of broad lamellar growth cones. We showed that Arp2/3 inhibition on this substrate causes growth cones to have deficiencies in cytoskeletal dynamics and guidance. In view of these results, we asked if such deficiencies would also arise on a substrate where growth cones are more compact and filopodial, and perhaps less dependent on the branched actin network organized by Arp2/3. For this reason we decided to use laminin, which is an ECM protein found in most organs and tissues and has also been shown to be an endogenous substrate for growing axons (McLoon et al., 1988).

Arp2/3 distribution in growth cones on laminin

To assess Arp2/3 function in growth cones on laminin, we first asked where was it localized. Through immunostaining, we found Arp2/3 subunit Arp3 to be localized homogeneously across the growth cone P-domain, without any enrichment at the leading edge (Fig. 6a-d). However, Mongiu et al. reported that chick DRG growth cones do have Arp2/3 subunits enriched at their veils through EM (2007). This discrepancy across labs is most likely due to the higher resolution and sensitivity of their screening methods. The fact that we were able to detect Arp2/3 subunit enrichment at the leading edge in growth cones on L1 through immunostaining might reflect a denser branched actin network on this substrate, than on laminin.

Arp2/3 motility and axon length

We showed that Arp2/3 was required for optimal growth cone motility on L1. Therefore, we asked if Arp2/3 was also required for motility on laminin. We made time-lapse videos of DRG explants with and without Arp2/3 inhibition. As before, explants were imaged for 1 hr and the velocity of individual growth cones measured. We found that Arp2/3 inhibition did not cause a significant deficit in migration velocity, compared to control growth cones (Table 1). This suggests that Arp2/3 is not crucial for effective growth cone motility on laminin, although it is on L1.

Even though growth cone motility on laminin over a 1 hr period was not significantly affected by Arp2/3 inhibition, we asked whether the prolonged effect of overnight inhibition would reduce axon elongation on laminin, as it did on L1. For this purpose, we made low density cultures of DRG neurons that were either transfected with EGFP-CA or treated with CK666 5 hrs after plating to inhibit Arp2/3, grown overnight, fixed and stained with anti-β3 tubulin. We found that Arp2/3 inhibition, by any of the two methods, reduced average axon length to 80% that of controls (Table 1). This shows that prolonged inhibition of Arp2/3 function will reduce axon length on laminin, although not as severely as it did on L1.

Arp2/3 effect on actin polymerization and filopodia

Arp2/3 inhibition led to a drastic reduction in the increase of F-actin on L1 after NGF stimulation. Consequently, we asked if Arp2/3 inhibition would have a similar effect on laminin, where growth cones are compact and filopodial. We pretreated DRG explants with DMSO or CK666 for 4 hrs, followed by global NGF stimulation, or media

as a control, for 15 minutes. Growth cones were then fixed, stained with Alexa-488 phalloidin, and imaged. We found NGF stimulation led to a large increase in total F-actin and growth cone surface area, whereas Arp2/3-inhibited growth cones responded with only a minor increase in F-actin and area after NGF treatment (Fig. 6e-j). Not only was there a quantitative difference in growth cone F-actin, but a qualitative difference as well. Arp2/3-inhibited growth cones had fewer veils than controls, consistent with Arp2/3 role in nucleating a branched actin network. This result shows that Arp2/3 mediates actin polymerization in growth cones on laminin after NGF stimulation, as it does on L1.

Similar to other groups using non-neuronal and neuronal cells (Machesky and Insall, 1998; Svitkina et al., 2003; Korobova and Svitkina, 2008), we found that Arp2/3 inhibition reduced the number of NGF-induced filopodia in growth cones on L1. Therefore, we asked whether Arp2/3 inhibition would have any effect on the number of NGF-induced filopodia in growth cones on laminin. We found that Arp2/3 inhibition led to a reduction in the number of filopodia in growth cones after NGF stimulation, like on L1 (Fig. 6k). These results suggest that Arp2/3 is involved in filopodia formation on laminin and L1.

Arp2/3 and the retrograde flow of actin

Arp2/3 inhibition led to a reduction in the rate of the actin retrograde flow along growth cone veils on L1. Presumably, this decreased rate was due to a reduced retrograde push exerted on the actin network, because of the reduced force exerted by actin polymerization against the leading edge membrane. Since Arp2/3 inhibition reduced actin polymerization in growth cones on laminin, we asked what effect Arp2/3 inhibition

would have on the actin retrograde flow on laminin. For this purpose, we did time-lapse videos of DRG neurons transfected with mCherry-actin and grown overnight. To our surprise, Arp2/3 inhibition led to an increased actin retrograde flow rate along growth cone veils but not filopodia on laminin, regardless of whether CK666 or EGFP-CA was used to inhibit Arp2/3 (Fig. 7a-h). Recently, Yang et al reported similar results in *Aplysia* neuronal growth cones and concluded that the actin network assembled by Arp2/3 restricts the myosin II-dependent contractility of the actin network in a ROCK-independent manner (Yang et al., 2012). When we measured phospho-myosin light chain 2 (Ser19), a regulatory subunit for myosin II and downstream target of ROCK, similar to our results on L1 and Yang et al, we found no difference in the myosin II activity after Arp2/3 inhibition (Fig. 7i-o). In addition, we found that the actin retrograde flow along filopodia was indistinguishable between control and Arp2/3-inhibited growth cones (Fig. 6h) further suggesting that the increased rate in the actin retrograde flow along veils is not a result of increased myosin II activity.

Because it is unlikely that Arp2/3 inhibition would increase the retrograde flow of actin by promoting actin polymerization, we examined integrin-based adhesions in growth cones on laminin, since the adhesion-based clutch is a determinant of the actin retrograde flow. Recent reports in non-neuronal cells have shown that Arp2/3 is recruited to nascent integrin-based adhesions and interacts with vinculin and FAK, as a way to couple actin polymerization to newly formed adhesions (DeMali et al., 2002; Serrels et al., 2007). We transfected DRG neurons with paxillin-GFP, a marker of integrin adhesions, and mCherry-CA, grew them overnight, and imaged cell-substrate interactions by TIRF microscopy. Consistent with the increased actin retrograde flow rate after

Arp2/3 inhibition, we found that the mean area of paxillin-GFP puncta was 70% that of controls (Fig. 8a-e). Moreover, these growth cones also had a reduced number of paxillin-GFP puncta compared to controls (Fig. 8f). It is likely that the smaller size and reduced number of adhesions are not as effective at engaging the overlying flow of actin filaments, and as a result the actin retrograde flow rate is faster. A recent report on fibroblasts showed that adhesion size was not affected by Arp2/3 inhibition, only their orientation relative to the leading edge (Wu et al., 2012). Our experiments suggest that on laminin the size and number of integrin-based adhesions in growth cones is influenced by Arp2/3 activity.

Arp2/3 and guidance

It is thought that local stimulation of actin polymerization steers the growth cone leading edge towards attractive guidance cues (Marsick et al., 2010; Dent et al., 2011). We know that Arp2/3 inhibition reduced the NGF-stimulated increase in F-actin content in growth cones on laminin. Arp2/3 inhibition also reduced actin polymerization in DRG and RGC growth cones on L1, which was associated with a guidance deficit towards the chemoattractants NGF and Netrin, respectively. Therefore, we asked if the reduction in actin polymerization on laminin after Arp2/3 inhibition would also affect growth cone chemoattraction towards NGF. As before, we applied NGF to one side of growth cones and measured their turning responses. Surprisingly, we found that Arp2/3 inhibition did not reduce chemoattraction towards NGF, but instead we observed an increase in the turning angles (Fig. 9a-e). This experiment suggests that Arp2/3-mediated actin

polymerization is not required for chemoattractive turning on laminin, as opposed to on L1.

Because Arp2/3 inhibition did not cause deficient attractive guidance towards NGF on laminin, we asked if its unilateral activation of Arp2/3 in a growth cone on laminin was sufficient to trigger turning. In our experiment on L1, unilateral activation of Arp2/3 by the Chariot™+VCA-GST complex did elicit a significant turning response toward the pipette over controls. As before, we used a micropipette to deliver a gradient of either Chariot™+VCA-GST or Chariot™+B-Galactosidase, as control. We found that the Chariot™+VCA-GST peptide complex could not elicit growth cone turning on laminin towards the gradient source (Fig. 9f). This indicates that localized activation of Arp2/3 is insufficient to trigger growth cone turning on laminin, as opposed to on an L1 substrate, and suggests that other cellular processes are required to execute attractive chemotactic turning on laminin.

Since Arp2/3 inhibition did not reduce chemoattraction towards NGF, we asked if Arp2/3 was also dispensable for contact-mediated chemorepulsion. When we performed this experiment on L1, we found that RGC axons exhibited a variety of guidance deficits. We made a boundary assay with alternating stripes of laminin or laminin + ephrin A2. E7 temporal retina stripes were laid perpendicular to the stripes and allowed to grow for 40 hrs, the final 24 hrs under the effect of DMSO or CK666. Explants were fixed, and axon trajectories revealed with anti-β3 tubulin and the integrity of the ephrin A2 lanes with anti-ephrin A2. Despite being shorter, Arp2/3 inhibited axons were just as responsive to the contact-mediated chemorepulsive effects of the ephrin A2-containing lanes as the

control group (Fig. 9g-l). This result suggests that Arp2/3 function is not required for efficient contact-mediated chemorepulsion on laminin, as it is on L1.

Figures and Tables

Table 1. Arp2/3 role in axon outgrowth rate and length		
	laminin	L1
Axon outgrowth rate# (μm/hr)		
-DMSO	20.68 ± 0.5881	15.26 ± 0.8684
-CK666	18.02 ± 0.8024	10.76 ± 0.5519
Axon length* (μm)		
-DMSO	235.2 ± 11.88	198.2 ± 11.10
-CK666	195.6 ± 12.61	153.0 ± 9.936
-EGFP	236.8 ± 11.21	239.5 ± 13.39
-EGFP-CA	182.2 ± 11.66	144.1 ± 12.01

Table 1: # Measurements were done from time lapse videos of E7 DRG explants' growth cones on L1 treated with DMSO or 50M CK666 4 hrs prior to imaging. *Measurements were done on dissociated low-density cultures on L1 from E7 DRG neurons grown for 24 hrs, fixed, and stained with antibodies against neuronal β3-tubulin. For pharmacological inhibition of Arp2/3 with CK666, neurons were allowed to adhere for 6 hrs before adding the drug.

Figure 1:

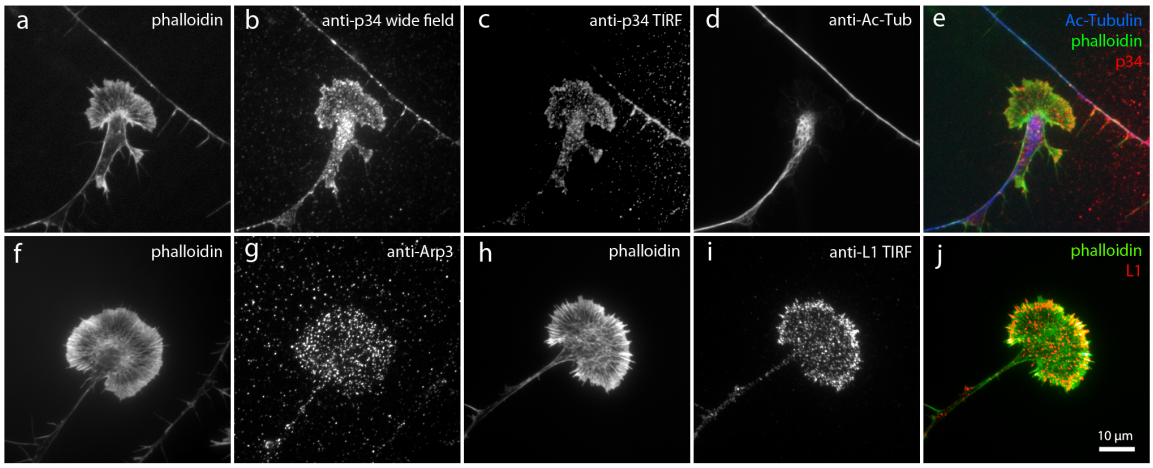

Figure 1. Arp2/3 is present in the leading edge of growth cones on L1. **(a-j)** E7 DRG explants were grown overnight on L1, treated globally with 50 ng/mL NGF for 15min., fixed, and stained with phalloidin and antibodies against acetylated α-tubulin (Ac-Tubulin), p34, Arp3, and L1 (8D9). Images were acquired with standard confocal microscopy; **(c)** p34 staining was also imaged with the TIRF modality to show its localization near the substrate.

Figure 2:

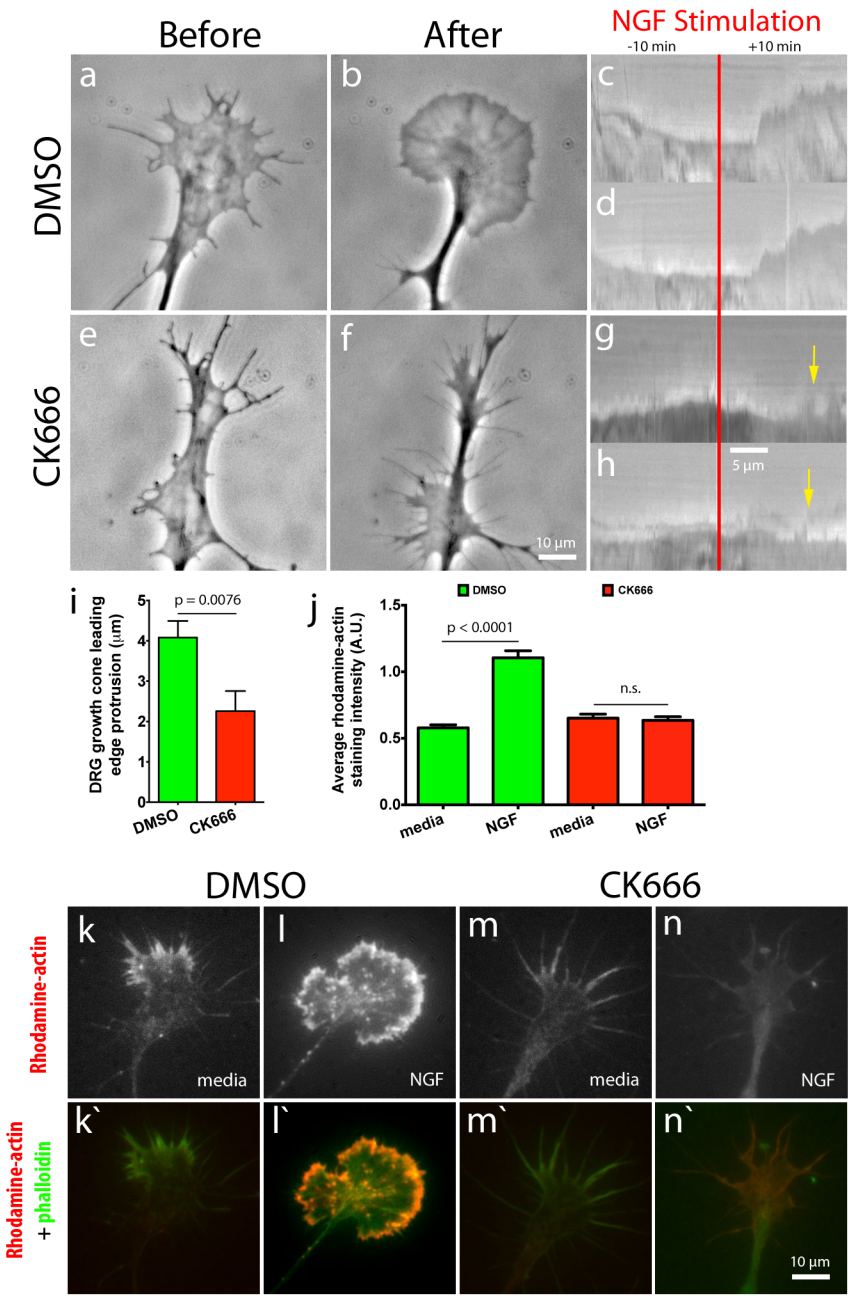
Before
After
NGF Stimulation
-10 min
+10 min
DMSO
CK666
a
b
c
d
e
f
g
h
10 µm
5 µm
i
DRG growth cone leading edge protrusion (µm)
p = 0.0076
DMSO
CK666
j
Average rhodamine-actin staining intensity (A.U.)
p < 0.0001
n.s.
media
NGF
media
NGF
DMSO
CK666
Rhodamine-actin
Rhodamine-actin + phalloidin
k
l
m
n
media
NGF
media
NGF
k`
l`
m`
n`
10 µm

Figure 2. Arp2/3 mediates leading edge protrusion and barbed end creation after global NGF stimulation on L1. **(a,b,e,f)** E7 DRG explants were grown overnight on L1 and treated with DMSO or 50 μM CK666 (Arp2/3 inhibitor) for 4hrs, growth cones were then imaged with phase contrast microscopy for 10min, before and after, global application of 50 ng/mL NGF. Representative kymographs depicting leading edge behavior during NGF stimulation (red bar) for **(c-d)** DMSO- and **(g-h)** CK666-treated growth cones. Yellow arrows point to leading edge collapse. **(i)** Quantification of leading edge protrusion 10min after global NGF application. **(k-n)** E7 DRG explants were grown on L1, treated with DMSO or CK666 for 4hrs, then with 50 ng/mL NGF globally for 10min, permeabilized with buffer containing phalloidin and Rhodamine-actin for 4min, then fixed. **(k`-n`)** Rhodamine-actin (red) and phalloidin (green) labeling were overlaid to show barbed end distribution in growth cones on L1. **(j)** Quantification of the average Rhodamine-actin incorporated into growth cones. Graphs show mean +/- standard error of the mean.

Figure 3:

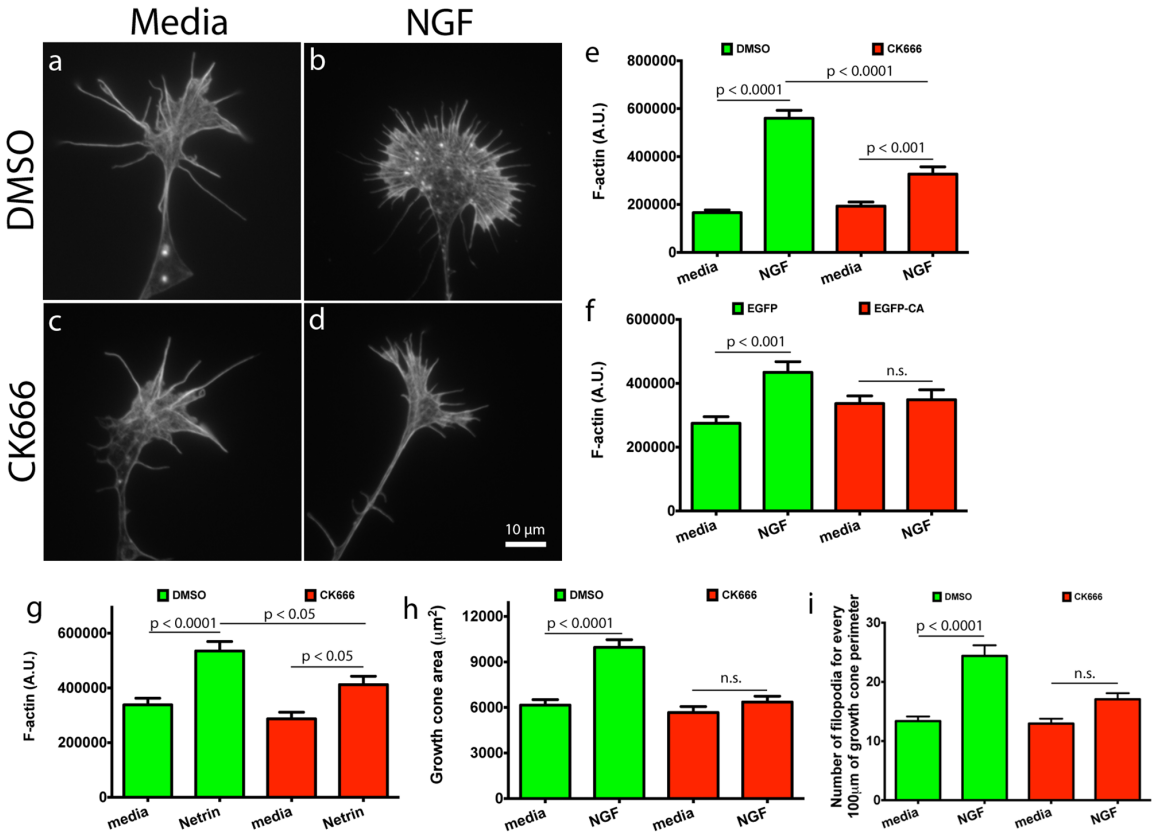
Media
NGF
DMSO
CK666
a
b
c
d
10 µm
e
DMSO
CK666
F-actin (A.U.)
p < 0.0001
p < 0.0001
p < 0.001
media
NGF
media
NGF
f
EGFP
EGFP-CA
F-actin (A.U.)
p < 0.001
n.s.
media
NGF
media
NGF
g
DMSO
CK666
F-actin (A.U.)
p < 0.0001
p < 0.05
p < 0.05
media
Netrin
media
Netrin
h
DMSO
CK666
Growth cone area (µm²)
p < 0.0001
n.s.
media
NGF
media
NGF
i
DMSO
CK666
Number of filopodia for every 100µm of growth cone perimeter
p < 0.0001
n.s.
media
NGF
media
NGF

Figure 3. Arp2/3 mediates actin polymerization, surface area expansion, and increase in filopodia numbers in growth cones on L1. **(a-d)** E7 DRG explants were grown overnight on L1, treated with DMSO or 50 μM CK666 for 4hrs, stimulated with 50 ng/mL NGF or control media for 15min, fixed, stained with Alexa Fluor 488 phalloidin, **(e)** and its fluorescent intensity quantified. **(f)** Quantification of Alexa Fluor 488 phalloidin fluorescent intensity bound to DRG growth cones transfected with EGFP, or the EGFP-CA (Arp2/3 dominant negative construct). **(g)** Quantification of Alexa Fluor 488 phalloidin fluorescent intensity bound to RGC growth cones treated with DMSO or 50 μM CK666 for 4hrs, stimulated with 500 ng/mL Netrin or media as a control for 15min, fixed and stained with phalloidin. **(h)** Measured DRG growth cone area. **(i)** Average number of filopodia for every 100μm of growth cone perimeter. Graphs show mean +/- standard error of the mean.

Figure 4:

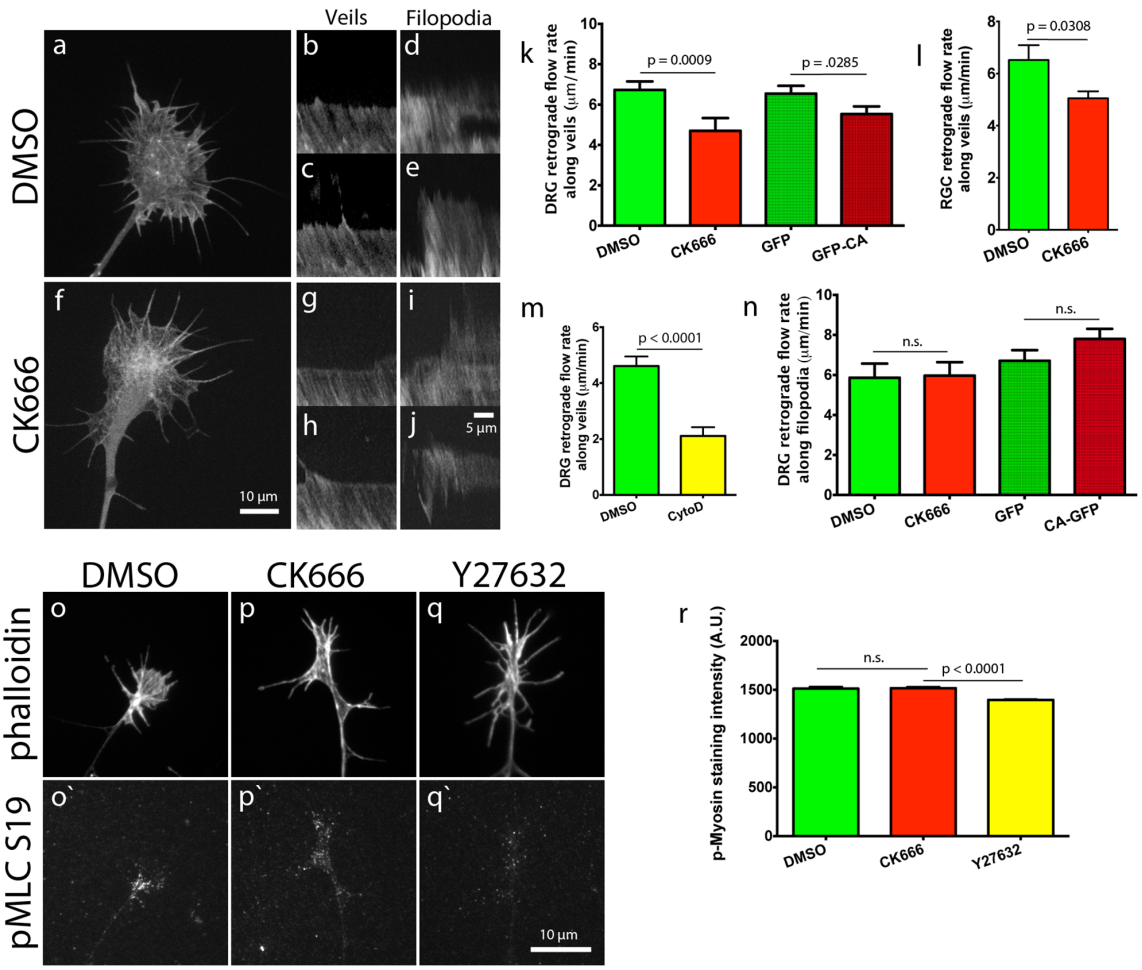
Veils
Filopodia
DMSO
CK666
a
b
c
d
e
f
g
h
i
j
10 µm
5 µm
k
DRG retrograde flow rate along veils (µm/min)
p = 0.0009
p = .0285
DMSO
CK666
GFP
GFP-CA
l
RGC retrograde flow rate along veils (µm/min)
p = 0.0308
DMSO
CK666
m
DRG retrograde flow rate along veils (µm/min)
p < 0.0001
DMSO
CytoD
n
DRG retrograde flow rate along filopodia (µm/min)
n.s.
n.s.
DMSO
CK666
GFP
CA-GFP
DMSO
CK666
Y27632
phalloidin
pMLC S19
o
p
q
o`
p`
q`
10 µm
r
p-Myosin staining intensity (A.U.)
n.s.
p < 0.0001
DMSO
CK666
Y27632

Figure 4. Arp2/3 inhibition reduces actin retrograde flow at the leading edge of growth cones on L1, independent of myosin II activity. **(a,f)** E7 DRG or RGC neurons were transfected with mCherry-actin and grown overnight on L1. Arp2/3 was inhibited by co-expression of EGFP-CA with mCherry-actin, or by 50 μM CK666 treatment 4hrs prior to imaging. Growth cones were imaged in a spinning disc confocal microscope and kymographs made from these time-lapse videos. **(b,c,g,h)** Representative kymographs along veils and **(d,e,i,j)** filopodia of DMSO- and CK666-treated growth cones. **(k-l)** Quantification of the actin retrograde flow along veils of DRG and RGC growth cones and **(m)** the effect that 2 μM Cytochalasin-D has on it. Note that in this experiment DMSO and Cytochalasin-D were added 3min before imaging, instead of the normal 4hrs, hence the different DMSO control rates. **(n)** Quantification of the actin retrograde flow along filopodia of DRG growth cones. **(o-q`)** As a control, DRG growth cones on L1 were treated with DMSO, 50 μM CK666, or 10 μM Y27632 for 4hrs, fixed, and stained with phalloidin and an antibody against phospho myosin light chain (Ser19), **(r)** and anti-pMLC average fluorescent intensity quantified. Graphs show mean +/- standard error of the mean.

Figure 5:

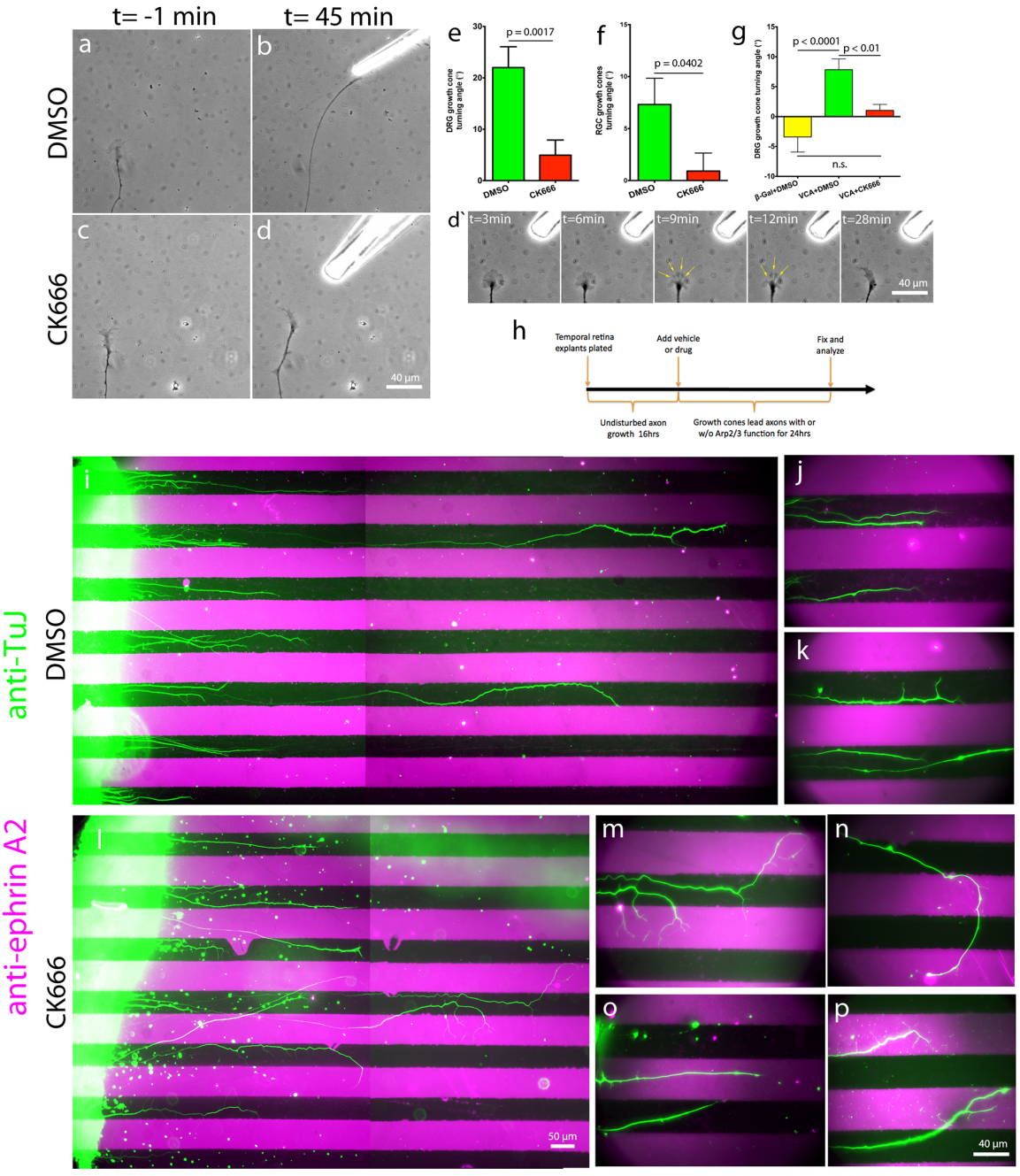
t= -1 min
t= 45 min
DMSO
CK666
a
b
c
d
40 µm
e
p = 0.0017
DRG growth cone turning angle (°)
DMSO
CK666
f
p = 0.0402
RGC growth cones turning angle (°)
DMSO
CK666
g
p < 0.0001
p < 0.01
n.s.
DRG growth cone turning angle (°)
β-Gal+DMSO
VCA+DMSO
VCA+CK666
d`
t=3min
t=6min
t=9min
t=12min
t=28min
40 µm
h
Temporal retina explants plated
Add vehicle or drug
Fix and analyze
Undisturbed axon growth 16hrs
Growth cones lead axons with or w/o Arp2/3 function for 24hrs
anti-TuJ
DMSO
i
j
k
anti-ephrin A2
CK666
l
m
n
o
p
50 µm
40 µm

Figure 5. Arp2/3 activity is necessary for efficient guidance and sufficient to trigger growth cone turning on L1. E7 DRG or RGC explants were grown on L1 overnight and treated with DMSO or 50 μM CK666 4hrs prior to the turning assay. NGF (DRG) or Netrin (RGC) gradients were established with a micropipette located at 45° and approximately 80 μm from the growth cone leading edge. **(a-d)** Representative images of DRG growth cones 1 min before and 45 min after positioning the micropipette. **(d`)** Montage of Arp2/3-inhibited growth cone response to the NGF gradient showing multiple points of veil collapse (yellow arrows). **(e-f)** DRG and RGC growth cone turning angle quantification. **(g)** Turning angle quantification for DRG growth cones on L1 in response to a gradient of Chariot™ complexed to VCA-GST or β-Galactosidase as a control, delivered as above. **(h)** Diagram depicting the experimental design for the substrate-bound ephrin A2 chemorepulsive assay. **(i,l)** Boundary assay for control (DMSO) and Arp2/3-inhibited (CK666) retina explants (on the left) with alternating lanes of laminin (black) and ephrin A2 + laminin (magenta) with axons stained with antibodies against the neuronal β3-tubulin (green). **(j-k)** Distal tips of control and **(m-p)** Arp2/3-inhibited axons shown at higher magnification, note the guidance deficits and the multiple processes sprouted by Arp2/3-inhibited axons over the ephrin A2 lanes. Graphs show mean +/- standard error of the mean.

Figure 6:

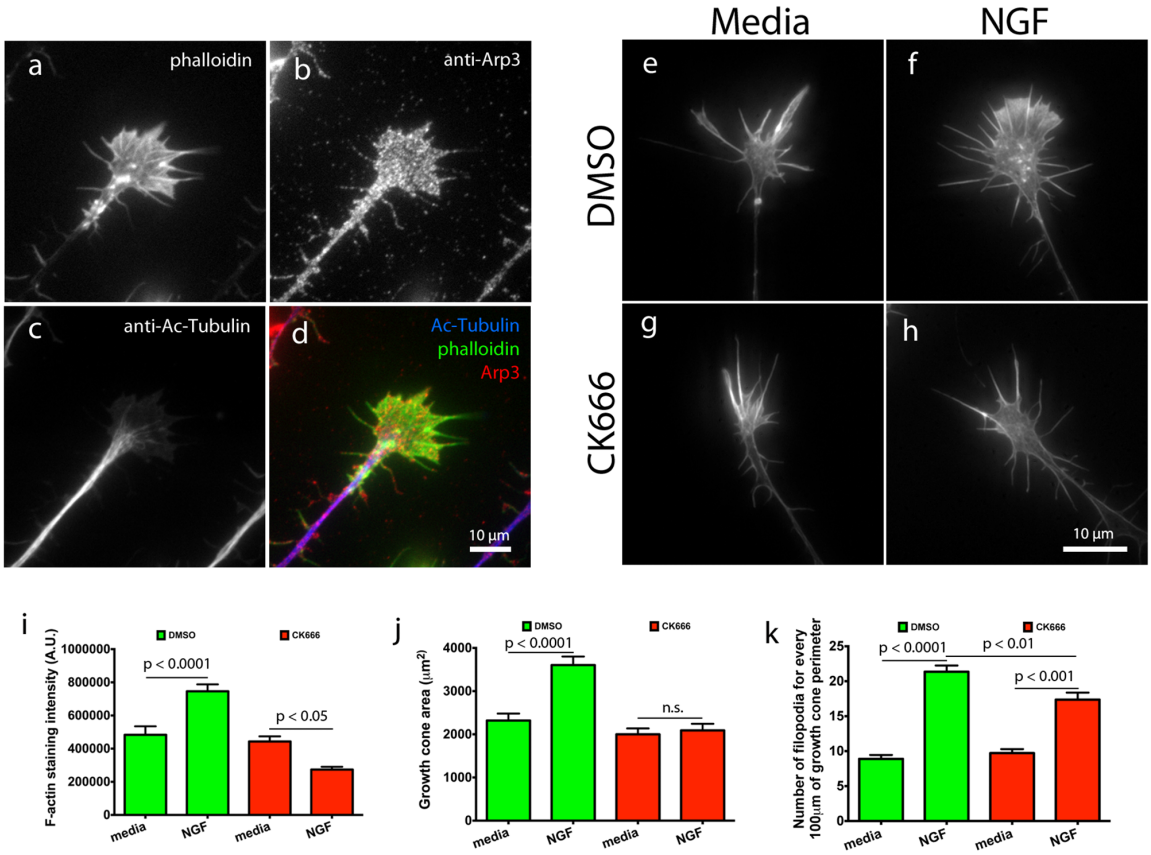
a
phalloidin
b
anti-Arp3
c
anti-Ac-Tubulin
d
Ac-Tubulin
phalloidin
Arp3
10 µm
Media
NGF
DMSO
CK666
e
f
g
h
10 µm
i
F-actin staining intensity (A.U.)
DMSO
CK666
p < 0.0001
p < 0.05
media
NGF
media
NGF
j
Growth cone area (µm²)
p < 0.0001
n.s.
k
Number of filopodia for every 100µm of growth cone perimeter
p < 0.0001
p < 0.01
p < 0.001

Figure 6. Arp2/3 mediates actin polymerization, surface area expansion, and increase in filopodium numbers in growth cones after NGF stimulation on laminin. **(a-d)** E7 DRG growth cones on laminin, treated with NGF, and stained with phalloidin and antibodies against Arp3 and acetylated α-tubulin (Ac-Tubulin). **(e-h)** E7 DRG growth cones on laminin treated with DMSO or CK666 for 4hrs, stimulated with NGF or media as control, fixed, stained with Alexa Fluor 488 phalloidin, **(i)** and phalloidin fluorescent intensity quantified. **(j)** Quantification of growth cone area. **(k)** Average number of filopodium for every 100μm of growth cone perimeter. Graphs show mean +/- standard error of the mean.

Figure 7:

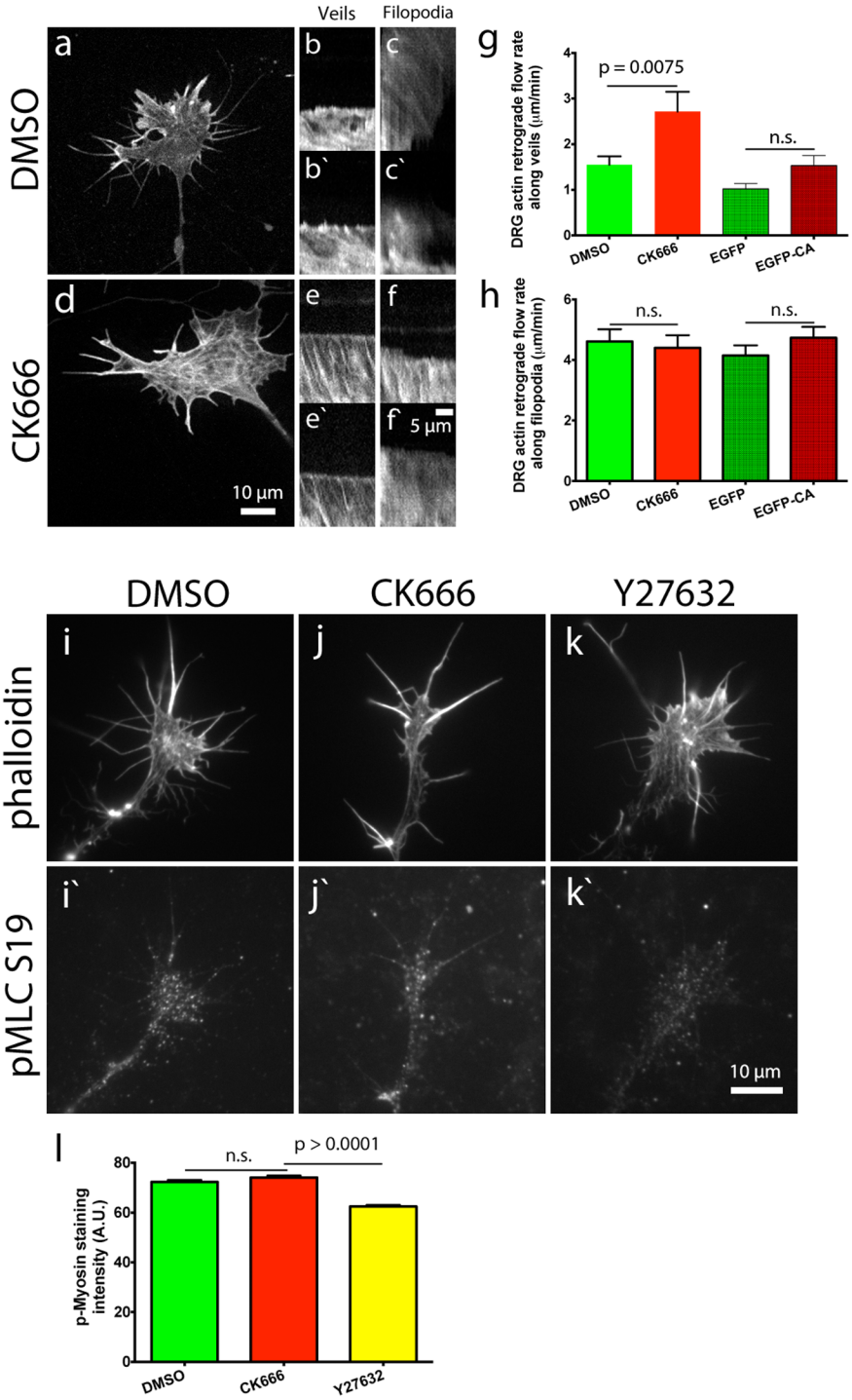
Veils
Filopodia
DMSO
CK666
a
b
c
b`
c`
d
e
f
e`
f`
5 µm
10 µm
g
DRG actin retrograde flow rate along veils (µm/min)
p = 0.0075
n.s.
DMSO
CK666
EGFP
EGFP-CA
h
DRG actin retrograde flow rate along filopodia (µm/min)
n.s.
n.s.
DMSO
CK666
EGFP
EGFP-CA
DMSO
CK666
Y27632
phalloidin
pMLC S19
i
j
k
i`
j`
k`
10 µm
l
p-Myosin staining intensity (A.U.)
n.s.
p > 0.0001
DMSO
CK666
Y27632

Figure 7. Arp2/3 inhibition increases the actin retrograde flow rate at the leading edge of growth cones on laminin in a myosin II-independent manner. **(a,d)** E7 DRG neurons were transfected with mCherry-actin and grown overnight on laminin. Arp2/3 was inhibited by co-expression of EGFP-CA with mCherry-actin, or by 50 μM CK666 treatment 4hrs prior to imaging. Growth cones were imaged in a spinning disc confocal and kymographs made from these time-lapse videos. **(b,b`,e,e`)** Representative kymographs along veils and **(c,c`,f,f`)** filopodia of DMSO- and CK666-treated growth cones. **(g-h)** Quantification of the actin retrograde flow rate along veils and filopodia. **(i-k`)** As a control, DRG growth cones on L1 were treated with DMSO, 50 μM CK666, or 10 μM Y27632 for 4hrs, fixed, and stained with phalloidin and an antibody against phospho myosin light chain (Ser19), **(l)** and anti-pMLC average fluorescent intensity quantified. Graphs show mean +/- standard error of the mean.

Figure 8:

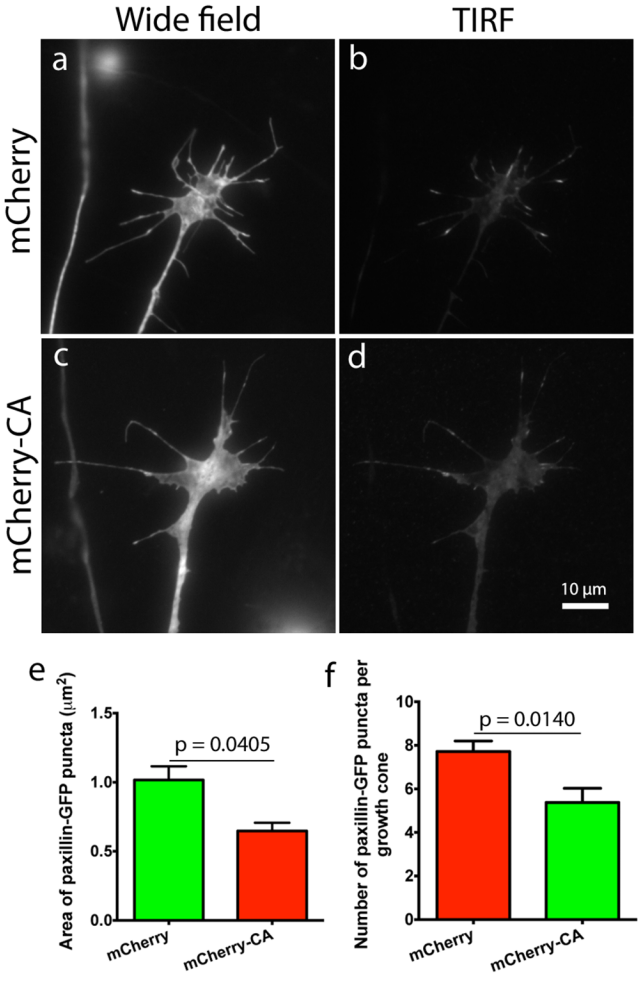
Wide field
TIRF
a
b
c
d
mCherry
mCherry-CA
10 µm
e
Area of paxillin-GFP puncta (µm²)
1.5
1.0
0.5
0.0
p = 0.0405
mCherry
mCherry-CA
f
Number of paxillin-GFP puncta per growth cone
10
8
6
4
2
0
p = 0.0140
mCherry
mCherry-CA

Figure 8. Arp2/3 inhibition reduces the area and number of paxillin-GFP puncta in growth cones on laminin. **(a-d)** E7 DRG neurons were transfected with paxillin-GFP and mCherry-CA, grown overnight on laminin, and imaged through wide field and TIRF microscopy. **(e-f)** Thresholded TIRF images were used to measure the area and number of paxillin-GFP puncta.

Figure 9:

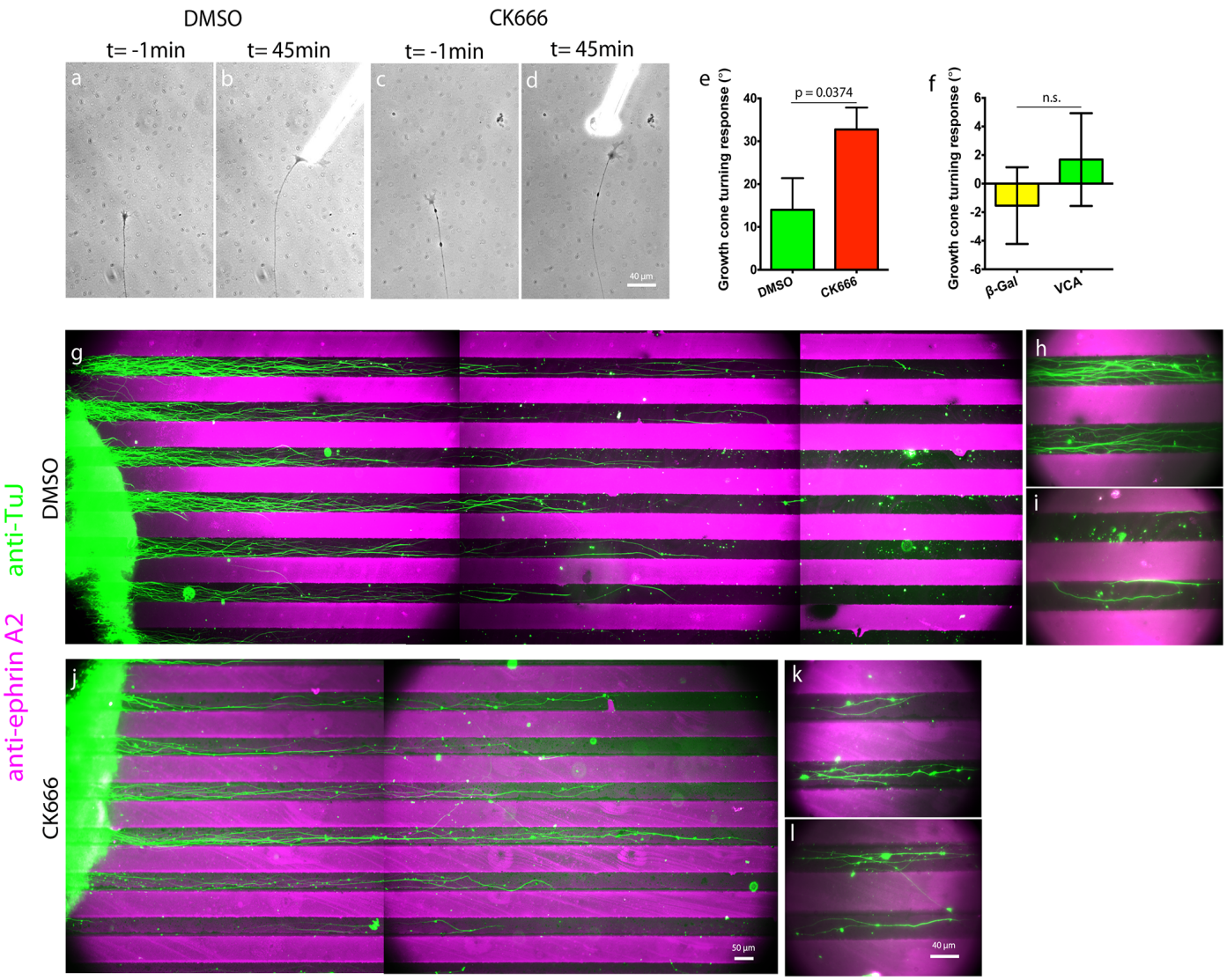
DMSO
CK666
t= -1min
t= 45min
t= -1min
t= 45min
a
b
c
d
40 µm
e
Growth cone turning response (°)
p = 0.0374
DMSO
CK666
f
Growth cone turning response (°)
n.s.
β-Gal
VCA
anti-TuJ
anti-ephrin A2
DMSO
CK666
g
h
i
j
k
l
50 µm
40 µm

Figure 9. Arp2/3 activity is not necessary for efficient guidance and insufficient to trigger growth cone turning on laminin. E7 DRG explants were grown on laminin and treated with DMSO or 50 μM CK666 4hrs prior to the turning assay. An NGF gradient was established with a micropipette located at 45° and approximately 80 μm from the growth cone leading edge. **(a-d)** Representative images of DRG growth cones 1 min before and 45 min after positioning the micropipette. **(e-f)** Growth cone turning angle quantification. **(g)** Growth cone turning angle quantification in response to a gradient of Chariot™ complexed to VCA-GST or β-Galactosidase as a control, delivered as above. **(h,k)** Boundary assay for control (DMSO) and Arp2/3-inhibited (CK666) retina explants (on the left) with alternating lanes of laminin (black) and ephrin A2 + laminin (magenta) with axons stained with antibodies against the neuronal β3-tubulin (green); **(i-j, l-m)** shows axons in close apposition to the ephrin A2 + laminin lanes at higher magnification.

Discussion

Here we investigated the role of Arp2/3 in growth cone leading edge protrusion, actin dynamics, and guidance. Furthermore, we examined how the substrate influenced these processes. We found that Arp2/3 inhibition reduced F-actin content, filopodium number, and axon length in DRG neurons regardless of the growing substrate. However, we found that Arp2/3 inhibition had substrate-dependent effects on the actin retrograde flow and growth cone guidance.

Similar to most reports on non-neuronal cells, we found Arp2/3 necessary for the NGF-induced growth cone leading edge protrusion on L1 (Fig. 2a-h). Interestingly, Arp2/3-inhibited veils would protrude in response to NGF but then collapse (Fig. 2g-h and 5d`), perhaps due to the reduced branch density in the actin network at the leading edge. It is possible that actin polymerization-mediated centrifugal leading edge expansion causes an increase in centripetal membrane tension that compresses the Arp2/3-inhibited actin network underneath it, thus leading to veil collapse (Craig et al., 2012) and explaining the actin filaments parallel to the leading edge during Arp2/3 inhibition, as described by Strasser et al. (2004). These results suggest that Arp2/3 is integral for the protrusion and stability of the leading edge on L1.

Consistent with Arp2/3 role in leading edge protrusion, we found subunits p34 and Arp3 at the leading edge through immunostaining (Fig. 1a-g). Moreover, during the barbed end assay most Rhodamine-actin incorporation occurred at the leading edge, colocalized with the distal tip of phalloidin staining, and was dependent on Arp2/3 function (Fig. 2j-n`). Thus, showing that Arp2/3-mediated actin polymerization promotes leading edge protrusion in growth cones on L1.

Arp2/3 inhibition reduced actin polymerization in growth cones regardless of the substrate, albeit incompletely (Fig. 3a-g and 6e-i). This suggests either: 1) incomplete inhibition of Arp2/3 and/or 2) there is also activation of other ABP's by NGF to promote barbed end creation and F-actin polymerization. Potential candidates are other actin nucleators like the formins, Ena/VASP proteins, and the F-actin severing protein ADF/cofilin (Marsick et al., 2010; Dent et al., 2011). Overall, this suggests that Arp2/3 is an important mediator of actin polymerization in growth cones on L1 and laminin.

In accordance with the convergent elongation model (Svitkina et al., 2003), Arp2/3 inhibition reduced filopodium numbers in growth cones on both substrates, but only during NGF stimulation (Fig. 3i and 6k). Thus, suggesting that actin branches created by Arp2/3 after NGF stimulation can mediate filopodium formation, regardless of growth cone substrate.

Interestingly, inhibition of the actin nucleator Arp2/3 led to differential changes in the rate of the actin retrograde flow. On L1, Arp2/3 inhibition reduced the rate of the actin retrograde flow along veils by 15-30%, which is likely due to the reduced number of barbed ends polymerizing actin at the leading edge. The idea is that the actin retrograde flow is influenced by the "pull" exerted by myosin II contractile activity along actin filaments, and by a "push back" from membrane tension, as polymerizing actin filaments expand the actin network and push against the leading edge (Henson et al., 1999; Medeiros et al., 2006; Craig et al., 2012). This model is supported by our experiments with Cytochalasin D (Fig. 4a-m), whereby inhibition of actin polymerization significantly reduced its retrograde flow. These results suggest that Arp2/3-dependent actin polymerization at the leading edge influences the rate of the actin retrograde flow.

In contrast to results on L1, Arp2/3 inhibition on laminin increased the actin retrograde flow along veils. Recently, Yang et al (2012) reported similar findings and concluded that the branched actin network assembled by Arp2/3 can restrict the myosin II-dependent component of the actin retrograde flow. This suggests that during myosin II contractility a higher branch density in the actin network can slow its retrograde flow, presumably due to increased interactions with other cytoskeletal components like microtubules, other actin structures, or adhesions. As an alternative and complementary explanation for the increased actin retrograde flow, we found that Arp2/3 inhibition led to a reduction in the area and total number of paxillin-GFP puncta per growth cones of 40% and a 20%, respectively (Fig. 8a-f). Therefore, Arp2/3-inhibited growth cones on laminin were less effective in engaging the "clutch" to slow the flow of actin filaments, leading to an increased retrograde flow rate. Notably, Arp2/3 inhibition in fibroblasts did not change adhesion size, only their organization relative to the leading edge (Wu et al., 2012). This discrepancy can be explained by the different in cell type, substrate, and adhesions studied, since growth cone adhesions are round and small, versus the long linear focal adhesions seen in non-neuronal cells.

Why are adhesions smaller after Arp2/3 inhibition? It is known that Arp2/3 is recruited to nascent integrin adhesions (DeMali et al., 2002; Serrels et al., 2007) and that the actin retrograde flow can transfer myosin II-generated tension to promote adhesion growth and maturation (Galbraith et al., 2002; Choi et al., 2008; Wolfenson et al., 2011). Consequently, we propose that Arp2/3 inhibition reduces the chance for adhesions to interact with the overhead actin network because of its reduced branch density, in turn, leading to reduced tension on adhesions by the retrograde flow, which could reduce their

maturation and/or stability. In agreement, Woo and Gomez (2006) showed that ROCK inhibition, a direct regulator of myosin II activity and actin retrograde flow, led to smaller and less stable growth cone adhesions on laminin.

Consistent with reports that actin polymerization is critical for guidance (Lanier et al., 1999; Marsick et al., 2010), growth cones exhibited reduced turning responses to chemoattractants (NGF or Netrin), and defective chemorepulsive responses (substrate-bound ephrin A2) on L1 during Arp2/3 inhibition. The reduced leading edge protrusion and the veil collapse during Arp2/3 inhibition would hamper growth cone turning towards an attractant. Similarly, on a striped ephrin-A2 substrate reduced protrusion at the growth cone side away from ephrin-A2 would cause defective evasion of ephrin-A2. Additionally, we also showed that unilateral Arp2/3 activation with Chariot™+VCA-GST was sufficient to trigger growth cone turning on L1. These results serve to highlight the central role the actin nucleator Arp2/3 plays during growth cone guidance on L1.

Nevertheless, performing the same attractive guidance assay on laminin during Arp2/3 inhibition caused no deficits. On the contrary, Arp2/3 inhibition led to an increased turning response during chemoattraction towards NGF. We can speculate as to why these growth cones have a larger turning response. We know Arp2/3-inhibited growth cones on laminin have less and smaller adhesions, which would allow for faster dismantling and, hence, substrate detachment on the side opposite to the chemoattractant. Thus, allowing growth cones to steer and follow the chemoattractant gradient more readily than controls. Alternatively, their larger turning response could result from the faster retrograde flow of actin. Neurotrophins increase the number of integrin adhesions in growth cones (Carlstrom et al., 2011), therefore NGF stimulation during turning could

trigger the strengthening or formation of new adhesions closer to its source. In turn, these adhesions could harness the faster actin retrograde flow and convert it into a greater turning response. Ultimately, even though Arp2/3 was inhibited, other actin nucleators like the formins and generation of barbed ends by ADF/cofilin severing activity could coordinate actin polymerization to steer growth cones towards the NGF source.

Similarly, Arp2/3 inhibition caused no defect on RGC growth cones response to avoid the ephrin A2 + laminin lanes on the boundary assay. Once again, other actin nucleators may be orchestrating actin filament polymerization to steer growth cones away from the ephrin A2 + laminin lanes. Alternatively, growth cones could steer away from the ephrin A2 + laminin lanes because of the reduced adhesivity they offer. It was shown that chemorepellent cues can dismantle integrin adhesions (Hines et al., 2010); therefore, on the boundary assay growth cones could remain on the laminin lanes because of their increased adhesivity, compared to the ephrin A2 + laminin ones. Also, supplementary to these results, we showed that delivery of the Chariot™+VCA-GST complex, to unilaterally activate Arp2/3 on one side of the growth cone, failed to trigger turning on laminin. Therefore, we conclude that Arp2/3 is dispensable for an attractive guidance response to a soluble chemoattractant and for a repulsive guidance response to a membrane-bound chemorepellent, when growth cones migrate on laminin.

In conclusion, during development growth cones migrate in association with diverse substrates and respond to different guidance cues. In doing so, diverse signaling pathways are activated to regulate different ABP's to organize actin structures and modulate their dynamics to ensure that growth cones reach their targets. We probed the role of the actin nucleator Arp2/3 during growth cone motility and found it crucial for

guidance on L1, but not on laminin. Previous studies have also shown the diversity of actin regulatory mechanisms in neuronal motility on different substrates. For example, Arp2/3-dependent actin structures were necessary for exocytosis and neuritogenesis on laminin, but not on PDL, where exocytosis and neuritogenesis relied on Ena/VASP-dependent actin structures (Gupton and Gertler, 2010). In addition, ENA/VASP null neurons cannot form neurites on PDL, but on laminin neurite formation by ENA/VASP null neurons is normal (Dent et al., 2007).

Chapter III: Ezrin/radixin/moesin family proteins mediate actin filament dynamics in attractive growth cone guidance to nerve growth factor

This chapter was modified from the original paper published by:

Bonnie M. Marsick, Jose E San Miguel-Ruiz, and Paul C. Letourneau

Ezrin/radixin/moesin family proteins mediate actin filament dynamics in attractive growth cone guidance to nerve growth factor

Journal of Neuroscience (2012), 32:282-296

*Jose E San Miguel-Ruiz contributed directly to the following figures: Figure 2 (A-C).

Introduction

Proper synaptic development depends on pathfinding by axonal growth cones (Mitchison and Kirschner, 1988; Letourneau and Cypher, 1991; Serafini et al., 1996; Lowery and Van Vactor, 2009; Kolodkin and Tessier-Lavigne, 2011). Growth cones detect extrinsic cues and respond by actin filament reorganization that drives growth cone motility (Serafini et al., 1996; Huber et al., 2003; Gallo and Letourneau, 2004; Kalil and Dent, 2005; Geraldo and Gordon-Weeks, 2009; Lowery and Van Vactor, 2009). Turning toward attractants involves leading edge protrusion toward the attractant (Lin and Forscher, 1993; Kalil and Dent, 2005). Previously, we reported that the attractant nerve growth factor (NGF) induces actin polymerization in growth cone regions closer to the attractant (Marsick et al., 2010). Activation of the actin-severing protein ADF/cofilin mediates this stimulated polymerization; yet it is unknown how these new actin filaments interact with the membrane to drive protrusion.

Few actin-regulatory proteins have well-characterized roles in axon guidance (Tanaka et al., 1995; Pak et al., 2008; Lowery and Van Vactor, 2009). The conserved ezrin/radixin/moesin (ERM) proteins often organize membrane-cytoskeletal interactions (Amieva and Furthmayr, 1995; Matsui et al., 1999; Bretscher et al., 2002; Niggli and Rossy, 2008). ERMs share a C-terminal actin-binding domain and an N-terminal FERM domain that binds membrane proteins, such as CD44, ICAM1, L1 cell adhesion molecule, and dystrophin (Bretscher et al., 2002; McClatchey and Fehon, 2009). ERMs also act as scaffolding for adaptor and signaling molecules. ERM activity is conformationally regulated. Phosphorylation of a conserved threonine residue disrupts an N-C termini interaction to allow ERMs to link F-actin and membranes (Tsukita et al., 1997;

Pietromonaco et al., 1998; Hayashi et al., 1999). Thus, ERM proteins are key components in organizing membranes, cytoskeletal-membrane interactions and cell signaling.

ERM proteins are expressed in growth cones and may mediate actin-membrane interactions (Paglini et al., 1998; Castelo and Jay, 1999; Niggli and Rossy, 2008) ERMs bind L1, an important axonal adhesion receptor (Dickson, 2002; Mintz et al., 2003; Cheng et al., 2005; Tang et al., 2007; Sakurai et al., 2008). Growth cone repulsion by Semaphorin 3A may involve ERM inactivation (Gallo, 2008; Mintz et al., 2008), and studies showing ERM activation downstream of NGF in PC12 cells make ERMs good candidates for mediating growth cone responses to NGF (Amieva and Furthmayr, 1995; Gonzalez-Agosti and Solomon, 1996; Jeon et al., 2010). Thus, ERMs could facilitate axon guidance by regulating F-actin organization and the distribution of membrane proteins.

We report here that gradients of attractive cues NGF and NT3 locally activate ERM proteins in growth cones of chick sensory neurons. Activated ERMs co-localize at the leading edge with L1, ADF/cofilin and F-actin barbed ends. When ERM protein levels are reduced, or ERM function is disrupted by a dominant negative construct (DN-ERM), neurite length and growth cone F-actin levels are reduced. Moreover, DN-ERM blocks NGF-induced increases in F-actin and filopodial adhesion receptors, as well as turning toward NGF. Directly increasing ADF/cofilin activity increases phospho-ERM levels and knockdown of the ERM binding partner L1, conversely, reduces filopodial phospho-ERM. These results provide insights into the role of ERM proteins in organizing actin filaments and adhesion receptors to promote leading edge protrusion and chemoattractive responses.

Methods

Materials

F-12 medium, B27 additives, laminin, poly-D-lysine (MW >300,000), Alexa Fluor 488 DNase1, Alexa Fluor 488- and 568–phalloidin, Alexa Fluor 488 and 568 secondary antibodies were purchased from Invitrogen. NGF, NT3, L1 and N-cadherin were purchased from R & D Systems. LY-294002 was purchased from Cell Signaling. Chariot was purchased from Active Motif. White Leghorn fertilized chicken eggs were purchased from Hy-Line North America, LLC. All other drugs and reagents were purchased from Sigma-Aldrich, unless otherwise indicated.

Neuronal culture

Glass coverslips (Gold Seal) were coated with 100ug/ml poly-D-lysine, rinsed three times with water, dried, coated with 5% nitrocellulose dissolved in 100% amyl acetate (Fischer Scientific), dried, and coated overnight with 20µg/ml laminin or 4µg/ml L1 in phosphate buffered solution (PBS; Roche). Video dishes were made by gluing (silicone aquarium sealant) a coverslip (18 mm x 18 mm; Gold Seal) over a hole (5mm) in the bottom of a culture dish (Falcon 35 mm x 10 mm), allowed to dry, rinsed with water, and coated as described. Embryonic day 7 (E7) dorsal root ganglia (DRG) were removed from chick embryos of either sex, according to procedures approved by the University of Minnesota Institutional Animal Care and Use Committee. Neural tissues were cultured on experimental substrates in F-12 with added B27, glutamine, sodium pyruvate and glucose, and buffered to pH 7.4 with 10 mM HEPES. For low calcium media, a 1:1 solution was made of F-12 and calcium-free Hank's balanced salt solution, with added B27, glutamine,

sodium pyruvate and glucose. For the high calcium condition, calcium chloride was added to 1.0 mM to this medium. Neural tissues were cultured overnight or 48 hrs in a humidified incubator at 37°C.

Neuronal transfection

DRGs were dissociated as described in Roche et al. (2009). Approximately 2 x 10^6 cells were transfected with one of the following: 1 μg of plasmid expressing GFP, 1 μg of a plasmid encoding GFP tagged to the N-terminus of ezrin (DN-ERM; a generous gift from Dr. Janis Burkhardt, University of Pennsylvania, Philadelphia PA), 0.5 ug of GFP combined with siRNA against chick radixin (10 nM) and moesin (10 nM), or 2 ug constitutively-active LIMK (CA-LIMK; a generous gift from Dr. James R. Bamburg, Colorado State University, Fort Collins, CO) mixed with 1 ug GFP plasmid using the G-13 program of the Lonza Nucleofector, and the chicken neuron Nucleofector reagents. To assess retrograde actin flow, or for barbed end or active ADF labeling studies, 2 μg GFP or DN-ERM were combined with 0.5 μg plasmids for RFP- or GFP-actin (a kind gift of James R. Bamburg, Colorado State University, Fort Collins, CO). Morpholinos against chick L1 and control morpholinos were purchased from Gene Tools; sequence and transfection protocol were described in Blackmore and Letourneau (2006a). Short interfering RNA (siRNA) oligos were purchased from invitrogen and sequences were as follows; chick radixin antisense: 5'-ACGUUGAUUGGUUUCGGCA; chick moesin antisense: 5'-ACGCUGAUCGUUUUCGGCA; scrambled control: 5'-UCCUGGAUCUUAGUGCGUU. Transfected cells were cultured 24 or 48 h, as indicated.

Immunocytochemistry

Neuronal cultures were fixed and blocked as described in (Roche et al., 2009)). Coverslips were incubated with primary antibodies diluted in PBS containing 10% goat serum overnight at 4º C. Affinity purified antibody 12977 (ADF) was used at 1:200 dilution and antibody 4321 (phospho-ADF/cofilin) was used at 1:1000 (generous gifts of Dr. James R. Bamburg, Colorado State University, Fort Collins, CO), ERM antibodies against ezrin, moesin, phospho-ERM and pan-ERM (Cell Signaling Technology) were used at 1:100, 13H9 (pan-ERM; a generous gift from Lorene Lanier, University of Minnesota, Minneapolis, MN) was used at 1:1000, antibody specific for radixin (R3653; Sigma-Aldrich) was used at 1:100, polyclonal antibody specific for radixin (457-3; a generous gift of Frank Solomon, Massachusetts Institute of Technology, Cambridge, MA) was used at 1:200, anti-β1 integrin (W1B10; Sigma-Aldrich) was used at 1:100, monoclonal anti-chick-L1 (8D9; Developmental Studies Hybridoma Bank, University of Iowa, Iowa City, IA) was used at 10μg/ml, anti-N-cadherin (ab12221; Abcam) was used at 1:100, polyclonal anti-chick-TrkA (ab22267; a kind gift from Dr. Frances Lefcort, Montana State University, Bozeman, MT), and anti-P-Akt (Cell Signaling Technology) was used at 1:50. Coverslips were then rinsed 3 times in PBS and incubated in PBS rinse for 1 h. For labeling F-actin, Alexa Fluor 568–phalloidin was applied at a 1:20 dilution, and mixed with secondary antibodies: Alexa Fluor 568 goat anti-rabbit or anti-mouse antibodies at 1:1000 dilution in PBS with 10% goat serum for 1 h. For labeling G-actin, 5 μg/ml Alexa Fluor 488 DNase1 in PBS was applied to coverslips for 1 h. For staining total active ADF, media was removed and cultures were incubated 1 min in

permeabilization buffer (described below) with 100 nM phalloidin, then fixed and stained. After rinsing 3 times in PBS, coverslips were mounted in *SlowFade* reagent (Invitrogen).

Time lapse microscopy

A Spot digital camera mounted on an Olympus XC-70 inverted microscope, and MetaMorph software (Molecular Devices) were used for all image acquisitions. In any one experiment, all images were acquired in one session. For repeat experiments, data were normalized to controls. For collection of fluorescent images, exposure time and gain settings on the digital camera were kept constant, and image acquisition and analysis was performed as described in Roche et al. (2009).

For experiments measuring growth cone fluorescence intensity values, a line tool in MetaMorph was used to outline the terminal 25 μm of each distal axon and growth cone, and background intensity value was subtracted from the fluorescence intensity value of the accompanying neuronal measurement. For phospho-ERM and L1 filopodial intensity measurements, growth cones were selected at random from phalloidin images and a line was drawn on each filopodium using the line tool; lines were then transferred to the corresponding phospho-ERM or L1 image and background-subtracted intensity values were recorded. To measure the intensity of β-integrin at filopodial tips, phalloidin images were used to draw a 20x20 pixel box at the tip of each filopodia. Box regions were then transferred to the corresponding integrin image and background-subtracted intensity values were recorded.

Central and peripheral region quantifications of active ADF/cofilin and barbed labeling were performed by hand-tracing GFP-actin images in Metamorph. A straight line

was then drawn across the growth cone width in at least 3 locations and the distance 25% from either side of the growth cone edge was noted and used to trace a central growth cone region. Regions were then transferred to the ADF/cofilin or rhodamine-actin image, where total and central growth cone intensities were measured. Peripheral growth cone intensities were later calculated by subtracting the central intensity from the total for each growth cone.

Proximal/distal filopodial intensity measurements in gradients were performed as follows. Growth cones were subjected to a gradient of BSA, NGF, NT3, chariot, or chariot + A3 and were imaged, fixed, and process for immunochemistry. In MetaMorph, a line along the neurite axis was extended forward to divide the growth cone in two. A line was drawn on each filopodium toward the cue source (proximal) and away from the cue source (distal), and the background-subtracted intensity values were measured. For each growth cone, the filopodia intensity values were averaged for each half, and used to calculate the proximal/distal ratio, as described in Marsick et al. (2010).

Retrograde flow measurements

To determine retrograde actin flow rates, DRGs were co-transfected to express RFP-actin and either GFP or DN-ERM, and cultured overnight with NGF. Co-transfected growth cones were identified, and RFP-actin was imaged every 3 s for 6 min. Kymographs were generated for the distal 10 μm of growth cones, and flow rates were measured by tracking bright RFP-actin features, which are formed by unequal incorporation of RFP- and non-RFP-actin monomers into polymerized filaments at the leading edge. Measuring retrograde flow using the movement of these features has been described previously

(Marsick et al., 2010), including a demonstrated sensitivity of this retrograde flow to the myosin-II inhibitior blebbistatin (Chan and Odde, 2008).

Pharmacological Inhibitors

Trk inhibitor K252a (500 nM), PI3K inhibitor LY-294002 (10 μM), PLC inhibitor U73122 (1 μM), or PKC inhibitor chelerythrine (1 μM) were added to cultures for 15 min prior to media or NGF addition. Controls were treated with the same volume of DMSO vehicle, which never exceeded 5 μl/ml.

Barbed end labeling

This protocol was adapted from Chan et al. (Chan et al., 1998) and is described in Marsick et al. (2009). For co-labeling with active ADF, cells were permeabilized and processed for barbed end labeling, fixed, then stained for total ADF (12977). For co-labeling with phospho-ERM, 0.1% glutaraldehyde and 0.1% paraformaldehyde was added to permeabilization buffer. Following Rh-actin labeling, cells were further fixed 30 min and stained for phospho-ERM.

Recombinant proteins and protein loading

Recombinant XAC proteins were generated as described previously (Gehler et al., 2004). Proteins were delivered into cells using Chariot reagent (Active Motif; Morris et al., 2001), according to the manufacture's instructions. Briefly, 6 μl Chariot was complexed with 1 μg XACA3 for 1 h, then added to the culture medium or immobilized onto a nitrocellulose-coated micropipette.

Growth cone turning assay

Turning was assessed as described previously (Roche et al., 2009; Marsick et al., 2010). Briefly, micropipette tips were dipped in a 1% nitrocellulose solution, dried, then dipped several times in a PBS solution of 1 µg/ml NGF or 1 ng/ml NT3. A growth cone was imaged at 30 or 60 s intervals for 15 min. The micropipette tip was then positioned 100 µm (NGF) or 50µm (NT3) from a growth cone at a 45° angle to the direction of axon elongation. Images were acquired for 60 min after introducing the micropipette tip. Growth cone turning angles were determined as the change in direction of growth cone migration between the beginning and end of the image acquisition period (Ming et al., 1997).

Results

Growth cone ERM proteins are activated by NGF

Similar to previous reports, we found that ERM proteins are expressed in chick embryo DRG growth cones. Antibodies that recognize all three ERM proteins (pan-ERM, 13H9) stained growth cones strongly and co-distributed in the peripheral domain (P-domain) with phalloidin labeled F-actin (Fig. 1A). Using antibodies specific to individual ERM proteins, we found strong radixin staining in the P-domain, similar to pan-ERM staining, whereas staining for ezrin and moesin was strongest in the growth cone C-domain and neurite shaft (Fig. 1A). These immunostaining data suggest that radixin is the predominant ERM protein present in the DRG growth cone leading margin and peripheral domain, consistent with previous reports (Castelo and Jay, 1999).

ERM activation can be immunologically assessed with an antibody specific to threonine-phosphorylated ERM proteins in their active conformation (phospho-ERM). Using this antibody, we found that acute addition of 40ng/ml NGF increases levels of active ERM proteins, most predominantly in growth cone lamellipodia and filopodia (Fig. 1B). Experiments with timed NGF exposures demonstrate that active ERM levels increase rapidly following NGF addition, and are then reduced and restored upon NGF removal and re-addition, respectively (Fig. 1B).

To assess ERM distribution in a model of axon guidance, a diffusible gradient of NGF was generated by placing an NGF-coated pipette tip near a growth cone for 5 min ((Marsick et al., 2010), then cells were fixed and stained for phospho-ERM. This resulted in elevated phospho-ERM in the growth cone regions closer to the NGF source, while no such asymmetry occurred in growth cones subjected to a gradient of BSA (Fig. 1C). These results indicate that acute NGF treatment increases active ERM levels in both a local and a global manner.

We next investigated the signaling that mediates NGF-induced ERM phosphorylation in DRG growth cones by using inhibitors of trkA activation and several downstream effectors. Previous studies have identified numerous kinases upstream of ERM phosphorylation, including molecules activated by neurotrophins or other growth factors (Gautreau et al., 1999; Matsui et al., 1999; Bretscher et al., 2002; Baumgartner et al., 2006; Gallo, 2008; Jeon et al., 2010; Antoine-Bertrand et al., 2011). DRG cultures were treated 15 min with 500 nM k252a (trkA), 10 μM LY294002 (PI3 kinase), 1 μM U73122 (PLC) or 1 μM chelerythrine (PKC) before the global addition of control media or 40 ng/ml NGF for 10 min. The trk inhibitor k252a completely blocked ERM

phosphorylation in response to NGF addition, while Inhibiting PI3K, PLC or PKC individually prior to NGF treatment lowered baseline phospho-ERM levels and resulted in lower phospho-ERM levels after NGF-addition, compared to DMSO+NGF (Fig. 1D). However, only the trkA inhibitor completely block the NGF-induced increase in phospho-ERM, and the other inhibitors significantly, but partially reduced the size of the NGF-induced increase in ERM phosphorylation (Fig. 1D). In agreement with previous studies, these data suggest multiple signaling pathways can simultaneously regulate phospho-ERM levels (Yonemura et al., 2002; Jeon et al., 2010; Antoine-Bertrand et al., 2011).

Neurotrophin-3 activates ERM proteins and induces attractive turning.

We next investigated if ERM activity is regulated by another attractive guidance cue. Neurotrophin-3 (NT3) attracts developing proprioceptive and trigeminal axons to their target tissues (O'Connor and Tessier-Lavigne, 1999; Genc et al., 2004) and facilitates the regeneration of adult sensory neurons (Ramer et al., 2000; 2002; Alto et al., 2009). Similar to NGF, we found that treatment of DRG explants for 15min with 50 ng/ml NT3 increased filopodial phospho-ERM levels (Fig. 2A). Exposure to a localized source of NT3 diffusing from a micropipette increased proximal phospho-ERM levels (Fig. 2B) and induced attractive growth cone turning (Fig. 2C). Acute NT3 treatment also increased the levels of growth cone F-actin and active (de-phosphorylated) ADF/cofilin (Fig. 2A). These data suggest that local activation of ADF/cofilin and ERM proteins mediate attractive growth cone turning to multiple guidance cues.

NGF treatment co-localizes phospho-ERM, ADF/cofilin and F-actin barbed ends at the leading edge and increases filopodial L1 and ß-1integrin expression

We previously reported that activation of ADF/cofilin mediates NGF-stimulated actin polymerization and growth cone turning towards an NGF source (Marsick et al., 2010). Here, we visualized the distribution of activated ERM in relation to ADF/cofilin and F-actin free barbed ends. As shown in Figure 3A, phospho-ERM co-distributes with active ADF/cofilin and rhodamine-labeled F-actin barbed ends at the leading edge of NGF-treated growth cones. Thus, active ERM proteins are appropriately localized so as to link new actin polymer to the growth cone leading margin and facilitate protrusion.

Adhesive contacts enable axon growth and guidance by stabilizing protrusions, providing traction for pulling forward, and influencing intracellular signaling. Three adhesion molecules important in axon growth and guidance are L1, N-cadherin and ß-integrin dimers (Neugebauer et al., 1988; Agius et al., 1996; McKerracher et al., 1996; Cheng and Lemmon, 2004; Kiryushko et al., 2004; Chen et al., 2005; Blackmore and Letourneau, 2006). Previous studies report that NGF treatment stimulates the accumulation of ß-integrin receptors at filopodial tips (Grabham and Goldberg, 1997; Grabham et al., 2000), which we also observed in our NGF-treated DRG growth cones (Fig. 3B, E). We also report for the first time that L1 expression along filopodial shafts was significantly higher after NGF treatment (Fig. 3C, E). Interestingly, this L1 accumulation co-localized with phospho-ERM, whereas ß1-integrin accumulation at filopodial tips was distal to phospho-ERM. Growth cone N-cadherin distribution was unchanged after NGF treatment, suggesting these changes in ß1-integrin and L1 distribution are selective (Fig. 3D, E).

In Marsick et al. (2010) we showed that a gradient of NGF locally increases F-actin, free barbed ends, ADF/cofilin activity, and here, phospho-ERM (Fig. 1C). Similarly, filopodial accumulations of ß1-integrin receptors and L1 were also greater in growth cone regions proximal to an NGF source (Fig. 3F), with no such asymmetry in gradients of BSA. Thus, an NGF gradient rapidly increases actin polymerization, active ERM proteins and adhesion receptors in the protruding growth cone region closer to the NGF source. With their dual binding functions ERM proteins may play a key role in harnessing both newly polymerized actin filaments and adhesion molecules to effectively protrude the leading margin and lead the growth cone toward the NGF source.

Disrupting ERM function disrupts growth cone F-actin and motility

To evaluate the function of ERM proteins in DRG growth cone migration and their responses to NGF, two approaches were used. We transfected DRG neurons to express a dominant-negative ezrin (DN-ERM) mutant comprised of the membrane-binding FERM domain fused with GFP, which competes with endogenous ERM proteins and prevents actin-membrane linkage (a kind gift from Dr. Janis Burkhardt; described in (Allenspach et al., 2001). Alternatively, we transfected DRG neurons to express a mixture of siRNA against radixin and moesin. Knockdown of radixin and moesin protein levels by siRNA was confirmed by Western blot (Fig. 4A) and immunocytochemistry (Fig. 4B,C).

To assess how disrupting ERM function affects growth cone actin organization, we used confocal microscopy to visualize phalloidin labeled F-actin. In GFP controls, F-actin is organized in peripheral filopodial bundles and lamellipodial structures and is less

prevalent in the C-domain where filaments are disassembled (Fig. 4D,E). In contrast, DN-ERM expressing growth cones exhibited less F-actin in the P-domain, with F-actin tangles more centrally located (Fig. 4D,E). This might occur because without ERM-mediated linkage to plasma membrane proteins, F-actin is more readily transported retrogradely from the P-domain into the C-domain. We probed this possibility by co-transfecting neurons to express DN-ERM-GFP or control GFP, as well as RFP-actin (Chan and Odde, 2008; Marsick et al., 2010). By tracking movement of bright red actin features, we found increased retrograde flow of F-actin at the leading margin of DN-ERM expressing growth cones compared to control GFP (Fig. 4F). Here, reduced ERM-mediated membrane linkage may facilitate retrograde F-actin flow, disrupting F-actin organization in the peripheral domain. In support of this we found lower growth cone F-actin levels (Fig. 4G) and fewer filopodia (Fig. 4H) in DN-ERM growth cones, suggesting that ERM-mediated linkage of actin to membrane proteins supports the establishment and/or maintenance of the F-actin network in the motile periphery.

To examine the effects of disrupted ERM function on motility, we used time-lapse imaging to assess the rate of growth cone advance. Compared to GFP expressing controls, DN-ERM growth cones advanced more slowly (Fig. 4J) and not surprisingly, axons of DN-ERM-expressing neurons were shorter than GFP controls after 48 hours in vitro (Fig. 4I). Together these data suggest that ERM proteins are important for the establishment and/or maintenance of actin filament organization in the growth cone leading margin.

Disrupting of ERM function impairs DRG responses to NGF

We next asked how growth cone responses to NGF are affected when ERM proteins are disrupted. Imaging was conducted for 60 min after introduction of the pipette to allow enough time for slower-moving DN-ERM and siRNA-expressing growth cones to advance at least 80 μm and execute a turning response. In both cases of reduced ERM function, siRNA treatment or DN-ERM expression, the turning of DRG growth cones toward a micropipette releasing NGF was significantly reduced compared to GFP expressing controls (Fig. 5A).

We previously showed that acute NGF exposure increases growth cone F-actin and decreases G-actin levels (Marsick et al., 2010), so we examined the effects of ERM inhibition on NGF-stimulated actin polymerization. When NGF was added globally to DRG neurons, the increase in total F-actin seen in control GFP-expressing neurons was absent in DN-ERM-expressing growth cones (Fig. 5B).

Because the NGF-induced increase in F-actin is mediated by ADF/cofilin activation, we wondered if this effect of DN-ERM expression on F-actin levels was due to a lack of ADF/cofilin activation. However, NGF-induced activation of ADF/cofilin, as indicated by reduced staining for the inactive phospho-ADF/cofilin (pAC), was still observed in DN-ERM expressing growth cones (Fig. 5C). Similarly, when ADF/cofilin activity in growth cones was directly increased by Chariot™-mediated incorporation of constitutively-active ADF/cofilin (Gehler et al., 2004; Marsick et al., 2010), DN-ERM-expressing growth cones did not exhibit the expected F-actin increase (Fig. 5D). Thus, the increased ADF/cofilin activity that normally triggers actin polymerization at the growth cone leading margin may be ineffective without ERM function to harness actin

filaments at the leading edge.

The NGF-induced increase in ADF/cofilin activity in DN-ERM growth cones (Fig. 5C) suggests that impaired ERM function does not block NGF signaling. To more directly probe this, we stained GFP and DN-ERM growth cones with an antibody against the high-affinity NGF receptor TrkA. DN-ERM growth cones did express TrkA, though with lower levels compared to control GFP growth cones (Fig. 5E). We therefore sought to assess if this reduced level of TrkA expression impaired DN-ERM expressing growth cones' ability to detect NGF and activate downstream signaling. We thus used an antibody against phospho-Akt, an activated downstream target of NGF signaling (Crowder and Freeman, 1998). As expected, NGF exposure increased phospho-Akt levels in GFP-expressing growth cones (Fig. 5F). Inhibition of PI3K (LY-294002), which has been implicated in ERM activation (Gautreau et al., 1999; Gallo, 2008; Jeon et al., 2010) and lies upstream of TrkA-mediated Akt activation, blocks this increase (Fig 5F). However, DN-ERM-expressing growth cones also had significantly increased levels of phospho-Akt following NGF (Fig. 5F), suggesting that disrupting ERM function does not interfere with NGF detection and signaling.

Thus, impaired ERM function blocks the NGF-induced increase in actin polymerization, despite evidence that TrkA-mediated signaling occurs and ADF/cofilin is activated. Even a direct increase in ADF/cofilin activity, independently of NGF signaling, failed to increase F-actin in DN-ERM-expressing growth cones (Fig. 5D). These data suggest that ERM-mediated F-actin-membrane linkage is required for increased ADF/cofilin activity to trigger actin polymerization at the leading margin.

Disruption of ERM function disrupts NGF-induced increase in active ADF/cofilin, F-actin barbed ends and adhesion proteins at the leading growth cone margin

Thus far, we have found NGF does not increase F-actin levels in DN-ERM expressing growth cones, despite ADF/cofilin activation. To further explore the effects of disrupting ERM function, we visualized the distribution of active ADF/cofilin and F-actin barbed ends in NGF-stimulated growth cones. To enable identification of transfected cells following the permeabilization step of barbed-end labeling, we co-transfected neurons to express GFP or DN-ERM and GFP-actin, which incorporates into detergent-resistant actin filaments. Following acute NGF treatment, active ADF/cofilin normally localizes to the growth cone leading margin, where it severs filaments to create free F-actin barbed ends (Fig. 3A, 6A; (Marsick et al., 2010). However, as shown in Figure 6A, active ADF/cofilin is more centrally located in DN-ERM expressing growth cones.

We then probed whether NGF-induced free barbed ends are also displaced when ERM function is disrupted. In growth cones transfected with GFP-actin and control GFP, most rhodamine-actin was incorporated at the leading margin, consistent with the localization of ADF/cofilin (Fig. 6B,C). However, in growth cones that also expressed DN-ERM, more rhodamine-actin was incorporated centrally and away from the leading margin, where the active ADF/cofilin was also mis-localized in the NGF treated DN-ERM expressing growth cones (Fig. 6B,C).

Together, these experiments suggest that ERM proteins play a critical role in attractive responses to growth cone guidance cues. When ERM function is reduced, F-actin is not organized into the typical peripheral bundles and networks. Rather, lamellipodia are absent, and more F-actin is centrally concentrated, perhaps because

retrograde actin flow is enhanced without ERM-mediated F-actin linkage to the plasma membrane (Fig. 4F). Upon NGF treatment, total F-actin content is not increased, although ADF/cofilin activity and F-actin barbed ends are increased, as normal. However, these components are mis-localized centrally in DN-ERM growth cones. Thus, ERM proteins may contribute to an attractive response by organizing actin filaments at the leading edge to allow an effective protrusion response, and by tethering newly created barbed ends to the plasma membrane for sustained actin polymerization.

We previously showed that NGF treatment increases filopodial expression of the adhesion molecules L1 and ß1-integrin (Fig. 3B, C, E). These increases were also blocked when ERM function was disrupted (Fig. 6D, E, F). The absence of L1 accumulation is likely related to a reduction in ERM-mediated linkage of L1 to filopodial F-actin, given that L1 and ERMs can physically interact (Dickson, 2002; Cheng et al., 2005), and that L1 co-localizes with active phospho-ERM in filopodia (Fig. 3C). However, the reduced ß1-integrin localization in filopodial tips may reflect other consequences of the disrupted F-actin arrays, given that ß1-integrin does not co-localize with phospho-ERM in filopodia (Fig. 3B). Finally, DN-ERM did not affect N-cadherin distribution (Fig. 6G), whose distribution is not affected by NGF treatment (Fig. 4D). Thus, the ability of NGF to induce changes in the distribution and organization of adhesion-mediating proteins on filopodia also depends on ERM function.

Increased ADF/cofilin activity increases the levels of phospho-ERM

An early biochemical study suggested that radixin binds preferentially to F-actin barbed ends (Tsukita et al., 1989). We have shown here that phospho-ERM, ADF/cofilin

and barbed ends co-localize at the leading growth cone margin following NGF treatment (Fig. 3A). We therefore wondered if the increased phospho-ERM levels following NGF might be due, at least in part, to the increased free F-actin barbed ends created by ADF/cofilin activity. In a previous study we showed that without adding NGF, a direct increase in growth cone ADF/cofilin activity increases free barbed ends (Marsick et al., 2010). Using this method, we introduced constitutively-active ADF/cofilin (A3) into cultured DRGs using Chariot™ for 1 hr, then fixed and assessed phospho-ERM levels. We found that similar to treatment with NGF, growth cones with elevated ADF/cofilin (char+A3) also exhibited increased filopodial phospho-ERM staining, while no such increase occurred with chariot+BSA controls (Fig. 7A). In Marsick et al. (2010) we also found that a gradient of cell-permeable, active ADF/cofilin (chariot+A3) was sufficient to locally increase growth cone F-actin and free barbed ends, as well as attractive growth cone turning toward the region of higher ADF/cofilin activity. We therefore subjected growth cones to this chariot+A3 gradient for 5 min before being fixed and stained for phospho-ERM. While a gradient of chariot+BSA resulted in symmetric phospho-ERM staining across growth cone widths, chariot+A3 gradients produced increased phospho-ERM closest to the source (Fig. 7B).

To determine if reducing ADF/cofilin activity conversely lowers phospho-ERM levels we transfected DRG neurons with constitutively-active form of LIM kinase (CA-LIMK) that phosphorylates and inactivates ADF/cofilin (Yang et al., 1998; Bernard, 2007). Neurons expressing CA-LIMK do not exhibit an NGF-induced increased in F-actin (Marsick et al., 2010). Compared to GFP controls, CA-LIMK expressing growth cones did not demonstrate a NGF-induced increase in filopodial phospho-ERM (Fig. 7C).

This finding of increased phospho-ERM levels following a direct increase in ADF/cofilin activity and free F-actin barbed ends, without adding NGF, suggest that ERM proteins may be activated or stabilized by binding to new F-actin barbed ends at the plasma membrane. In this sense, activation of ADF/cofilin lies upstream of ERM activation in growth cones responding to NGF signaling.

Filopodial phospho-ERM expression is reduced by L1 knockdown

ERM proteins can stabilize peripheral growth cone F-actin via N-terminal linkage to cytoplasmic domains of membrane proteins. Thus far we have shown that L1 and active ERM proteins co-localize in filopodia, and previous studies have shown direct interaction of these proteins in neurons (Dickson, 2002; Cheng et al., 2005). These data suggested to us that L1 may often participate with ERM proteins in forming the membrane link that helps to organize dynamic actin-rich growth cone structures. To test this possibility we reduced expression of L1 by electroporating an anti-L1 FITC-tagged morpholino into DRG neurons. As shown in Blackmore and Letourneau (2006a), DRG explants treated with L1 morpholino (L1 MO) do not extend neurites on L1, but they do on laminin. Also, as expected (Fig. 8A) growth cones treated with the L1 morpholino (L1 MO) 48 hrs *in vitro* demonstrate reduced staining for L1 compared to controls. To assess F-actin organization when L1 levels are reduced, we imaged phalloidin-labeled F-actin in morpholino-treated growth cones. Similar to DN-ERM-expressing growth cones, growth cones with reduced L1 were smaller (Fig. 8B) and had fewer filopodia (Fig. 8C). In addition, after 48 of knockdown of L1 growth cone migration was greatly reduced, with many growth cones making little to no progress (Fig. 8D). As predicted by our suggestion, growth cones with reduced L1 expression also exhibited reduced phospho-ERM staining

(Fig. 8E). The increase in F-actin following NGF addition was also blocked in growth cones with reduced L1 expression (Fig. 8F). We were prevented from assessing turning to NGF due to the reduced growth cone migration rates in anti-L1 morphoplino expressing neurons after 48 hr (Fig. 8D). These data support the idea that L1 is the major membrane protein that is harnessed by ERM proteins to organize actin filaments and stabilize new actin polymer in filopodia and at the dynamic growth cone leading margin.

The calcium-dependent adhesion receptor N-cadherin is linked to the actin cytoskeleton via catenins (Bard et al., 2008; Shapiro and Weis, 2009). N-cadherin coated beads on a growth cone surface exhibit retrograde transport (Lambert et al., 2002) and immobilized beads induce local accumulations of F-actin (Bard et al., 2008). To determine if the effects of L1 knockdown on phospho-ERM and F-actin are specific, we manipulated the calcium concentration of the culture medium to disrupt N-cadherin-dependent growth(Letourneau et al., 1990; Blackmore and Letourneau, 2006). DRG explant outgrowth on an N-cadherin substrate is robust in media with 1.0mM calcium but significantly reduced in media containing 0.1mM calcium We thus grew DRG explants on laminin with 1.0mM or 0.1mM calcium and measured NGF-induced changes in phospho-ERM and F-actin. As shown in Figure 8G, growth cones cultured with either high or low calcium showed similarly increased filopodial phospho-ERM and phalloidin (F-actin) staining with NGF treatment. These results suggest that the NGF-induced increase in F-actin depends specifically on ERM-mediated linkage of L1 to the cytoskeleton.

Figure 1:

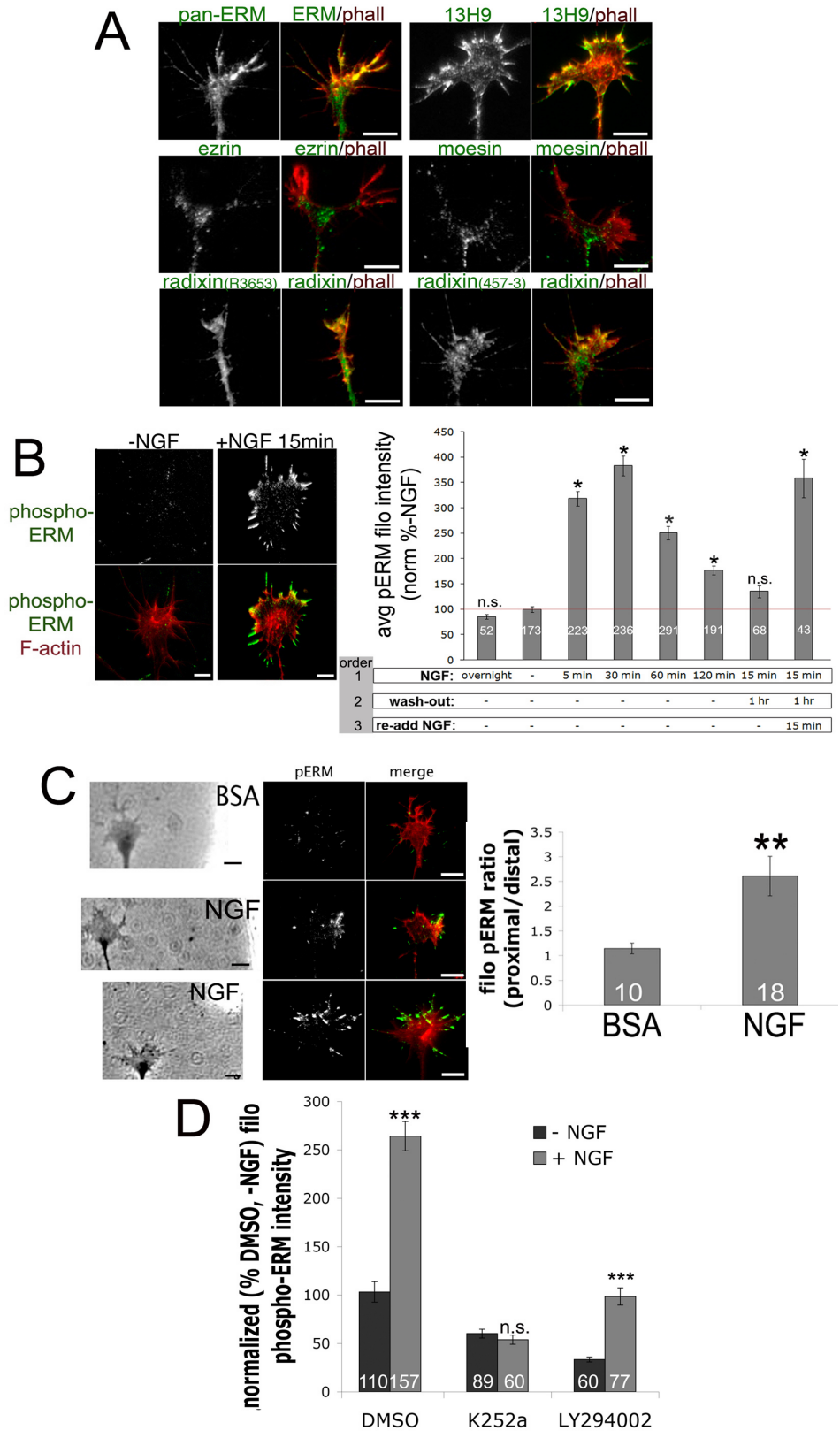
A
pan-ERM
ERM/phall
13H9
13H9/phall
ezrin
ezrin/phall
moesin
moesin/phall
radixin(R3653)
radixin/phall
radixin(457-3)
radixin/phall
B
-NGF
+NGF 15min
phospho-ERM
phospho-ERM F-actin
avg pERM filo intensity (norm %-NGF)
n.s.
52
173
223
236
291
191
68
43
order
NGF: overnight - 5 min 30 min 60 min 120 min 15 min 15 min
wash-out: - - - - - - 1 hr 1 hr
re-add NGF: - - - - - - - 15 min
C
pERM
merge
BSA
NGF
NGF
filo pERM ratio (proximal/distal)
10
18
BSA
NGF
D
normalized (% DMSO, -NGF) filo phospho-ERM intensity
- NGF
+ NGF
110 157
89 60
60 77
n.s.
DMSO
K252a
LY294002

Figure 1. **Nerve Growth Factor globally and locally activates ERM proteins.** (A) Embryonic day 7 (E7) DRG explants were cultured overnight on laminin with 40 ng/ml nerve growth factor (NGF), fixed and stained with Alexa Fluor 568-phalloidin (phall; red) and antibodies against all three ERMs (pan-ERM, 13H9), or individual ERM proteins: ezrin, moesin, or radixin (R3653, 457-3). (B) E7 DRG explants were cultured overnight without NGF (except in first bar, 40 ng/ml NGF overnight), then NGF (40 ng/ml) was bath applied for the times indicated, washed out as indicated, cells were fixed, stained for F-actin (phall; red) and phospho-ERM (green), and filopodial phospho-ERM intensities were measured. (C) A BSA- or NGF- coated micropipette was lowered to one side of a growth cone for 5 min, then cells were fixed and stained for F-actin (phalloidin; red) and phospho-ERM (green). The ratio of filopodial phospho-ERM distribution was measured as proximal/distal intensity relative to NGF source. (D) DRG cultures were treated 15 min with DMSO, 500 nM k252a, 10 μM LY294002, 1 μM U73122 or 1 μM chelerythrine, treated with NGF for 10 min, then fixed. Filopodial phospho-ERM staining intensity was quantified and normalized to the DMSO -NGF condition. Statistical significance using Student's *t* test. Data are means ± SEM; *P<.05, **P<.01, ***P<.001. Scale bars, 10 μm.

Figure 2:

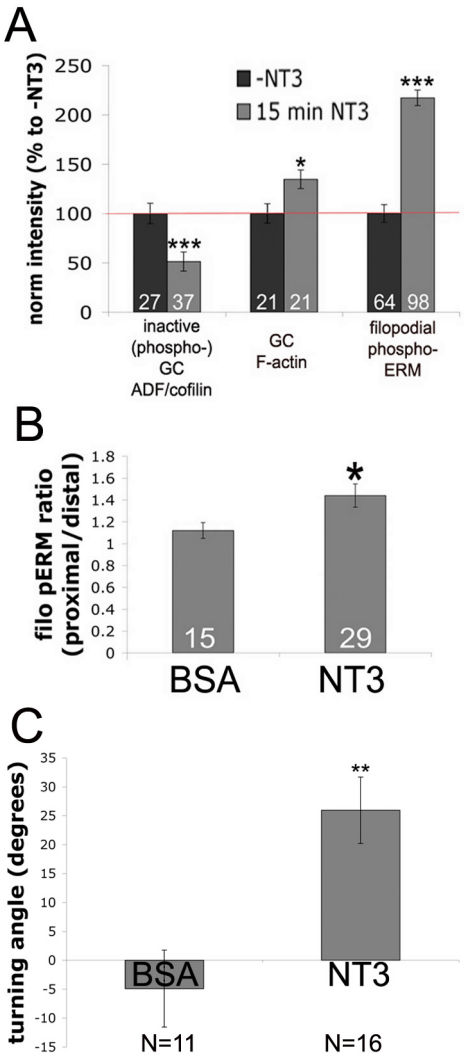
A
norm intensity (% to -NT3)
250
200
150
100
50
0
-NT3
15 min NT3
***
*
***
27 37
21 21
64 98
inactive (phospho-) GC ADF/cofilin
GC F-actin
filopodial phospho-ERM
B
filo pERM ratio (proximal/distal)
1.8
1.6
1.4
1.2
1
0.8
0.6
0.4
0.2
0
*
15
29
BSA
NT3
C
turning angle (degrees)
35
30
25
20
15
10
5
0
-5
-10
-15
**
BSA
NT3
N=11
N=16

Figure 2. Attractive guidance cue neurotrophin-3 (NT3) activates ERM proteins. (A) DRG explants cultured overnight and treated 15 min with 40 ng/ml NT3, fixed, and stained for phospho-ADF/cofilin, F-actin (phalloidin), or phospho-ERM. (B) a BSA- or NT3- coated micropipette was lowered to one side of a growth cone for 5 min, then cells were fixed and stained for F-actin and phospho-ERM. The ratio of filopodial phospho-ERM distribution was measured as proximal/distal intensity relative to the NT3 source. (C) DRG explants were growth overnight with 0.3 ng/ml NT3. Growth cones were imaged 15 min, then subjected to NT3 diffusing from a micropipette to one side and imaged for an additional 45 min, and mean turning angles were measured. Statistical significance using Student's *t* test. Data are means ± SEM; *P<.05, **P<.001, ***P<.0001.

Figure 3:

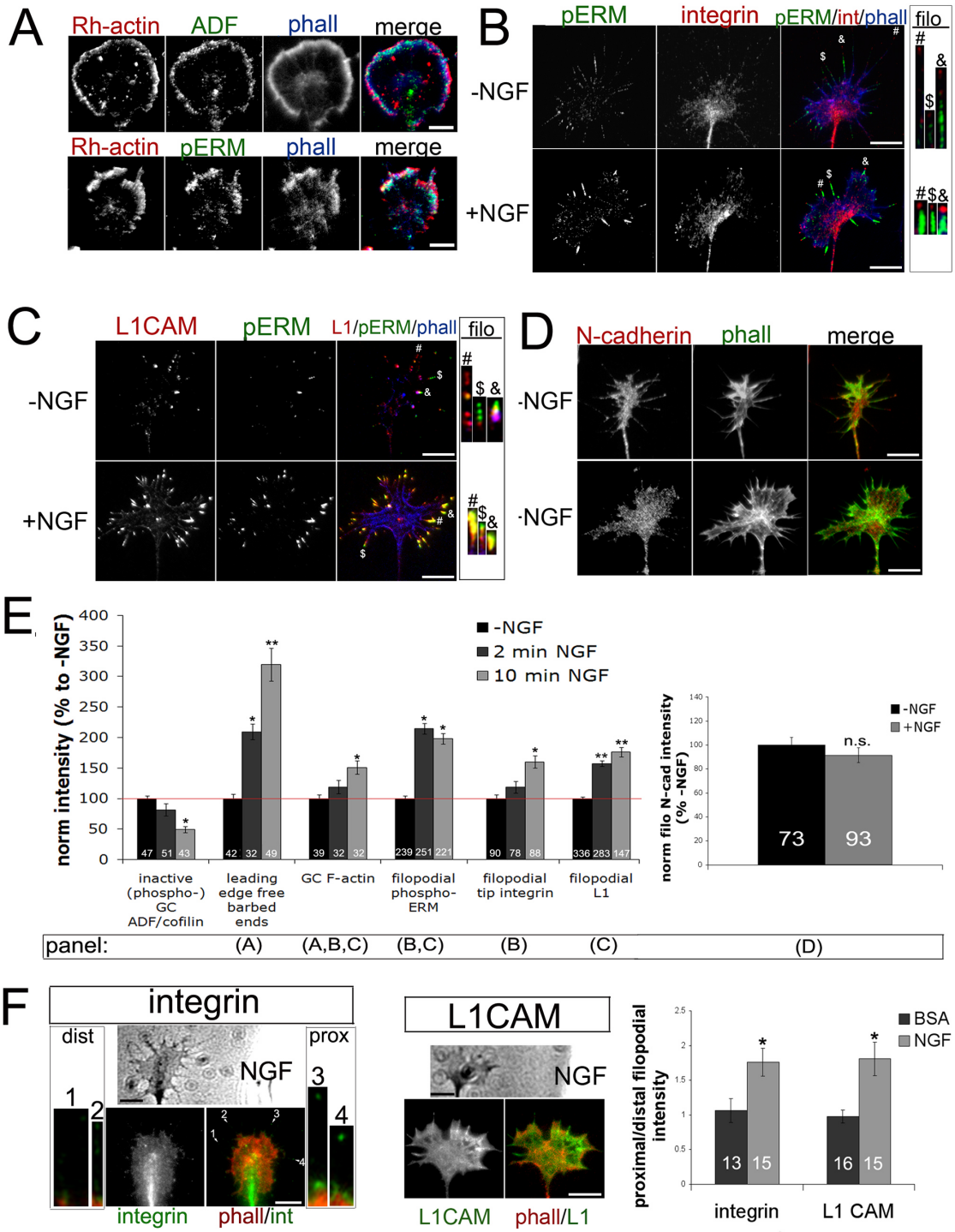
A
Rh-actin
ADF
phall
merge
Rh-actin
pERM
phall
merge
B
pERM
integrin
pERM/int/phall
filo
-NGF
+NGF
C
L1CAM
pERM
L1/pERM/phall
filo
-NGF
+NGF
D
N-cadherin
phall
merge
-NGF
-NGF
E
norm intensity (% to -NGF)
-NGF
2 min NGF
10 min NGF
47 51 43
42 32 49
39 32 32
239 251 221
90 78 88
336 283 147
inactive (phospho-) GC ADF/cofilin
leading edge free barbed ends
GC F-actin
filopodial phospho-ERM
filopodial tip integrin
filopodial L1
norm filo N-cad intensity (% -NGF)
-NGF
+NGF
n.s.
73
93
panel:
(A)
(A,B,C)
(B,C)
(B)
(C)
(D)
F
integrin
dist
prox
NGF
integrin
phall/int
L1CAM
NGF
L1CAM
phall/L1
proximal/distal filopodial intensity
BSA
NGF
13 15
16 15
integrin
L1 CAM

Figure 3. **NGF treatment co-localizes phospho-ERM and ADF/cofilin at the leading edge and increases filopodial L1 and ß-integrin expression.** DRG explants were cultured overnight without NGF, and treated 10 min with 40ng/ml NGF. (A) For the ADF condition, cells were permeabilized 1 min with Alexa Fluor 350-phalloidin (phalloidin; blue), Rh-actin labeling was performed 4 min (red), then cells were fixed and stained for ADF (ab12977; green). For the phospho-ERM condition, cells were permeabilized 1 min with buffer containing Alexa Fluor 350-phalloidin (blue), 0.1% gluteraldehyde and 0.1% paraformaldehyde. Rh-actin labeling was performed 4 min (red), then, cells were further fixed 30 min and stained for phospho-ERM (green). (B-D) DRG explants were cultured overnight, treated with media or 40 ng/ml NGF for 10 min, fixed and stained for phospho-ERM (green), phalloidin (B, C, blue; D, green), and ß1-integrin (B, red), L1 (C, red) or N-cadherin (D, red). (E) Intensity measurements were performed as described in methods. (F) A BSA- or NGF-coated micropipette was lowered to one side of a growth cone for 5 min, then cells were fixed and stained for phalloidin (red) and ß-integrin or L1 (green). The ratio of filopodial ß-integrin or L1 intensity distribution was measured as proximal/distal relative to pipette source. For insets at integrin image, filopodia enlarged 300%. Statistical significance was determined using Student's *t* test. Data are means ± SEM; *P<.05, **P<.01. Scale bars, 10 μm.

Figure 4:

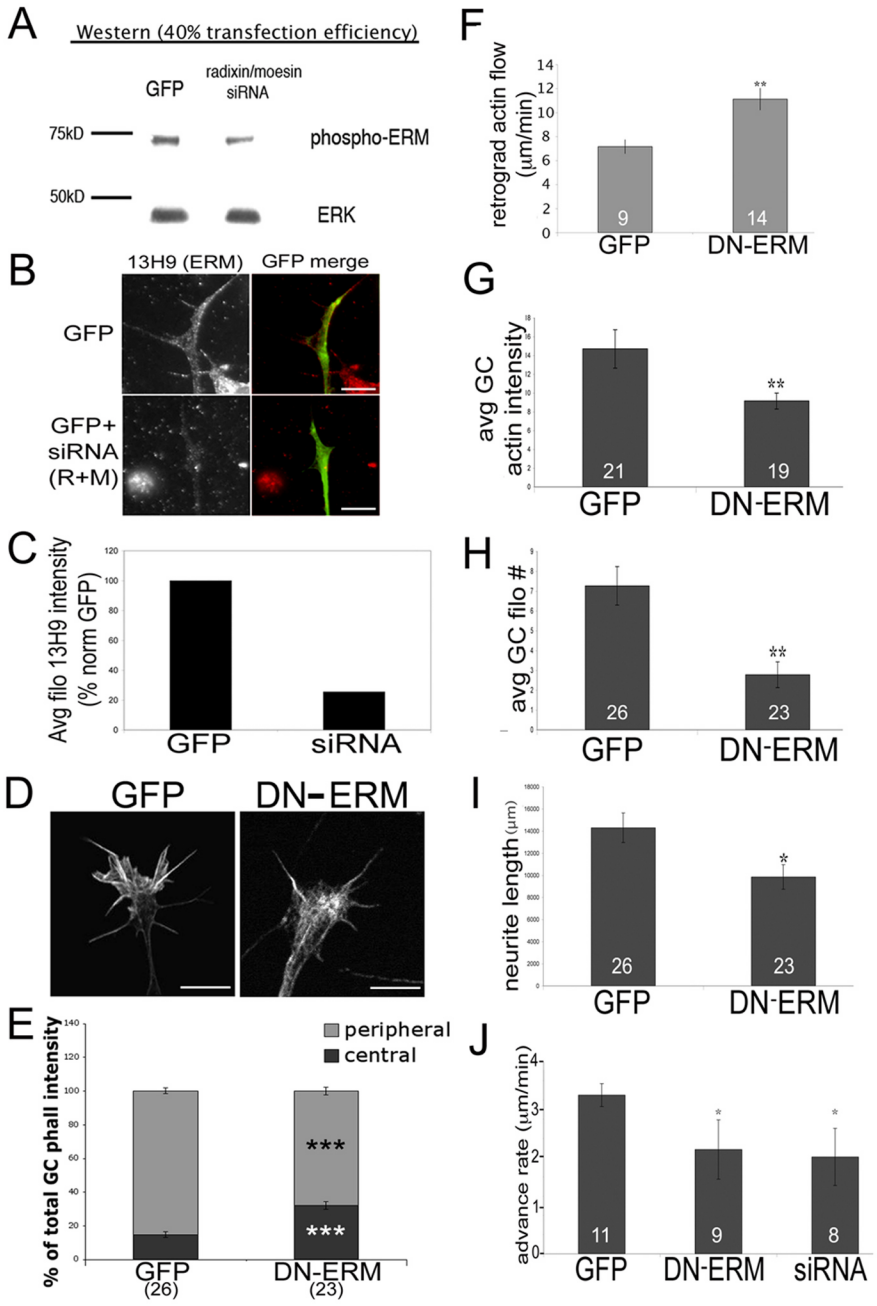
A
Western (40% transfection efficiency)
GFP
radixin/moesin siRNA
75kD
phospho-ERM
50kD
ERK
B
13H9 (ERM)
GFP merge
GFP
GFP+ siRNA (R+M)
C
Avg filo 13H9 intensity (% norm GFP)
GFP
siRNA
D
GFP
DN-ERM
E
peripheral
central
% of total GC phall intensity
***
***
GFP (26)
DN-ERM (23)
F
retrograd actin flow (μm/min)
**
9
14
GFP
DN-ERM
G
avg GC actin intensity
**
21
19
GFP
DN-ERM
H
avg GC filo #
**
26
23
GFP
DN-ERM
I
neurite length (μm)
*
26
23
GFP
DN-ERM
J
advance rate (μm/min)
*
*
11
9
8
GFP
DN-ERM
siRNA

Figure 4. Disrupting ERM function results in smaller and less motile growth cones with disorganized actin filaments. DRGs were transfected with GFP control or siRNA against radixin and moesin, and cultured 48 hrs with 40 ng/ml NGF. Cells were lysed and probed for phospho-ERM via western blot (A), or fixed and stained with an antibody against ERMs (13H9) (B), and intensities were quantified (C). (D) DRGs were transfected with GFP or DN-ERM, cultured overnight with NGF, fixed, stained with phalloidin, and imaged using confocal microscopy. The following parameters were quantified: phalloidin intensities in the peripheral and central growth cone regions (E), growth cone actin intensity (G), or filopodial number (H). For panel F, DRGs were co-transfected with RFP-actin and GFP or DN-ERM and cultured overnight. Growth cones were imaged for 6 min at 3 sec intervals and bright RFP-actin features were tracked to calculate retrograde flow rates. (J) GFP, DN-ERM, or siRNA transfected growth cones were imaged every min for 1 hr to calculate advance rate. (I) Neurite lengths were measured for GFP and DN-ERM expressing DRGs cultured overnight with NGF. Statistical significance was determined using Student's *t* test. Data are means ± SEM; *P<.05, **P<.01. Scale bars, 10 μm.

Figure 5:

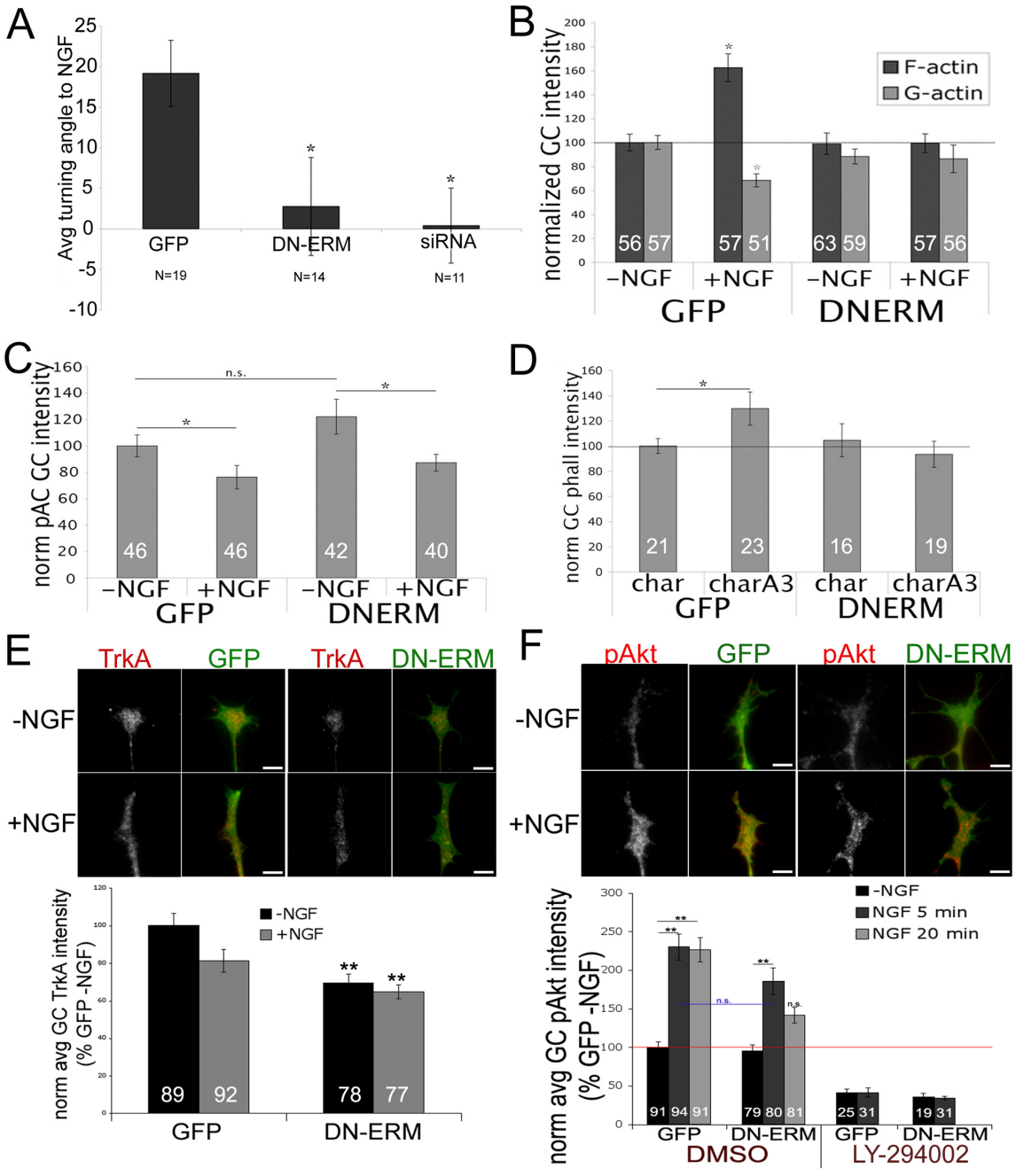
A
Avg turning angle to NGF
GFP
N=19
DN-ERM
N=14
siRNA
N=11
B
normalized GC intensity
F-actin
G-actin
56 57
57 51
63 59
57 56
−NGF
+NGF
−NGF
+NGF
GFP
DNERM
C
norm pAC GC intensity
n.s.
46
46
42
40
−NGF
+NGF
−NGF
+NGF
GFP
DNERM
D
norm GC phall intensity
21
23
16
19
char
charA3
char
charA3
GFP
DNERM
E
TrkA
GFP
TrkA
DN-ERM
-NGF
+NGF
norm avg GC TrkA intensity (% GFP -NGF)
-NGF
+NGF
89
92
78
77
GFP
DN-ERM
F
pAkt
GFP
pAkt
DN-ERM
-NGF
+NGF
norm avg GC pAkt intensity (% GFP -NGF)
-NGF
NGF 5 min
NGF 20 min
91 94 91
79 80 81
25 31
19 31
GFP
DN-ERM
GFP
DN-ERM
DMSO
LY-294002

Figure 5. Disrupting ERM function impairs DRG responses to NGF. (A) DRGs were transfected with GFP control, DN-ERM, or a mixture of GFP and siRNA against radixin and moesin, and cultured 48 hrs without NGF. Transfected growth cones were imaged 15 min, then subjected to NGF diffusing from a micropipette to one side and imaged for an additional 60 min, and mean turning angles were measured. (B-C) DRGs were transfected with GFP or DN-ERM, cultured overnight without NGF, treated with media or NGF 15 min, fixed, then stained with Alexa Fluor 568-phalloidin (F-actin) and FITC-conjugated DNase1 (G-actin; B), or phospho-ADF/cofilin (pAC; C), and growth cone intensities were measured. (D) Cultures were treated with chariot alone or chariot +A3 (active ADF/cofilin) for 1 hr, fixed, stained with Alexa Fluor 568-phalloidin. (E) GFP and DN-ERM cultures were treated with media or NGF 15 min, fixed and stained for TrkA (red). (F) GFP and DN-ERM cultures were treated 10 min with DMSO or LY-294002 (10 μM), then media or NGF 5 or 20 min, then fixed and stained for pAkt (red). Statistical significance was determined using Student's *t* test (A-E) or ANOVA (F). Data are means ± SEM; *P<.05, **P<.01. Scale bars, 10 μm.

Figure 6:

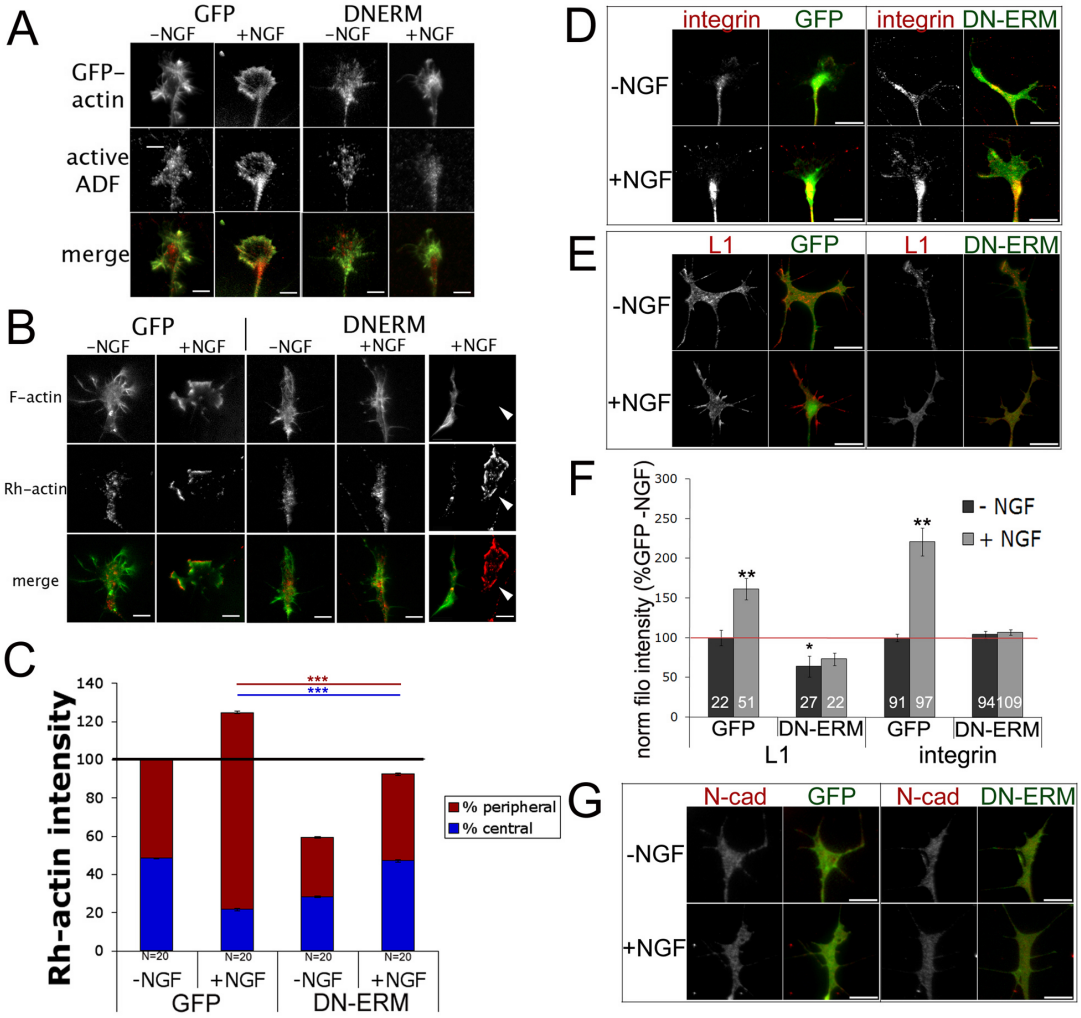
A
GFP
DNERM
−NGF
+NGF
−NGF
+NGF
GFP–actin
active ADF
merge
B
GFP
DNERM
−NGF
+NGF
−NGF
+NGF
+NGF
F-actin
Rh-actin
merge
C
Rh-actin intensity
140
120
100
80
60
40
20
0
***
***
% peripheral
% central
N=20
N=20
N=20
N=20
-NGF
+NGF
-NGF
+NGF
GFP
DN-ERM
D
integrin
GFP
integrin
DN-ERM
-NGF
+NGF
E
L1
GFP
L1
DN-ERM
-NGF
+NGF
F
norm filo intensity (%GFP -NGF)
300
250
200
150
100
50
0
- NGF
+ NGF
**
**
*
22
51
27
22
91
97
94
109
GFP
DN-ERM
GFP
DN-ERM
L1
integrin
G
N-cad
GFP
N-cad
DN-ERM
-NGF
+NGF

Figure 6. Disrupting ERM function disrupts NGF-induced increase in leading edge active ADF/cofilin and F-actin barbed ends, and filopodial L1 and ß-integrin. DRGs were transfected with GFP or DN-ERM, cultured overnight, and treated 15 min with media or 40 ng/ml NGF. (A) Cell were permeabilized for 1 min, then fixed and stained with an antibody against total ADF (12977). (B-C) Cells were permeabilized 1 min, barbed end labeling was performed for 4 min, then cells were fixed and imaged. Barbed end labeling quantification in peripheral vs central regions was performed as described in methods. Arrowheads in Panel B mark an untransfected growth cone in DN-ERM culture that shows normal Rh-actin barbed end labeling (D-G) Cells were fixed and stained for ß1-integrin (D), L1 (E), or N-cadherin (G). Intensities of L1 in filopodia or ß1-integrin at filopodial tips were measured (F). Statistical significance was determined using Student's *t* test. Data are means ± SEM; *P<.05, **P<.01, ***P<.001. Scale bars, 10 μm.

Figure 7:

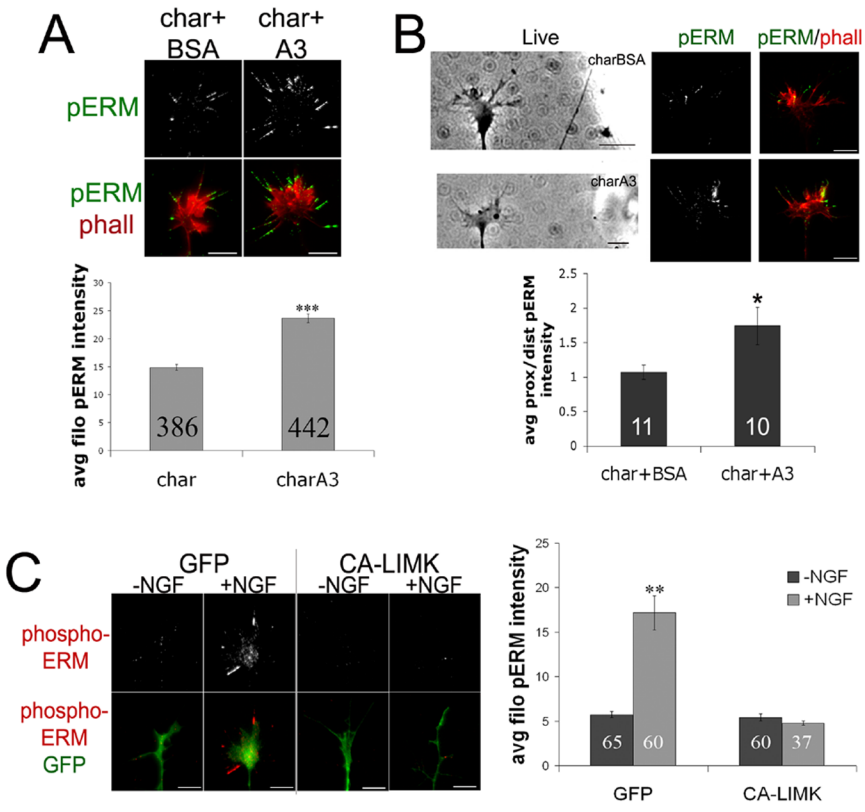
A
char+ BSA
char+ A3
pERM
pERM phall
avg filo pERM intensity
***
386
442
char
charA3
B
Live
pERM
pERM/phall
charBSA
charA3
avg prox/dist pERM intensity
*
11
10
char+BSA
char+A3
C
GFP
CA-LIMK
-NGF
+NGF
-NGF
+NGF
phospho-ERM
phospho-ERM GFP
avg filo pERM intensity
**
65
60
60
37
-NGF
+NGF
GFP
CA-LIMK

Figure 7. Increasing ADF/cofilin activity increases phospho-ERM. DRG explants were cultured overnight without NGF, then treated 1 hr with chariot alone or chariot + A3 (active ADF/cofilin; A), or a micropipette coated with chariot + A3 was brought to one side of a growth cone for 5 min (B). Cells were fixed, and stained for phospho-ERM (green) and Alexa Fluor 568-phalloidin (red). The intensities of filopodial phospho-ERM were measured for growth cones (A) or the proximal/distal ratio relative to the NGF source (B). (C) DRGs were transfected with GFP or GFP + constitutively-active LIMK (CA-LIMK), cultured overnight, treated with media or 40 ng/ml NGF 15 min, fixed and stained for phospho-ERM (red), and filopodial intensities were measured. Statistical significance was determined using Student's *t* test. Data are means ± SEM; *P<.05, **P<.01, ***P<.001. Scale bars, 10 μm.

Figure 8:

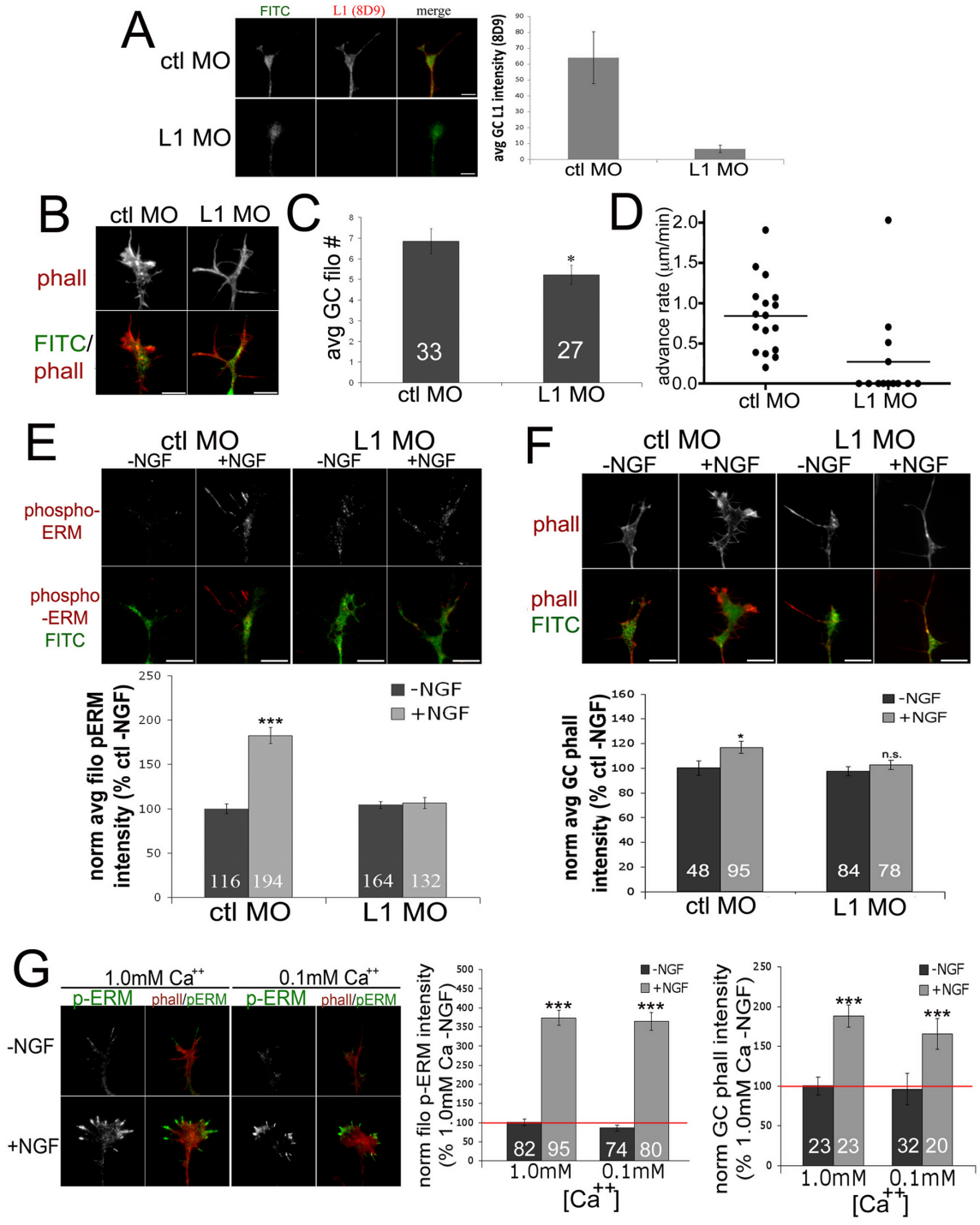
A
FITC
L1 (8D9)
merge
ctl MO
L1 MO
avg GC L1 intensity (8D9)
ctl MO
L1 MO
B
ctl MO
L1 MO
phall
FITC/
phall
C
avg GC filo #
33
27
*
ctl MO
L1 MO
D
advance rate (μm/min)
ctl MO
L1 MO
E
ctl MO
L1 MO
-NGF
+NGF
-NGF
+NGF
phospho-
ERM
phospho
-ERM
FITC
norm avg filo pERM
intensity (% ctl -NGF)
-NGF
+NGF
***
116
194
164
132
ctl MO
L1 MO
F
ctl MO
L1 MO
-NGF
+NGF
-NGF
+NGF
phall
phall
FITC
norm avg GC phall
intensity (% ctl -NGF)
-NGF
+NGF
*
n.s.
48
95
84
78
ctl MO
L1 MO
G
1.0mM Ca++
0.1mM Ca++
p-ERM
phall/pERM
p-ERM
phall/pERM
-NGF
+NGF
norm filo p-ERM intensity
(% 1.0mM Ca -NGF)
-NGF
+NGF
***
***
82
95
74
80
1.0mM
0.1mM
[Ca++]
norm GC phall intensity
(% 1.0mM Ca -NGF)
-NGF
+NGF
***
***
23
23
32
20
1.0mM
0.1mM
[Ca++]

Figure 8. Filopodial phospho-ERM expression is reduced by L1 knockdown. (A-D) DRG explants were transfected with FITC-tagged morpholinos against chick L1 (L1 MO) or control (ctl MO) and cultured on laminin 48 hrs with 40 ng/ml NGF. (A) Cells were fixed and stained for L1 (8D9; red) and growth cone intensities were measured. (B) Representative growth cones transfected with morpholino, fixed and stained with Alexa Fluor 568-phalloidin. (C) Average number of filopodia of morpholino-transfected growth cones. (D) Growth cone advance rate for control (ctl MO) or anti-L1 morpholino (L1 MO). (E-F) Transfected DRGs were cultured 24 hrs with 40 ng/ml NGF, an additional 24 hrs without NGF, then cells were treated with media or NGF 15 min, fixed, stained with phospho-ERM (E) or Alexa Fluor 568-phalloidin (F), imaged, and intensities were measured. (G) DRG explants were cultured overnight on laminin with media containing 1.0 mM or 0.1 mM calcium. Cells were treated with media or NGF 15 min, fixed and stained with Alexa Fluor 568-phalloidin (red) and phospho-ERM (green), then imaged, and intensities were measured. Statistical significance was determined using Student's *t* test. Data are means ± SEM; *P<.05, **P<.01, ***P<.001. Scale bars, 10 μm.

Discussion

ERM (ezrin moesin, radixin) proteins are multi-domain proteins that link actin filaments to plasma membrane proteins. ERMs also serve as scaffolding for adaptor proteins and signaling molecules. Previous studies of ERM functions in neurons reported that reducing ERM synthesis slowed neurite growth and reduced growth cone size, while inhibiting growth cone ERMs with micro-CALI (chromophore-assisted laser inactivation) locally destabilized lamellipodia (Paglini et al., 1998; Castelo and Jay, 1999). These papers implicated ERM proteins in stabilizing membrane cytoskeletal associations. In other studies the binding of the cytoplasmic domain of the adhesion molecule L1 to ERM proteins was implicated in mediating neurite branch formation on L1 substrates and in transmitting growth cone traction at L1-mediated adhesion sites (Cheng et al., 2005; Sakurai et al., 2008).

Here we investigated the role of ERMs in chemotactic growth cone guidance. Like previous papers, we found that inhibiting ERM function reduces growth cone migration, filopodia and actin content. Our new finding is that ERM proteins are necessary for the chemotropic turning of DRG growth cones to multiple attractive guidance cues. Moreover, our results emphasize a key function of ERM proteins in organizing the actin filament network and adhesive properties of the growth cone leading margin.

Activation of ERM proteins by phosphorylation is a critical part of a dynamic response that protrudes a DRG growth cone leading membrane towards an NGF or NT3 source. Within two minutes of neurotrophin stimulation, P-domain phospho-ERM levels are significantly elevated and co-localize with ADF/cofilin and F-actin barbed ends at the growth cone leading margin. Our immunocytochemistry indicates that radixin is the

dominant ERM protein in the DRG growth cone leading margin, in agreement with Castelo and Jay (1999). Radixin was initially characterized as an actin barbed-end binding protein (Tsukita et al., 1989), suggesting radixin may link F-actin barbed ends that created by ADF/cofilin-mediated filament severing to the leading edge. Thus, the spatially and temporally coordinated activation of ADF/cofilin and ERM proteins in the growth cone region that is closer to an NGF or NT3 source may connect new actin polymer to the leading edge to effectively harness actin polymerization for driving membrane protrusion toward an attractant source.

We found that TrkA mediates the NGF-induced activation of ERM proteins and ADF/cofilin in DRG growth cones. Jeon et al (2010) found in PC12 cells that NGF-stimulated phosphorylation of moesin is mediated by AKT kinase, through its upstream activator PI3 Kinase. Similarly, we found that NGF increases AKT phosphorylation in DRG growth cones in a PI3 kinase-dependent manner, and the PI3 kinase inhibitor LY294002 reduces the NGF-mediated increase in filopodial phospho-ERM staining. Our data also suggest other TrkA-activated kinases, such as PLC and PKC may also contribute to ERM phosphorylation in response to NGF (Pietromonaco et al., 1998). In addition, our finding that ERM phosphorylation is stimulated by directly increasing ADF/cofilin and F-actin barbed ends in growth cones, without NGF-mediated signaling, suggests that the active unfolded conformation of ERM proteins is promoted or stabilized by binding to actin polymer. In this, active ERMs could function as positive feedback for continued growth cone protrusion toward an attractive cue source.

The necessity for ERM function in growth cone chemotaxis was indicated by the absence of NGF-induced increase in F-actin content and growth cone turning, when ERM

function was disrupted by a dominant negative ERM or siRNA against radixin and moesin. This occurred despite evidence in ERM-inhibited growth cones of trk signaling (increased phospho-AKT) and activation of ADF/cofilin (reduced phospho-ADF/cofilin). However, beyond the disruption of growth cone turning toward NGF, the effects of reduced ERM function indicated a basic role for ERMs in organizing F-actin at the growth cone leading margin.

Along with the reduced total F-actin content in ERM-inhibited growth cones, we found a greater fraction of F-actin was located in the growth cone center. In addition, when DN-ERM expressing growth cones were stimulated with NGF, the active ADF/cofilin and resultant F-actin barbed ends were centrally located in growth cones, instead of being concentrated at the leading margin. This disrupted actin organization is related to our finding that retrograde flow of F-actin is faster in ERM-inhibited growth cones. This result suggests that F-actin-ERM linkage to the plasma membrane contributes to the molecular "clutch" that counteracts myosin II-powered retrograde actin flow. By linking polymerizing actin filaments to sites of substrate adhesion, the "clutch" enhances protrusion of the leading margin and transmits traction forces that advance the growth cone. Without ERM-mediated linkage of F-actin to the plasma membrane the "clutch" may slip more frequently, and retrograde F-actin movement from the leading margin may be more rapid than normal, accounting for the more central F-actin localization. A "clutch" that slips more will also be less effective in exerting traction to advance the growth cone, which is consistent with our observed slower migration of ERM-inhibited growth cones.

In addition to the locally increased actin polymerization, turning of growth cones

toward NGF may be promoted by the enhanced expression of adhesion-mediating molecules on filopodia that are closer to an NGF source. After NGF treatment phospho-ERM and L1 levels are increased and co-localize along filopodial shafts, but when ERM function is disrupted, L1 accumulation along filopodia is blocked. ERM binding may mediate L1 localization to filopodia in several ways. Linkage to ERM proteins may anchor filopodial L1, which reaches filopodia by lateral movement in the membrane and by exocytosis of vesicular L1 (Kamiguchi and Lemmon, 2000; Dequidt et al., 2007). In addition, ERM binding to the RSLE cytoplasmic region of L1 may reduce endocytic removal of L1 from filopodial surfaces by competing with binding of the clathrin-associated adaptor AP-2 (Long et al., 2001; Cheng et al., 2005).

The NGF-induced selective co-localization of L1 and phospho-ERM along filopodial shafts illustrates a functional coordination of these two proteins. Homophilic L1 adhesions, as well as heterophilic interactions between L1 and extracellular matrix proteins, mediate neurite outgrowth and neuronal polarization. The concentrated L1/ERM linkage to actin filaments along growth cone filopodia may be particularly effective in providing traction that can turn a growth cone or can initiate cytoskeletal rearrangements to form a neuritic branch (Cheng and Lemmon, 2004). Another aspect of the strong filopodial expression of L1 is that L1 may be the major ERM binding partner in dynamic growth cone regions for linking F-actin to the plasma membrane and providing a scaffold for other membrane and signaling proteins. We might not expect that knock down of L1 synthesis would have blocked the NGF-induced increase in filopodial p-ERM staining, if other plasma membrane binding partners for ERMs were available. Furthermore, growth cones of L1-depleted neurons resembled growth cones with disrupted ERM function, as

they had few filopodia, a slow migration rate and a lack of increased F-actin in response to NGF treatment.

NGF also induces local accumulation of ß1-integrin receptors at filopodial tips, distal to the p-ERM that is concentrated along filopodial shafts. However, disrupting ERM function also blocks this response. ERM proteins may act to increase ß1-integrin expression at filopodial tips by stabilizing parallel bundles of actin filaments, which serve as rails for myosin-mediated anterograde transport of ß1-integrin to filopodial tips (Grabham and Goldberg, 1997; Grabham et al., 2000). Alternatively, ERMs may provide scaffolding for signaling components of integrin adhesions, such as PKA or Epac1 (Gloerich et al., 2010), a GEF for Rap GTPase, which promotes integrin-mediated cell adhesion to ECM molecules (Boettner and Van Aelst, 2009).

In our previous report on the role of ADF/cofilin in attractive growth cone turning toward a soluble guidance cue, we showed that the local stimulation of growth cone protrusion involves increased actin polymerization at the leading growth cone margin. Here we show that ERM proteins have an equally important role in attractive guidance by NGF and NT3 by stabilizing new actin polymer at the leading edge so that actin polymerization effectively drives the leading edge forward. In addition, ERM proteins may contribute to the clutch mechanism that transmits mechanical energy from actomyosin contractility to exert traction on substrate adhesions. ERM proteins contribute to the activity of the clutch by linking actin filament to the plasma membrane to slow retrograde actin flow and by mediating the dynamic expression of L1 and ß1 integrin adhesion molecules on filopodia. These data point to ERM proteins as central to the coordinated remodeling of growth cone adhesions and F-actin downstream of guidance

cues.

In summary, axonal navigation involves signaling by extrinsic guidance cues to regulate the cytoskeletal mechanisms of growth cone migration. The diverse actin binding proteins that orchestrate actin filament dynamics and organization are targets of this signaling, and our studies reported here illustrate how spatial and temporal activation of ADF/cofilin and ERM proteins are coordinated to generate attractive growth cone turning responses to multiple guidance cues. Our conclusion is supported by a recent report that ERM proteins are also activated by the chemoattractant netrin-1 (Antoine-Bertrand et al., 2011).

Chapter IV: The role of Arp2/3 during in-vivo axon guidance in the chick embryo

Introduction

During development, newborn neurons send axons to establish connections with their synaptic targets. The growth cone at the tip of that axon is responsible for steering it correctly, based on the guidance cues present in the extracellular environment. These guidance cues modulate the cytoskeleton inside the growth cone, particularly actin-binding proteins (ABP's), to elicit advance, turning, branching, or retraction (Gomez and Letourneau, 2013). A thoroughly studied ABP is Arp2/3 (Goley and Welch, 2006), however, whether it is required for the correct wiring of particular circuits during development is uncertain.

The few available studies on the role of Arp2/3 during development show that the lack of its activity leads to defects in axonal guidance. For example, studies in *Drosophila* and *Caenorhabditis elegans* show that disruption of Arp2/3 activity causes clear deficits during axonal guidance (Zallen et al., 2002; Shakir et al., 2008). In chick embryos, it has been shown that Arp2/3 is required for axonal branching in the developing spinal cord (Spillane et al., 2011). The absence of more studies detailing the role of Arp2/3 during developmental guidance has been attributed to the lethality associated with the lack of Arp2/3 activity during development (Harborth et al., 2001; Fujiwara et al., 2002; Zallen et al., 2002; Dahl et al., 2003; Sawa et al., 2003). Therefore, studying the role of Arp2/3 during developmental guidance requires a system amenable for tissue-specific or mosaic downregulation of Arp2/3 activity.

In-ovo transfection of chicken embryos provides such a model system (Vergara and Canto-Soler, 2012). This versatile organism provides easy accessibility to central and peripheral nervous system neurons for transfection while in-ovo, which allows for easy

manipulation of Arp2/3 function during active periods of guidance. For this reason, we decided to study the role of Arp2/3 in axonal guidance during the development of the retinotectal projections and sensory-motor innervation of the hindlimb. The chick retinotectal projections are composed of retinal ganglion cells axons as they leave the developing eye and migrate towards the contralateral optic tectum (Mey and Thanos, 2000; Thanos and Mey, 2001). The sensory-motor axons are composed of motor axons from the ventral spinal cord and sensory axons from the dorsal root ganglia (DRG) as they migrate and innervate the embryo hindlimb. As a result, these two guidance systems can shed light on the role of Arp2/3 during axonal guidance.

Here we report that inhibition of the Arp2/3 complex during sensory-motor innervation of the hindlimb led to a reduced number of nerve branches in the embryo's hindlimb. In the retinotectal projections, we found that retinal ganglion cells had no trouble exiting the eye or reaching the optic tectum.

Methods

In-ovo transfection

Embryonic day 3 embryos were wiped with 70% ethanol-soaked tissues and a 1.5 centimeter diameter window was opened on the egg shell. The inner shell membrane was removed without disturbing the vitelline membrane. A micropipette needle, prepared from a glass capillary tube, was filled with a plasmid solution of 5 μg/μl and fast green (0.025%), EGFP was used for controls and EGFP-CA for the experimental group. For the retinotectal projections, the needle was pierced through the vitelline membrane,

sclera and retina and the solution injected. For labeling sensory-motor axons, the inner shell membrane was removed and the needle inserted through the vitelline membrane and into the neural tube cavity at the lumbar region level. At this point, 300 µl of F12 media were added on top of the embryo, enough to cover the electrode tips, and five pulses of 50mV for 50 ms were applied, at intervals of 950ms. The opening on the egg shell was sealed with clear scotch tape, labeled, and returned to the incubator. Embryos were then harvested at different stages, and imaged as whole mounts with wide field microscopy.

Results

Proper functioning of the adult nervous system requires correct wiring during development. This process relies on growth cones to steer axons to their targets based on guidance cues present in the extracellular environment. These guidance cues will modulate the activity of actin binding proteins to change actin dynamics at the leading edge of the growth cone to cause retraction, protrusion and advance, turning, or branching. We wanted to know what role, if any, is played by the actin nucleator Arp2/3 during in-vivo guidance by sensory-motor axons in the hindlimb and the retinotectal projections of the chick embryo.

Lumbar plexus axons

Briefly, plasmid solution containing either EGFP or EGFP-CA was injected into the neural tube cavity at the lumbar region of E3 embryos, and neural tube cells were transfected via electroporation. Animals were then dissected and imaged at various days

after electroporation. GFP fluorescent signal could be observed in the spinal cord and DRG's of the lumbar region of electroporated animals by whole mount imaging 48 hrs after electroporation. Ventral spinal cord and DRG neuron transfection was corroborated by culturing explants of these tissues overnight, the next morning GFP-positive axons could be seen growing outside of the explants.

To study sensory-motor innervation, transfected embryos were allowed to continue developing in the incubator until E8. At this point, embryos were dissected, and imaged with wide field microscopy, both dorsally and ventrally. To compare the effect of axon guidance in the hindlimb, we imaged and compared the branching pattern of sensory-motor nerves in the hindlimb region. We found that Arp2/3-inhibited animals had nerves with fewer branches than aged-matched controls (Fig. 1). Nonetheless, Arp2/3-inhibited axons could be seen to have reached the distal-most part of the hindlimb, just as control animals did. These results suggest that the actin nucleator Arp2/3 might be necessary for the formation of nerve branches during axon guidance in the hindlimb. Similar in-vivo results have been published before, showing that Arp2/3 was necessary for normal axonal branching in the chick embryo spinal cord (Spillane et al., 2011).

Retinotectal projections

E3 animals were injected with plasmid solution containing EGFP or GFP-CA in the space between the dorso-temporal retina and the vitreous body, electroporated, placed in the incubator, then dissected and imaged at different stages to study retinal ganglion cell axon migration at different stages. At E5, 48 hrs after transfection, GFP-positive retinal axons from the dorso-temporal retina were seen at the optic nerve head and

presumably inside the optic nerve. At this point, no visible guidance defects were observed in the Arp2/3-inhibited group, when compared to controls. Axon terminals that had not yet reached the optic nerve head, had a straight trajectory pointing towards it. Retinal axon migration was not directly studied in the optic nerve, chiasm, or tract. However, we found no GFP-positive axons in the ipsilateral tectum, suggesting that Arp2/3 inhibition caused no misrouting at the optic chiasm. Arp 2/3-inhibited embryos dissected at E9 were found to have retinal axon terminals with a similar distribution and density in the contralateral antero-ventral optic tectum, as did their age-matched control counterparts (Fig. 2). These results suggest that Arp2/3 activity is dispensable during retinotectal projection axon guidance during the ages of E3 and E9.

Figure 1:

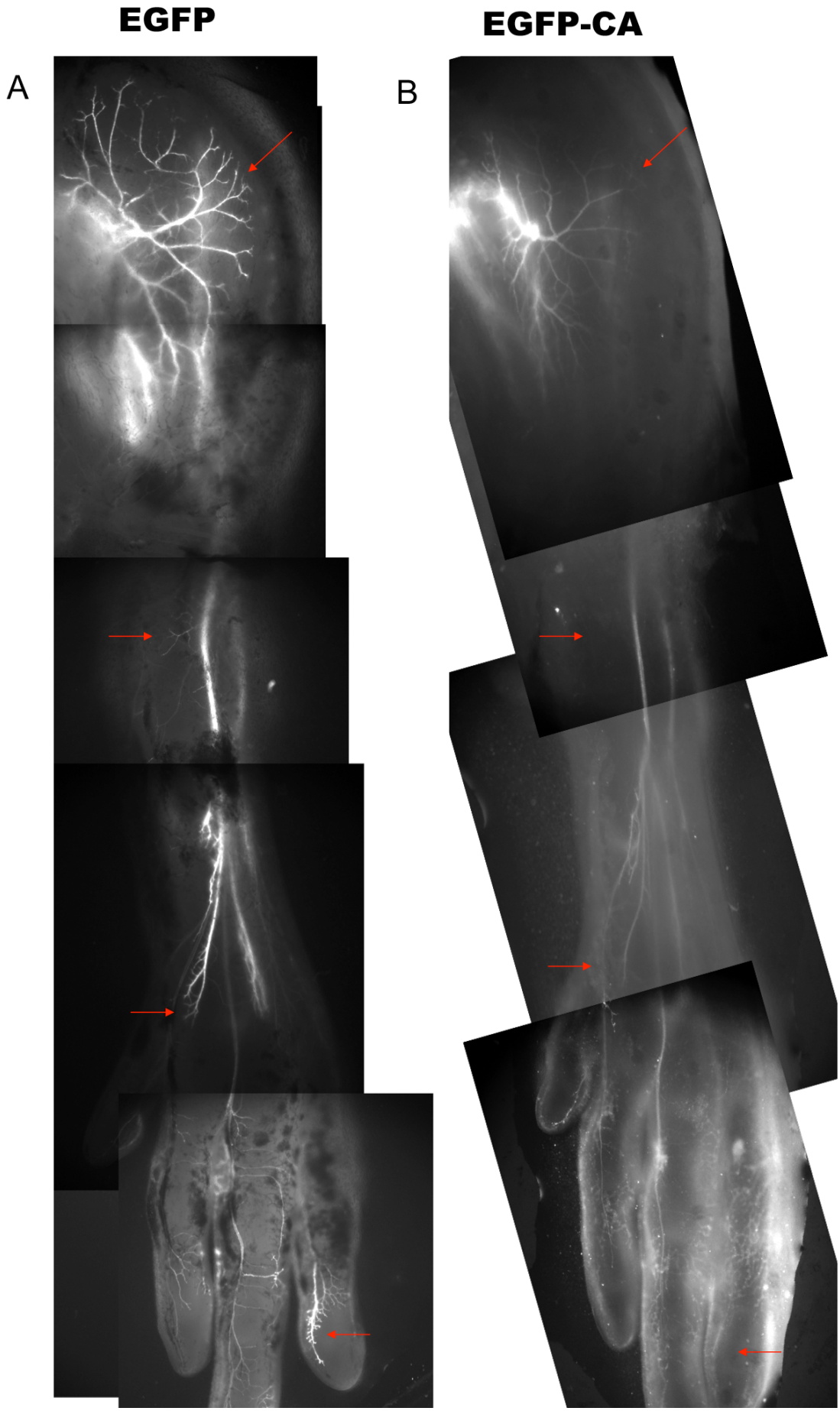

Figure 1: Effect of Arp2/3 inhibition during sensory-motor innervation of the chick hindlimb. E3 embryos were injected with a plasmid solution containing either EGFP or EGFP-CA into the neural tube of the lumbar region, electroporated, dissected and imaged at E8. (A) Dorsal view of the control hindlimb transfected with EGFP showing nerve branching along the hindlimb in control embryo. (B) Dorsal view of the Arp2/3-inhibited hindlimb showing the reduced number of nerve branches as compared to control embryos (red arrows). Scale bar: 1mm.

Figure 2:

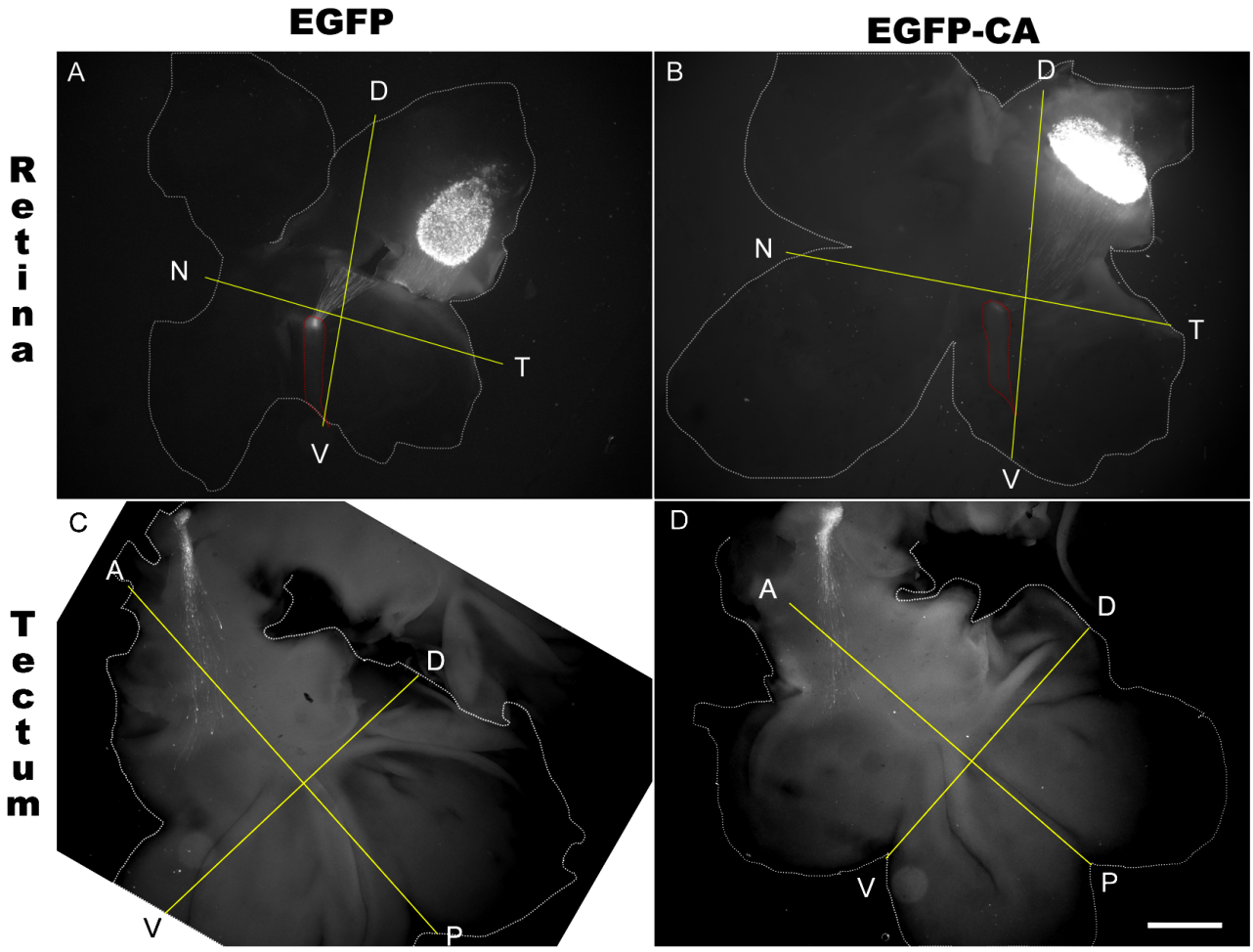

Figure 2: Effect of Arp2/3 inhibition on during retinotectal projection development. E3 embryos were injected with a plasmid solution containing either EGFP or EGFP-CA in the space between the dorso-temporal retina and the vitreous body, electroporated, dissected and imaged at E9. (A-B) Whole-mount of E9 retina showing transfected area and axons that have migrated into the optic nerve head in control and Arp2/3-inhibited animals, respectively. (C-D) Whole-mount showing axons occupying the antero-ventral aspect of the E9 tectum in control and Arp2/3-inhibited embryos. Optic fissure is delineated in red dotted lines. Yellow lines demarcate tissues planes; A-anterior, P-posterior, D-dorsal, V-ventral, N-nasal, or T-temporal. Scale bar: 1.5 mm.

Discussion

Our experiments were aimed at elucidating the role of the actin nucleator Arp2/3 during in-vivo axon guidance. To this end we performed in-ovo transfection to study retinotectal projections and sensory-motor axon innervation of the hindlimb. This approach allowed us to study Arp2/3 function only in neurons, thus ensuring that if guidance deficits arise they were not secondary to tissue disruption associated with whole-embryo Arp2/3 inhibition.

Transfection of the spinal cord and dorsal root ganglia at the lumbar level of E3 chicks allowed us to study axon guidance during innervation of the hindlimb by motor and sensory neurons. Unfortunately, our plasmid delivery method does not allow us to differentiate the identity of axons, motor vs. sensory, during whole mount imaging, thus forcing us to treat them as one population during analysis. At E8, we found that Arp2/3 inhibition led to a reduction in the number of nerve branches along the hindlimb, compared to age-matched controls (Fig. 1). A possible interpretation of this result is that Arp2/3 is necessary for responding to guidance cues that instruct axonal defasciculation from the main nerve and the formation of a new branch. Alternatively, it could suggest that Arp2/3-inhibited axons are delayed in their migration rate because of their reduced actin polymerization capacity. These results suggest that Arp2/3 activity is required for normal nerve branching during the innervation of the chick hindlimb. Similar results have been reported before in the chick spinal cord (Spillane et al., 2011).

In the retinotectal system, we found that Arp2/3 inhibited neurons had no trouble exiting the eye and migrating into the optic nerve. We did not study axonal bundling or migration inside the optic nerve, chiasm, or tract. However, the chick retinotectal system

is a crossed one, meaning that retinal ganglion cells project to the contralateral tectum. We did look for GFP-positive axon terminals in the ipsilateral tectum to rule out guidance deficits at the optic chiasm and found none in control or Arp2/3-inhibited animals. Thus suggesting, that at this stage of development Arp2/3 is not necessary for correct guidance at the optic chiasm. It has been shown that during development there are transient ipsilateral retinotectal connections, but these eventually regress and disappear. Most likely, our lack of transient GFP-positive fibers in the ipsilateral tectum is due to the small number of labeled fibers compared to the total population. Upon reaching the contralateral tectum, GFP-positive fibers from the dorso-temporal retinas of control and Arp2/3-inhibited animals, could be seen occupying a similar region on the antero-ventral surface of the tectum. Their position at this time is consistent with normal development, where the temporal retina axons project and synapse to the anterior tectum. These results suggest that Arp2/3 is not required for retinal axon guidance in the tectum.

Our findings with the retinotectal system suggest that the actin nucleator Arp2/3 is not required for efficient axon guidance in the developing chick visual system. Even though actin polymerization has been shown to be required for efficient in-vivo axon guidance before, it is not the first time that an ABP is abolished with no harm to the development of the retinotectal projections (Dwivedy et al., 2007). Thus, suggesting that the system might have a redundancy of mechanisms to generate actin barbed ends capable of sustaining polymerization to drive leading edge protrusion and guidance. However, we do have to raise a concern with our current experimental setup, and it is the fact that at the developmental stage in which we transfected our embryos (E3) there was a population of older retinal ganglion cells that had already left the eye. This initial axonal

layer could serve as a tract that younger axons could fasciculate onto and successfully exit the eye. This brings into question whether our experiment is set up to study the role of Arp2/3 during active axon guidance, or whether it is studying the role of Arp2/3 during passive axonal fasciculation? Future experiments to establish the role of Arp2/3 during retinotectal development will have to tease apart these two processes.

At this point, we believe that our results are not ready for publication for various reasons. While studying sensory-motor innervation of the chick hindlimb we still have to corroborate the identity of transfected neurons, the relative number of transfected neurons between control and experimental animals, and whether or not Arp2/3 affects neuritogenesis, which could be a confounding factor in our guidance analysis. In the retinotectal system we have repeat our experiments with Arp2/3 inhibition in younger RGC neurons. Doing so, would allow us to definitively determine the role of Arp2/3 during chick retinotectal projection development, as opposed to its role in fasciculation. Answering these questions, would further improve our understanding on the role of Arp2/3 during in-vivo axon guidance.

Chapter V: Final Discussion

Development of the nervous system requires newborn neurons to establish connections with other cells to ensure their survival and adequate functioning during adulthood. The embryonic extracellular environment provides the nervous system with molecular cues that enable the growth cone with guidance instructions to find its particular target (Gomez and Letourneau, 2013). These guidance cues can modulate the growth cone cytoskeleton, particularly ABP's, to provide the motile response needed to advance, turn, retract, or branch. However, to this day, our understanding of how these ABP's mediate all these growth cone motile responses in different environments, developmental stages, and in response to multiple attractive and repulsive guidance cues remains imprecise. This dissertation provides data on the role and mechanisms of two of these ABP's involved in growth cone guidance.

The first chapter addresses the role of the actin nucleator Arp2/3 during attractive and repulsive growth cone guidance on two different substrates: the ECM protein laminin and the CAM L1. We found that the increase in F-actin, filopodia number, and surface area in growth cones commonly associated with NGF and Netrin stimulation are dependent on Arp2/3 activity on both substrates. Moreover, through a barbed-end assay we found that the actin nucleating activity of Arp2/3 was restricted to the growth cone leading edge, consistent with immunostaining results for its subunits. However, we found that Arp2/3 activity was only required for attractive and repulsive guidance on L1, but that its inhibition had no effect during guidance on laminin. Additionally, we found that Arp2/3 inhibition led to a reduction in the size and number of paxillin-positive substrate adhesions on laminin with a concomitant increase in the actin retrograde flow, whereas its rate was reduced on L1. These data support a model whereby the Arp2/3 actin

nucleating activity is localized to the growth cone leading edge and is required for attractive and repulsive growth cone guidance on L1, but not on laminin. Thus, suggesting that the role of the ABP Arp2/3 is substrate-dependent.

The next chapter presents data supporting the role that the ERM family of cytoskeletal linker proteins have during attractive growth cone guidance to NGF and NT3. ERM proteins link actin filaments to the cytoplasmic domains of several transmembrane proteins, including a major neuronal adhesion protein L1 CAM. ERM proteins are localized with ADF/cofilin at the leading margin of growth cones stimulated by NGF and NT3. We found that signaling from both NGF and NT3 can phosphorylate and activate ERM proteins in DRG and RGC neurons. Moreover, the increase in F-actin and growth cone protrusion caused by NGF and NT3 stimulation was abolished if ERM protein function was disrupted. Additionally, the data supports a role for ERM protein activity with the correct placement of substrate adhesions in growth cones. Finally, disruption of ERM protein function diminishes attractive growth cone guidance responses and causes mislocalization of ADF/cofilin, an active binding protein previously shown by our group to be required for correct guidance. These results suggest that actin polymerization and substrate adhesions in growth cones are closely associated and dependent on ERM proteins activity and necessary for correct growth cone guidance.

The final chapter of this dissertation deals with the role of the actin nucleator Arp2/3 during in-vivo guidance. For this purpose we studied axon guidance in the retinotectal projections and during sensory-motor innervation of the hindlimb. We found that during development of the retinotectal projections, Arp2/3 activity was not required

for RGC axons to be guided towards the optic nerve head and leave the retina. Moreover, Arp2/3 activity was not required for RGC axons to reach the contralateral tectum and occupy their corresponding region based on topographical connectivity. The fact that we did not find misrouted axons in the ipsilateral tectum suggests that axon guidance at the optic chiasm was unaffected by Arp2/3 inhibition. On the other hand, we found that Arp2/3 inhibition did cause guidance deficits during sensory-motor innervation of the chick hindlimb. Particularly, we saw that Arp2/3 inhibited animals had nerves with reduced number of branches, compared to control animals, suggesting that Arp2/3 activity plays an important role in the correct wiring and innervation of the embryonic hindlimb by sensory-motor nerves.

Taken together, the data presented in these chapters support a model whereby the role of the actin nucleator Arp2/3 during growth cone migration and guidance is substrate dependent. Receptors for substrate molecules in growth cones are capable of activating signaling cascades and changing the signaling milieu inside the growth cone, potentially changing the way they respond to the environment. The effect that different substrates have on growth cone signaling has been documented before (Hopker et al., 1999; Ooashi et al., 2005). Additionally, substrate effects are also evident upon growing the same type of neuron on different substrates, where growth cones can undergo drastic changes in terms of their morphology, size, migration speed, response to guidance cues, and F-actin distribution and structures (filopodia veils). For example, in our experiments, growth cones on L1 are broad and lamellar, whereas on laminin they are compact and filopodial.

Our experiments suggest that unstimulated growth cones on L1 have a have a baseline level of Arp2/3 activity that maintains F-actin levels, leading edge protrusion,

and migration speed, since inhibition of Arp2/3 reduces these three parameters. This is supported by the fact that stimulation by NGF or Netrin causes DRG and RGC neurons respectively, to increase the number of barbed ends, F-actin content, push the leading edge forward, and turn towards the chemoattractant source in an Arp2/3-dependent manner. Thus, showing that these guidance cues can activate Arp2/3 beyond it baseline activity level. On the other hand, our experiment with the repulsive guidance cue ephrin A2 show that reducing Arp2/3 activity beyond that baseline level will impair efficient chemorepulsive responses by growth cones. These results show that the broad and lamellar growth cones on L1 have a baseline level of Arp2/3 activity that is necessary for efficient guidance, since reducing it hampers chemorepulsion and increasing it is necessary for chemoattraction.

Similarly, we found that the compact and filopodial growth cones on laminin would have reduced F-actin levels after Arp2/3 inhibition, suggesting that this substrate also promotes a baseline level of Arp2/3 activity. However, Arp2/3 inhibition did not affect attractive or repulsive growth cone guidance on this substrate, suggesting that other ABP's can mediate the formation of barbed ends to support actin polymerization needed for correct guidance on laminin. For example, it would be possible that compact filopodial growth cones on laminin would not require veil protrusion for efficient guidance and that they not only use filopodia as sensory organelles to search for guidance cues, but that these are integral for their motile response, as well. It has been shown that attractive guidance cues can promote the formation of substrate adhesions, particularly at the end of filopodial tips. Therefore, it is possible that growth cone locomotion requires filopodial- and lamellar-based protrusions on laminin and L1, respectively. These

protrusions then anchor themselves to the substrate to allow growth cone advance through the action of myosin contractile activity.

In such a model, the signaling pathways activated by substrate receptors influence and limit the collection of active ABP's, which in turn dictate growth cone morphology and how it responds to the environment. On L1, growth cones use lamellar protrusions to steer towards or away from guidance cues, whereas on laminin they might require filopodial protrusions. Future experiments, will have to address how important are filopodial protrusion for migration and guidance on laminin. However, from our experiments with ERM proteins, we know that chemoattraction towards NGF and NT3 preferentially increases active ERM levels along filopodia and that inhibition of ERM activity abolishes chemoattraction. Thus, suggesting that the integrity of filopodial protrusions is required for correct chemoattraction on laminin.

Our in-vivo results show that the role of Arp2/3 during axon guidance is required in some tissues. We found that inhibition of Arp2/3 during sensory-motor innervation of the hindlimb led to deficiencies in the complexity and branching pattern of nerves throughout the hindlimb. Our experiments show that Arp2/3-inhibited axons can migrate down the hindlimb but that they have trouble branching off the main nerve to form smaller nerve branches. Similar results have been published before by Spillane et al (2011), where they found out that Arp2/3 inhibition impaired filopodia and axonal branch formation in spinal cord neurons. This finding is suggestive of impaired de-fasciculation off from the main nerve in response to guidance cues that promote branching during development. In our experiments, the retinotectal projections seem to be unaffected by Arp2/3 inhibition. However, at the stage at which we conducted our experiments there

were already RGC axons on their way to the tectum. This means that the neurons in which we inhibited Arp2/3 could have fasciculated onto older axons to reach the tectum, as opposed to finding their own way based on responses to guidance cues.

Our results expand on the limited body of knowledge on the actin nucleator Arp2/3 during growth cone guidance. We show that its role on growth cone guidance is substrate dependent, thus reconciling previous contradictory reports on the role of Arp2/3 in growth cones. However, we still need a comprehensive understanding of how Arp2/3 functions in growth cones during developmental guidance and what are the implications of our findings in-vivo, where the substrate is likely to be a composite of adhesive molecules. Moreover, we need a better understanding of Arp2/3 in other biological processes that we did not address in this thesis but are relevant to growth cone migration, such as: microtubule dynamics, endocytosis, vesicle trafficking, and membrane delivery to the leading edge. Additionally, we need detailed in-vivo studies that can clarify the role of Arp2/3 during axon guidance. Finally, it would be useful to know whether Arp2/3 activity could be manipulated to make growth cones bypass inhibitory cues, like our boundary assay with ephrin A2. Such a finding could encourage studies to address whether adult neurons with upregulated Arp2/3 activity could bypass the inhibitory environment of a lesion and improve their regenerative capacity.

References

Agius E, Sagot Y, Duprat AM, Cochard P (1996) Antibodies directed against the beta 1-integrin subunit and peptides containing the IKVAV sequence of laminin perturb neurite outgrowth of peripheral neurons on immature spinal cord substrata. Neuroscience 71:773-786.

Albers KM, Wright DE, Davis BM (1994) Overexpression of nerve growth factor in epidermis of transgenic mice causes hypertrophy of the peripheral nervous system. The Journal of neuroscience : the official journal of the Society for Neuroscience 14:1422-1432.

Allenspach EJ, Cullinan P, Tong J, Tang Q, Tesciuba AG, Cannon JL, Takahashi SM, Morgan R, Burkhardt JK, Sperling AI (2001) ERM-dependent movement of CD43 defines a novel protein complex distal to the immunological synapse. Immunity 15:739-750.

Amann KJ, Pollard TD (2001) Direct real-time observation of actin filament branching mediated by Arp2/3 complex using total internal reflection fluorescence microscopy. Proceedings of the National Academy of Sciences of the United States of America 98:15009-15013.

Amieva MR, Furthmayr H (1995) Subcellular localization of moesin in dynamic filopodia, retraction fibers, and other structures involved in substrate exploration, attachment, and cell-cell contacts. Experimental cell research 219:180-196.

Andrews TJ, Cowen T (1994) Nerve growth factor enhances the dendritic arborization of sympathetic ganglion cells undergoing atrophy in aged rats. Journal of neurocytology 23:234-241.

Andrianantoandro E, Pollard TD (2006) Mechanism of actin filament turnover by severing and nucleation at different concentrations of ADF/cofilin. Molecular cell 24:13-23.

Antoine-Bertrand J, Ghogha A, Luangrath V, Bedford FK, Lamarche-Vane N (2011) The activation of ezrin-radixin-moesin proteins is regulated by netrin-1 through Src kinase and RhoA/Rho kinase activities and mediates netrin-1-induced axon outgrowth. Molecular biology of the cell 22:3734-3746.

Bamburg JR (1999) Proteins of the ADF/cofilin family: essential regulators of actin dynamics. Annual review of cell and developmental biology 15:185-230.

Bard L, Boscher C, Lambert M, Mege RM, Choquet D, Thoumine O (2008) A molecular clutch between the actin flow and N-cadherin adhesions drives growth cone migration. The Journal of neuroscience : the official journal of the Society for Neuroscience 28:5879-5890.

Baum B, Kunda P (2005) Actin nucleation: spire - actin nucleator in a class of its own. Current biology : CB 15:R305-308.

Baumgartner M, Sillman AL, Blackwood EM, Srivastava J, Madson N, Schilling JW, Wright JH, Barber DL (2006) The Nck-interacting kinase phosphorylates ERM proteins for formation of lamellipodium by growth factors. Proceedings

of the National Academy of Sciences of the United States of America 103:13391-13396.
Bentley D, Toroian-Raymond A (1986) Disoriented pathfinding by pioneer neurone growth cones deprived of filopodia by cytochalasin treatment. Nature 323:712-715.
Bernard O (2007) Lim kinases, regulators of actin dynamics. The international journal of biochemistry & cell biology 39:1071-1076.
Betz T, Koch D, Lu YB, Franze K, Kas JA (2011) Growth cones as soft and weak force generators. Proceedings of the National Academy of Sciences of the United States of America 108:13420-13425.
Bibel M, Barde YA (2000) Neurotrophins: key regulators of cell fate and cell shape in the vertebrate nervous system. Genes & development 14:2919-2937.
Biyasheva A, Svitkina T, Kunda P, Baum B, Borisy G (2004) Cascade pathway of filopodia formation downstream of SCAR. Journal of cell science 117:837-848.
Blackmore M, Letourneau PC (2006) L1, beta1 integrin, and cadherins mediate axonal regeneration in the embryonic spinal cord. Journal of neurobiology 66:1564-1583.
Bovolenta P, Mason C (1987) Growth cone morphology varies with position in the developing mouse visual pathway from retina to first targets. The Journal of neuroscience : the official journal of the Society for Neuroscience 7:1447-1460.
Bresnick AR (1999) Molecular mechanisms of nonmuscle myosin-II regulation. Current opinion in cell biology 11:26-33.
Bretscher A, Edwards K, Fehon RG (2002) ERM proteins and merlin: integrators at the cell cortex. Nature reviews Molecular cell biology 3:586-599.
Bridgman PC, Dave S, Asnes CF, Tullio AN, Adelstein RS (2001) Myosin IIB is required for growth cone motility. The Journal of neuroscience : the official journal of the Society for Neuroscience 21:6159-6169.
Bugyi B, Carlier MF (2010) Control of actin filament treadmilling in cell motility. Annual review of biophysics 39:449-470.
Burden-Gulley SM, Lemmon V (1996) L1, N-cadherin, and laminin induce distinct distribution patterns of cytoskeletal elements in growth cones. Cell motility and the cytoskeleton 35:1-23.
Burden-Gulley SM, Payne HR, Lemmon V (1995) Growth cones are actively influenced by substrate-bound adhesion molecules. The Journal of neuroscience : the official journal of the Society for Neuroscience 15:4370-4381.
Butler B, Cooper JA (2009) Distinct roles for the actin nucleators Arp2/3 and hDia1 during NK-mediated cytotoxicity. Current biology : CB 19:1886-1896.
Campellone KG, Welch MD (2010) A nucleator arms race: cellular control of actin assembly. Nature reviews Molecular cell biology 11:237-251.
Campenot RB (1977) Local control of neurite development by nerve growth factor. Proceedings of the National Academy of Sciences of the United States of America 74:4516-4519.

Carlier MF, Ressad F, Pantaloni D (1999) Control of actin dynamics in cell motility. Role of ADF/cofilin. The Journal of biological chemistry 274:33827-33830.

Carlier MF, Laurent V, Santolini J, Melki R, Didry D, Xia GX, Hong Y, Chua NH, Pantaloni D (1997) Actin depolymerizing factor (ADF/cofilin) enhances the rate of filament turnover: implication in actin-based motility. The Journal of cell biology 136:1307-1322.

Carlstrom LP, Hines JH, Henle SJ, Henley JR (2011) Bidirectional remodeling of beta1-integrin adhesions during chemotropic regulation of nerve growth. BMC biology 9:82.

Castellani V, Chedotal A, Schachner M, Faivre-Sarrailh C, Rougon G (2000) Analysis of the L1-deficient mouse phenotype reveals cross-talk between Sema3A and L1 signaling pathways in axonal guidance. Neuron 27:237-249.

Castelo L, Jay DG (1999) Radixin is involved in lamellipodial stability during nerve growth cone motility. Molecular biology of the cell 10:1511-1520.

Chan AY, Raft S, Bailly M, Wyckoff JB, Segall JE, Condeelis JS (1998) EGF stimulates an increase in actin nucleation and filament number at the leading edge of the lamellipod in mammary adenocarcinoma cells. Journal of cell science 111 (Pt 2):199-211.

Chan CE, Odde DJ (2008) Traction dynamics of filopodia on compliant substrates. Science 322:1687-1691.

Chen L, Zhou S (2010) "CRASH"ing with the worm: insights into L1CAM functions and mechanisms. Developmental dynamics : an official publication of the American Association of Anatomists 239:1490-1501.

Chen Q, Chen TJ, Letourneau PC, Costa Lda F, Schubert D (2005) Modifier of cell adhesion regulates N-cadherin-mediated cell-cell adhesion and neurite outgrowth. The Journal of neuroscience : the official journal of the Society for Neuroscience 25:281-290.

Chen TJ, Gehler S, Shaw AE, Bamburg JR, Letourneau PC (2006) Cdc42 participates in the regulation of ADF/cofilin and retinal growth cone filopodia by brain derived neurotrophic factor. Journal of neurobiology 66:103-114.

Cheng HJ, Nakamoto M, Bergemann AD, Flanagan JG (1995) Complementary gradients in expression and binding of ELF-1 and Mek4 in development of the topographic retinotectal projection map. Cell 82:371-381.

Cheng L, Lemmon V (2004) Pathological missense mutations of neural cell adhesion molecule L1 affect neurite outgrowth and branching on an L1 substrate. Molecular and cellular neurosciences 27:522-530.

Cheng L, Itoh K, Lemmon V (2005) L1-mediated branching is regulated by two ezrin-radixin-moesin (ERM)-binding sites, the RSLE region and a novel juxtamembrane ERM-binding region. The Journal of neuroscience : the official journal of the Society for Neuroscience 25:395-403.

Choi CK, Vicente-Manzanares M, Zareno J, Whitmore LA, Mogilner A, Horwitz AR (2008) Actin and alpha-actinin orchestrate the assembly and maturation of nascent adhesions in a myosin II motor-independent manner. Nature cell biology 10:1039-1050.

Clegg DO, Wingerd KL, Hikita ST, Tolhurst EC (2003) Integrins in the development, function and dysfunction of the nervous system. Frontiers in bioscience : a journal and virtual library 8:d723-750.

Colavita A, Culotti JG (1998) Suppressors of ectopic UNC-5 growth cone steering identify eight genes involved in axon guidance in Caenorhabditis elegans. Developmental biology 194:72-85.

Conover JC, Yancopoulos GD (1997) Neurotrophin regulation of the developing nervous system: analyses of knockout mice. Reviews in the neurosciences 8:13-27.

Cooper JA, Buhle EL, Jr., Walker SB, Tsong TY, Pollard TD (1983) Kinetic evidence for a monomer activation step in actin polymerization. Biochemistry 22:2193-2202.

Craig EM, Van Goor D, Forscher P, Mogilner A (2012) Membrane tension, myosin force, and actin turnover maintain actin treadmill in the nerve growth cone. Biophysical journal 102:1503-1513.

Crowder RJ, Freeman RS (1998) Phosphatidylinositol 3-kinase and Akt protein kinase are necessary and sufficient for the survival of nerve growth factor-dependent sympathetic neurons. The Journal of neuroscience : the official journal of the Society for Neuroscience 18:2933-2943.

Crowley C, Spencer SD, Nishimura MC, Chen KS, Pitts-Meek S, Armanini MP, Ling LH, McMahon SB, Shelton DL, Levinson AD, et al. (1994) Mice lacking nerve growth factor display perinatal loss of sensory and sympathetic neurons yet develop basal forebrain cholinergic neurons. Cell 76:1001-1011.

Dahl JP, Wang-Dunlop J, Gonzales C, Goad ME, Mark RJ, Kwak SP (2003) Characterization of the WAVE1 knock-out mouse: implications for CNS development. The Journal of neuroscience : the official journal of the Society for Neuroscience 23:3343-3352.

Dang I et al. (2013) Inhibitory signalling to the Arp2/3 complex steers cell migration. Nature 503:281-284.

Davenport RW, Dou P, Rehder V, Kater SB (1993) A sensory role for neuronal growth cone filopodia. Nature 361:721-724.

de la Torre JR, Hopker VH, Ming GL, Poo MM, Tessier-Lavigne M, Hemmati-Brivanlou A, Holt CE (1997) Turning of retinal growth cones in a netrin-1 gradient mediated by the netrin receptor DCC. Neuron 19:1211-1224.

Deiner MS, Kennedy TE, Fazeli A, Serafini T, Tessier-Lavigne M, Sretavan DW (1997) Netrin-1 and DCC mediate axon guidance locally at the optic disc: loss of function leads to optic nerve hypoplasia. Neuron 19:575-589.

DeMali KA, Barlow CA, Burridge K (2002) Recruitment of the Arp2/3 complex to vinculin: coupling membrane protrusion to matrix adhesion. The Journal of cell biology 159:881-891.

Dent EW, Gupton SL, Gertler FB (2011) The growth cone cytoskeleton in axon outgrowth and guidance. Cold Spring Harbor perspectives in biology 3.

Dent EW, Barnes AM, Tang F, Kalil K (2004) Netrin-1 and semaphorin 3A promote or inhibit cortical axon branching, respectively, by reorganization of the

cytoskeleton. The Journal of neuroscience : the official journal of the Society for Neuroscience 24:3002-3012.

Dent EW, Kwiatkowski AV, Mebane LM, Philippar U, Barzik M, Rubinson DA, Gupton S, Van Veen JE, Furman C, Zhang J, Alberts AS, Mori S, Gertler FB (2007) Filopodia are required for cortical neurite initiation. Nature cell biology 9:1347-1359.

Di Nardo A, Cicchetti G, Falet H, Hartwig JH, Stossel TP, Kwiatkowski DJ (2005) Arp2/3 complex-deficient mouse fibroblasts are viable and have normal leading-edge actin structure and function. Proceedings of the National Academy of Sciences of the United States of America 102:16263-16268.

Dickson BJ (2001) Rho GTPases in growth cone guidance. Current opinion in neurobiology 11:103-110.

Dickson BJ (2002) Molecular mechanisms of axon guidance. Science 298:1959-1964.

Doherty P, Walsh FS (1996) CAM-FGF Receptor Interactions: A Model for Axonal Growth. Molecular and cellular neurosciences 8:99-111.

Dontchev VD, Letourneau PC (2002) Nerve growth factor and semaphorin 3A signaling pathways interact in regulating sensory neuronal growth cone motility. The Journal of neuroscience : the official journal of the Society for Neuroscience 22:6659-6669.

Dontchev VD, Letourneau PC (2003) Growth cones integrate signaling from multiple guidance cues. The journal of histochemistry and cytochemistry : official journal of the Histochemistry Society 51:435-444.

Duleh SN, Welch MD (2010) WASH and the Arp2/3 complex regulate endosome shape and trafficking. Cytoskeleton 67:193-206.

Dwivedy A, Gertler FB, Miller J, Holt CE, Lebrand C (2007) Ena/VASP function in retinal axons is required for terminal arborization but not pathway navigation. Development 134:2137-2146.

Elowe S, Holland SJ, Kulkarni S, Pawson T (2001) Downregulation of the Ras-mitogen-activated protein kinase pathway by the EphB2 receptor tyrosine kinase is required for ephrin-induced neurite retraction. Molecular and cellular biology 21:7429-7441.

Engle EC (2010) Human genetic disorders of axon guidance. Cold Spring Harbor perspectives in biology 2:a001784.

Ernst AF, Jurney WM, McLoon SC (1998) Mechanisms involved in development of retinotectal connections: roles of Eph receptor tyrosine kinases, NMDA receptors and nitric oxide. Progress in brain research 118:115-131.

Ernst AF, Wu HH, El-Fakahany EE, McLoon SC (1999) NMDA receptor-mediated refinement of a transient retinotectal projection during development requires nitric oxide. The Journal of neuroscience : the official journal of the Society for Neuroscience 19:229-235.

Ernst AF, Gallo G, Letourneau PC, McLoon SC (2000) Stabilization of growing retinal axons by the combined signaling of nitric oxide and brain-derived neurotrophic factor. The Journal of neuroscience : the official journal of the Society for Neuroscience 20:1458-1469.

Evsyukova I, Plestant C, Anton ES (2013) Integrative mechanisms of oriented neuronal migration in the developing brain. Annual review of cell and developmental biology 29:299-353.
Fass JN, Odde DJ (2003) Tensile force-dependent neurite elicitation via anti-beta1 integrin antibody-coated magnetic beads. Biophysical journal 85:623-636.
Flanagan LA, Ju YE, Marg B, Osterfield M, Janmey PA (2002) Neurite branching on deformable substrates. Neuroreport 13:2411-2415.
Frade JM, Barde YA (1998) Microglia-derived nerve growth factor causes cell death in the developing retina. Neuron 20:35-41.
Fransen E, Lemmon V, Van Camp G, Vits L, Coucke P, Willems PJ (1995) CRASH syndrome: clinical spectrum of corpus callosum hypoplasia, retardation, adducted thumbs, spastic paraparesis and hydrocephalus due to mutations in one single gene, L1. European journal of human genetics : EJHG 3:273-284.
Fujiwara I, Suetsugu S, Uemura S, Takenawa T, Ishiwata S (2002) Visualization and force measurement of branching by Arp2/3 complex and N-WASP in actin filament. Biochemical and biophysical research communications 293:1550-1555.
Galbraith CG, Yamada KM, Sheetz MP (2002) The relationship between force and focal complex development. The Journal of cell biology 159:695-705.
Gallo G (2008) Semaphorin 3A inhibits ERM protein phosphorylation in growth cone filopodia through inactivation of PI3K. Developmental neurobiology 68:926-933.
Gallo G, Letourneau PC (1998a) Localized sources of neurotrophins initiate axon collateral sprouting. The Journal of neuroscience : the official journal of the Society for Neuroscience 18:5403-5414.
Gallo G, Letourneau PC (1998b) Axon guidance: GTPases help axons reach their targets. Current biology : CB 8:R80-82.
Gallo G, Letourneau PC (2000) Neurotrophins and the dynamic regulation of the neuronal cytoskeleton. Journal of neurobiology 44:159-173.
Gallo G, Letourneau PC (2004) Regulation of growth cone actin filaments by guidance cues. Journal of neurobiology 58:92-102.
Gallo G, Lefcort FB, Letourneau PC (1997) The trkA receptor mediates growth cone turning toward a localized source of nerve growth factor. The Journal of neuroscience : the official journal of the Society for Neuroscience 17:5445-5454.
Gallo G, Yee HF, Jr., Letourneau PC (2002) Actin turnover is required to prevent axon retraction driven by endogenous actomyosin contractility. The Journal of cell biology 158:1219-1228.
Gautreau A, Poullet P, Louvard D, Arpin M (1999) Ezrin, a plasma membrane-microfilament linker, signals cell survival through the phosphatidylinositol 3-kinase/Akt pathway. Proceedings of the National Academy of Sciences of the United States of America 96:7300-7305.
Gehler S, Gallo G, Veien E, Letourneau PC (2004) p75 neurotrophin receptor signaling regulates growth cone filopodial dynamics through modulating

RhoA activity. The Journal of neuroscience : the official journal of the Society for Neuroscience 24:4363-4372.
Geraldo S, Gordon-Weeks PR (2009) Cytoskeletal dynamics in growth-cone steering. Journal of cell science 122:3595-3604.
Giancotti FG, Ruoslahti E (1999) Integrin signaling. Science 285:1028-1032.
Glebova NO, Ginty DD (2004) Heterogeneous requirement of NGF for sympathetic target innervation in vivo. The Journal of neuroscience : the official journal of the Society for Neuroscience 24:743-751.
Goldberg DJ (1988) Local role of Ca2+ in formation of veils in growth cones. The Journal of neuroscience : the official journal of the Society for Neuroscience 8:2596-2605.
Goldberg DJ, Burmeister DW (1986) Stages in axon formation: observations of growth of Aplysia axons in culture using video-enhanced contrast-differential interference contrast microscopy. The Journal of cell biology 103:1921-1931.
Goley ED, Welch MD (2006) The ARP2/3 complex: an actin nucleator comes of age. Nature reviews Molecular cell biology 7:713-726.
Gomez TM, Letourneau PC (1994) Filopodia initiate choices made by sensory neuron growth cones at laminin/fibronectin borders in vitro. The Journal of neuroscience : the official journal of the Society for Neuroscience 14:5959-5972.
Gomez TM, Letourneau PC (2013) Actin dynamics in growth cone motility and navigation. Journal of neurochemistry.
Gomez TM, Robles E, Poo M, Spitzer NC (2001) Filopodial calcium transients promote substrate-dependent growth cone turning. Science 291:1983-1987.
Gonzalez-Agosti C, Solomon F (1996) Response of radixin to perturbations of growth cone morphology and motility in chick sympathetic neurons in vitro. Cell motility and the cytoskeleton 34:122-136.
Grabham PW, Goldberg DJ (1997) Nerve growth factor stimulates the accumulation of beta1 integrin at the tips of filopodia in the growth cones of sympathetic neurons. The Journal of neuroscience : the official journal of the Society for Neuroscience 17:5455-5465.
Grabham PW, Foley M, Umeojiako A, Goldberg DJ (2000) Nerve growth factor stimulates coupling of beta1 integrin to distinct transport mechanisms in the filopodia of growth cones. Journal of cell science 113 (Pt 17):3003-3012.
Gundersen RW, Barrett JN (1979) Neuronal chemotaxis: chick dorsal-root axons turn toward high concentrations of nerve growth factor. Science 206:1079-1080.
Gupton SL, Gertler FB (2010) Integrin signaling switches the cytoskeletal and exocytic machinery that drives neuritogenesis. Developmental cell 18:725-736.
Halloran MC, Kalil K (1994) Dynamic behaviors of growth cones extending in the corpus callosum of living cortical brain slices observed with video microscopy. The Journal of neuroscience : the official journal of the Society for Neuroscience 14:2161-2177.

Hamelin M, Zhou Y, Su MW, Scott IM, Culotti JG (1993) Expression of the UNC-5 guidance receptor in the touch neurons of C. elegans steers their axons dorsally. Nature 364:327-330.
Hammarback JA, Letourneau PC (1986) Neurite extension across regions of low cell-substratum adhesivity: implications for the guidepost hypothesis of axonal pathfinding. Developmental biology 117:655-662.
Harborth J, Elbashir SM, Bechert K, Tuschl T, Weber K (2001) Identification of essential genes in cultured mammalian cells using small interfering RNAs. Journal of cell science 114:4557-4565.
Hayashi K, Yonemura S, Matsui T, Tsukita S (1999) Immunofluorescence detection of ezrin/radixin/moesin (ERM) proteins with their carboxyl-terminal threonine phosphorylated in cultured cells and tissues. Journal of cell science 112 (Pt 8):1149-1158.
Heidemann SR, Lamoureux P, Buxbaum RE (1990) Growth cone behavior and production of traction force. The Journal of cell biology 111:1949-1957.
Henson JH, Svitkina TM, Burns AR, Hughes HE, MacPartland KJ, Nazarian R, Borisy GG (1999) Two components of actin-based retrograde flow in sea urchin coelomocytes. Molecular biology of the cell 10:4075-4090.
Hines JH, Abu-Rub M, Henley JR (2010) Asymmetric endocytosis and remodeling of beta1-integrin adhesions during growth cone chemorepulsion by MAG. Nature neuroscience 13:829-837.
Hong K, Hinck L, Nishiyama M, Poo MM, Tessier-Lavigne M, Stein E (1999) A ligand-gated association between cytoplasmic domains of UNC5 and DCC family receptors converts netrin-induced growth cone attraction to repulsion. Cell 97:927-941.
Hopker VH, Shewan D, Tessier-Lavigne M, Poo M, Holt C (1999) Growth-cone attraction to netrin-1 is converted to repulsion by laminin-1. Nature 401:69-73.
Huber AB, Kolodkin AL, Ginty DD, Cloutier JF (2003) Signaling at the growth cone: ligand-receptor complexes and the control of axon growth and guidance. Annual review of neuroscience 26:509-563.
Hufner K, Higgs HN, Pollard TD, Jacobi C, Aepfelbacher M, Linder S (2001) The verprolin-like central (vc) region of Wiskott-Aldrich syndrome protein induces Arp2/3 complex-dependent actin nucleation. The Journal of biological chemistry 276:35761-35767.
Ichetovkin I, Han J, Pang KM, Knecht DA, Condeelis JS (2000) Actin filaments are severed by both native and recombinant dictyostelium cofilin but to different extents. Cell motility and the cytoskeleton 45:293-306.
Jeon S, Park JK, Bae CD, Park J (2010) NGF-induced moesin phosphorylation is mediated by the PI3K, Rac1 and Akt and required for neurite formation in PC12 cells. Neurochemistry international 56:810-818.
Jurney WM, Gallo G, Letourneau PC, McLoon SC (2002) Rac1-mediated endocytosis during ephrin-A2- and semaphorin 3A-induced growth cone collapse. The

Journal of neuroscience : the official journal of the Society for Neuroscience 22:6019-6028.
Kaethner RJ, Stuermer CA (1994) Growth behavior of retinotectal axons in live zebrafish embryos under TTX-induced neural impulse blockade. Journal of neurobiology 25:781-796.
Kalil K, Dent EW (2005) Touch and go: guidance cues signal to the growth cone cytoskeleton. Current opinion in neurobiology 15:521-526.
Kamiguchi H, Lemmon V (1997) Neural cell adhesion molecule L1: signaling pathways and growth cone motility. Journal of neuroscience research 49:1-8.
Kennedy TE, Serafini T, de la Torre JR, Tessier-Lavigne M (1994) Netrins are diffusible chemotropic factors for commissural axons in the embryonic spinal cord. Cell 78:425-435.
Kennedy TE, Wang H, Marshall W, Tessier-Lavigne M (2006) Axon guidance by diffusible chemoattractants: a gradient of netrin protein in the developing spinal cord. The Journal of neuroscience : the official journal of the Society for Neuroscience 26:8866-8874.
Ketschek AR, Jones SL, Gallo G (2007) Axon extension in the fast and slow lanes: substratum-dependent engagement of myosin II functions. Developmental neurobiology 67:1305-1320.
Kholmanskikh SS, Dobrin JS, Wynshaw-Boris A, Letourneau PC, Ross ME (2003) Disregulated RhoGTPases and actin cytoskeleton contribute to the migration defect in Lis1-deficient neurons. The Journal of neuroscience : the official journal of the Society for Neuroscience 23:8673-8681.
Kim MD, Kamiyama D, Kolodziej P, Hing H, Chiba A (2003) Isolation of Rho GTPase effector pathways during axon development. Developmental biology 262:282-293.
Kiryushko D, Berezin V, Bock E (2004) Regulators of neurite outgrowth: role of cell adhesion molecules. Annals of the New York Academy of Sciences 1014:140-154.
Kolodkin AL, Tessier-Lavigne M (2011) Mechanisms and molecules of neuronal wiring: a primer. Cold Spring Harbor perspectives in biology 3.
Kolodziej PA, Timpe LC, Mitchell KJ, Fried SR, Goodman CS, Jan LY, Jan YN (1996) frazzled encodes a Drosophila member of the DCC immunoglobulin subfamily and is required for CNS and motor axon guidance. Cell 87:197-204.
Korobova F, Svitkina T (2008) Arp2/3 complex is important for filopodia formation, growth cone motility, and neuritogenesis in neuronal cells. Molecular biology of the cell 19:1561-1574.
Kurisu S, Takenawa T (2009) The WASP and WAVE family proteins. Genome biology 10:226.
Kwiatkowski AV, Rubinson DA, Dent EW, Edward van Veen J, Leslie JD, Zhang J, Mebane LM, Philippar U, Pinheiro EM, Burds AA, Bronson RT, Mori S, Fassler R, Gertler FB (2007) Ena/VASP Is Required for neuritogenesis in the developing cortex. Neuron 56:441-455.

Lai Wing Sun K, Correia JP, Kennedy TE (2011) Netrins: versatile extracellular cues with diverse functions. Development 138:2153-2169.

Lambert M, Choquet D, Mege RM (2002) Dynamics of ligand-induced, Rac1-dependent anchoring of cadherins to the actin cytoskeleton. The Journal of cell biology 157:469-479.

Lanier LM, Gates MA, Witke W, Menzies AS, Wehman AM, Macklis JD, Kwiatkowski D, Soriano P, Gertler FB (1999) Mena is required for neurulation and commissure formation. Neuron 22:313-325.

Lebrand C, Dent EW, Strasser GA, Lanier LM, Krause M, Svitkina TM, Borisy GG, Gertler FB (2004) Critical role of Ena/VASP proteins for filopodia formation in neurons and in function downstream of netrin-1. Neuron 42:37-49.

Lee AC, Suter DM (2008) Quantitative analysis of microtubule dynamics during adhesion-mediated growth cone guidance. Developmental neurobiology 68:1363-1377.

Lee JS, Chien CB (2004) When sugars guide axons: insights from heparan sulphate proteoglycan mutants. Nature reviews Genetics 5:923-935.

Lemmon V, McLoon SC (1986) The appearance of an L1-like molecule in the chick primary visual pathway. The Journal of neuroscience : the official journal of the Society for Neuroscience 6:2987-2994.

Letourneau PC, Cypher C (1991) Regulation of growth cone motility. Cell motility and the cytoskeleton 20:267-271.

Letourneau PC, Shattuck TA, Roche FK, Takeichi M, Lemmon V (1990) Nerve growth cone migration onto Schwann cells involves the calcium-dependent adhesion molecule, N-cadherin. Developmental biology 138:430-442.

Levi-Montalcini R, Booker B (1960) Destruction of the Sympathetic Ganglia in Mammals by an Antiserum to a Nerve-Growth Protein. Proceedings of the National Academy of Sciences of the United States of America 46:384-391.

Li X, Saint-Cyr-Proulx E, Aktories K, Lamarche-Vane N (2002) Rac1 and Cdc42 but not RhoA or Rho kinase activities are required for neurite outgrowth induced by the Netrin-1 receptor DCC (deleted in colorectal cancer) in N1E-115 neuroblastoma cells. The Journal of biological chemistry 277:15207-15214.

Lin CH, Forscher P (1993) Cytoskeletal remodeling during growth cone-target interactions. The Journal of cell biology 121:1369-1383.

Lin CH, Espreafico EM, Mooseker MS, Forscher P (1996) Myosin drives retrograde F-actin flow in neuronal growth cones. Neuron 16:769-782.

Liu RY, Schmid RS, Snider WD, Maness PF (2002) NGF enhances sensory axon growth induced by laminin but not by the L1 cell adhesion molecule. Molecular and cellular neurosciences 20:2-12.

Lowery LA, Van Vactor D (2009) The trip of the tip: understanding the growth cone machinery. Nature reviews Molecular cell biology 10:332-343.

Machesky LM, Insall RH (1998) Scar1 and the related Wiskott-Aldrich syndrome protein, WASP, regulate the actin cytoskeleton through the Arp2/3 complex. Current biology : CB 8:1347-1356.

Madrid R, Aranda JF, Rodriguez-Fraticelli AE, Ventimiglia L, Andres-Delgado L, Shehata M, Fanayan S, Shahheydari H, Gomez S, Jimenez A, Martin-Belmonte F, Byrne JA, Alonso MA (2010) The formin INF2 regulates basolateral-to-apical transcytosis and lumen formation in association with Cdc42 and MAL2. Developmental cell 18:814-827.

Maness PF, Schachner M (2007) Neural recognition molecules of the immunoglobulin superfamily: signaling transducers of axon guidance and neuronal migration. Nature neuroscience 10:19-26.

Marsick BM, Letourneau PC (2011) Labeling F-actin barbed ends with rhodamine-actin in permeabilized neuronal growth cones. J Vis Exp.

Marsick BM, San Miguel-Ruiz JE, Letourneau PC (2012a) Activation of ezrin/radixin/moesin mediates attractive growth cone guidance through regulation of growth cone actin and adhesion receptors. The Journal of neuroscience : the official journal of the Society for Neuroscience 32:282-296.

Marsick BM, Roche FK, Letourneau PC (2012b) Repulsive axon guidance cues ephrin-A2 and slit3 stop protrusion of the growth cone leading margin concurrently with inhibition of ADF/cofilin and ERM proteins. Cytoskeleton 69:496-505.

Marsick BM, Flynn KC, Santiago-Medina M, Bamburg JR, Letourneau PC (2010) Activation of ADF/cofilin mediates attractive growth cone turning toward nerve growth factor and netrin-1. Developmental neurobiology 70:565-588.

Mason C, Erskine L (2000) Growth cone form, behavior, and interactions in vivo: retinal axon pathfinding as a model. Journal of neurobiology 44:260-270.

Mason CA, Wang LC (1997) Growth cone form is behavior-specific and, consequently, position-specific along the retinal axon pathway. The Journal of neuroscience : the official journal of the Society for Neuroscience 17:1086-1100.

Matsui T, Yonemura S, Tsukita S, Tsukita S (1999) Activation of ERM proteins in vivo by Rho involves phosphatidyl-inositol 4-phosphate 5-kinase and not ROCK kinases. Current biology : CB 9:1259-1262.

McClatchey AI, Fehon RG (2009) Merlin and the ERM proteins--regulators of receptor distribution and signaling at the cell cortex. Trends in cell biology 19:198-206.

McKerracher L, Chamoux M, Arregui CO (1996) Role of laminin and integrin interactions in growth cone guidance. Molecular neurobiology 12:95-116.

McLoon LK, McLoon SC (1988) Schwann cell-conditioned medium promotes neurite outgrowth from explants of fetal rat retina and tectum in vitro. Brain research 467:61-68.

McLoon SC, McLoon LK, Palm SL, Furcht LT (1988) Transient expression of laminin in the optic nerve of the developing rat. The Journal of neuroscience : the official journal of the Society for Neuroscience 8:1981-1990.

Meberg PJ (2000) Signal-regulated ADF/cofilin activity and growth cone motility. Molecular neurobiology 21:97-107.

Medeiros NA, Burnette DT, Forscher P (2006) Myosin II functions in actin-bundle turnover in neuronal growth cones. Nature cell biology 8:215-226.

Meriane M, Tcherkezian J, Webber CA, Danek EI, Triki I, McFarlane S, Bloch-Gallego E, Lamarche-Vane N (2004) Phosphorylation of DCC by Fyn mediates Netrin-1 signaling in growth cone guidance. The Journal of cell biology 167:687-698.

Merrifield CJ, Qualmann B, Kessels MM, Almers W (2004) Neural Wiskott Aldrich Syndrome Protein (N-WASP) and the Arp2/3 complex are recruited to sites of clathrin-mediated endocytosis in cultured fibroblasts. Eur J Cell Biol 83:13-18.

Mey J, Thanos S (1992) Development of the visual system of the chick--a review. Journal fur Hirnforschung 33:673-702.

Mey J, Thanos S (2000) Development of the visual system of the chick. I. Cell differentiation and histogenesis. Brain research Brain research reviews 32:343-379.

Miao H, Burnett E, Kinch M, Simon E, Wang B (2000) Activation of EphA2 kinase suppresses integrin function and causes focal-adhesion-kinase dephosphorylation. Nature cell biology 2:62-69.

Miao H, Wei BR, Peehl DM, Li Q, Alexandrou T, Schelling JR, Rhim JS, Sedor JR, Burnett E, Wang B (2001) Activation of EphA receptor tyrosine kinase inhibits the Ras/MAPK pathway. Nature cell biology 3:527-530.

Ming GL, Song HJ, Berninger B, Holt CE, Tessier-Lavigne M, Poo MM (1997) cAMP-dependent growth cone guidance by netrin-1. Neuron 19:1225-1235.

Mintz CD, Dickson TC, Gripp ML, Salton SR, Benson DL (2003) ERMs colocalize transiently with L1 during neocortical axon outgrowth. The Journal of comparative neurology 464:438-448.

Mintz CD, Carcea I, McNickle DG, Dickson TC, Ge Y, Salton SR, Benson DL (2008) ERM proteins regulate growth cone responses to Sema3A. The Journal of comparative neurology 510:351-366.

Mitchell KJ, Doyle JL, Serafini T, Kennedy TE, Tessier-Lavigne M, Goodman CS, Dickson BJ (1996) Genetic analysis of Netrin genes in Drosophila: Netrins guide CNS commissural axons and peripheral motor axons. Neuron 17:203-215.

Mitchison T, Kirschner M (1988) Cytoskeletal dynamics and nerve growth. Neuron 1:761-772.

Mongiu AK, Weitzke EL, Chaga OY, Borisy GG (2007) Kinetic-structural analysis of neuronal growth cone veil motility. Journal of cell science 120:1113-1125.

Monschau B, Kremoser C, Ohta K, Tanaka H, Kaneko T, Yamada T, Handwerker C, Hornberger MR, Loschinger J, Pasquale EB, Siever DA, Verderame MF, Muller BK, Bonhoeffer F, Drescher U (1997) Shared and distinct functions of RAGS and ELF-1 in guiding retinal axons. The EMBO journal 16:1258-1267.

Moreau V, Galan JM, Devilliers G, Haguenauer-Tsapis R, Winsor B (1997) The yeast actin-related protein Arp2p is required for the internalization step of endocytosis. Molecular biology of the cell 8:1361-1375.

Mukai Y, Iwaya K, Ogawa H, Mukai K (2005) Involvement of Arp2/3 complex in MCP-1-induced chemotaxis. Biochemical and biophysical research communications 334:395-402.

Mullins RD, Stafford WF, Pollard TD (1997) Structure, subunit topology, and actin-binding activity of the Arp2/3 complex from Acanthamoeba. The Journal of cell biology 136:331-343.

Mullins RD, Heuser JA, Pollard TD (1998) The interaction of Arp2/3 complex with actin: nucleation, high affinity pointed end capping, and formation of branching networks of filaments. Proceedings of the National Academy of Sciences of the United States of America 95:6181-6186.

Myers JP, Gomez TM (2011) Focal adhesion kinase promotes integrin adhesion dynamics necessary for chemotropic turning of nerve growth cones. The Journal of neuroscience : the official journal of the Society for Neuroscience 31:13585-13595.

Myers JP, Robles E, Ducharme-Smith A, Gomez TM (2012) Focal adhesion kinase modulates Cdc42 activity downstream of positive and negative axon guidance cues. Journal of cell science 125:2918-2929.

Nakamura N, Oshiro N, Fukata Y, Amano M, Fukata M, Kuroda S, Matsuura Y, Leung T, Lim L, Kaibuchi K (2000) Phosphorylation of ERM proteins at filopodia induced by Cdc42. Genes to cells : devoted to molecular & cellular mechanisms 5:571-581.

Nakamura Y, Lee S, Haddox CL, Weaver EJ, Lemmon VP (2010) Role of the cytoplasmic domain of the L1 cell adhesion molecule in brain development. The Journal of comparative neurology 518:1113-1132.

Neugebauer KM, Tomaselli KJ, Lilien J, Reichardt LF (1988) N-cadherin, NCAM, and integrins promote retinal neurite outgrowth on astrocytes in vitro. The Journal of cell biology 107:1177-1187.

Ng J, Luo L (2004) Rho GTPases regulate axon growth through convergent and divergent signaling pathways. Neuron 44:779-793.

Niggli V, Rossy J (2008) Ezrin/radixin/moesin: versatile controllers of signaling molecules and of the cortical cytoskeleton. The international journal of biochemistry & cell biology 40:344-349.

Nishimura K, Yoshihara F, Tojima T, Ooashi N, Yoon W, Mikoshiba K, Bennett V, Kamiguchi H (2003) L1-dependent neuritogenesis involves ankyrinB that mediates L1-CAM coupling with retrograde actin flow. The Journal of cell biology 163:1077-1088.

Nolen BJ, Tomasevic N, Russell A, Pierce DW, Jia Z, McCormick CD, Hartman J, Sakowicz R, Pollard TD (2009) Characterization of two classes of small molecule inhibitors of Arp2/3 complex. Nature 460:1031-1034.

Norris AD, Dyer JO, Lundquist EA (2009) The Arp2/3 complex, UNC-115/abLIM, and UNC-34/Enabled regulate axon guidance and growth cone filopodia formation in Caenorhabditis elegans. Neural development 4:38.

O'Connor TP, Duerr JS, Bentley D (1990) Pioneer growth cone steering decisions mediated by single filopodial contacts in situ. The Journal of neuroscience : the official journal of the Society for Neuroscience 10:3935-3946.
Ooashi N, Futatsugi A, Yoshihara F, Mikoshiba K, Kamiguchi H (2005) Cell adhesion molecules regulate Ca2+-mediated steering of growth cones via cyclic AMP and ryanodine receptor type 3. The Journal of cell biology 170:1159-1167.
Oshiro N, Fukata Y, Kaibuchi K (1998) Phosphorylation of moesin by rho-associated kinase (Rho-kinase) plays a crucial role in the formation of microvilli-like structures. The Journal of biological chemistry 273:34663-34666.
Paglini G, Kunda P, Quiroga S, Kosik K, Caceres A (1998) Suppression of radixin and moesin alters growth cone morphology, motility, and process formation in primary cultured neurons. The Journal of cell biology 143:443-455.
Pak CW, Flynn KC, Bamburg JR (2008) Actin-binding proteins take the reins in growth cones. Nature reviews Neuroscience 9:136-147.
Parra LM, Zou Y (2010) Sonic hedgehog induces response of commissural axons to Semaphorin repulsion during midline crossing. Nature neuroscience 13:29-35.
Patel TD, Jackman A, Rice FL, Kucera J, Snider WD (2000) Development of sensory neurons in the absence of NGF/TrkA signaling in vivo. Neuron 25:345-357.
Payne HR, Burden SM, Lemmon V (1992) Modulation of growth cone morphology by substrate-bound adhesion molecules. Cell motility and the cytoskeleton 21:65-73.
Pfender S, Kuznetsov V, Pleiser S, Kerkhoff E, Schuh M (2011) Spire-type actin nucleators cooperate with Formin-2 to drive asymmetric oocyte division. Current biology : CB 21:955-960.
Pietromonaco SF, Simons PC, Altman A, Elias L (1998) Protein kinase C-theta phosphorylation of moesin in the actin-binding sequence. The Journal of biological chemistry 273:7594-7603.
Pollard TD (1986) Rate constants for the reactions of ATP- and ADP-actin with the ends of actin filaments. The Journal of cell biology 103:2747-2754.
Pollard TD (2007) Regulation of actin filament assembly by Arp2/3 complex and formins. Annual review of biophysics and biomolecular structure 36:451-477.
Pollard TD, Blanchoin L, Mullins RD (2000) Molecular mechanisms controlling actin filament dynamics in nonmuscle cells. Annual review of biophysics and biomolecular structure 29:545-576.
Rajagopalan S, Vivancos V, Nicolas E, Dickson BJ (2000) Selecting a longitudinal pathway: Robo receptors specify the lateral position of axons in the Drosophila CNS. Cell 103:1033-1045.
Ranscht B (2000) Cadherins: molecular codes for axon guidance and synapse formation. International journal of developmental neuroscience : the official journal of the International Society for Developmental Neuroscience 18:643-651.

Rathjen FG, Schachner M (1984) Immunocytological and biochemical characterization of a new neuronal cell surface component (L1 antigen) which is involved in cell adhesion. The EMBO journal 3:1-10.

Reichardt LF, Tomaselli KJ (1991) Extracellular matrix molecules and their receptors: functions in neural development. Annual review of neuroscience 14:531-570.

Ren XR, Ming GL, Xie Y, Hong Y, Sun DM, Zhao ZQ, Feng Z, Wang Q, Shim S, Chen ZF, Song HJ, Mei L, Xiong WC (2004) Focal adhesion kinase in netrin-1 signaling. Nature neuroscience 7:1204-1212.

Rice FL, Albers KM, Davis BM, Silos-Santiago I, Wilkinson GA, LeMaster AM, Ernfors P, Smeyne RJ, Aldskogius H, Phillips HS, Barbacid M, DeChiara TM, Yancopoulos GD, Dunne CE, Fundin BT (1998) Differential dependency of unmyelinated and A delta epidermal and upper dermal innervation on neurotrophins, trk receptors, and p75LNGFR. Developmental biology 198:57-81.

Robles E, Huttenlocher A, Gomez TM (2003) Filopodial calcium transients regulate growth cone motility and guidance through local activation of calpain. Neuron 38:597-609.

Roche FK, Marsick BM, Letourneau PC (2009) Protein synthesis in distal axons is not required for growth cone responses to guidance cues. The Journal of neuroscience : the official journal of the Society for Neuroscience 29:638-652.

Rogers SL, Edson KJ, Letourneau PC, McLoon SC (1986) Distribution of laminin in the developing peripheral nervous system of the chick. Developmental biology 113:429-435.

Rohatgi R, Ho HY, Kirschner MW (2000) Mechanism of N-WASP activation by CDC42 and phosphatidylinositol 4, 5-bisphosphate. The Journal of cell biology 150:1299-1310.

Rose R, Weyand M, Lammers M, Ishizaki T, Ahmadian MR, Wittinghofer A (2005) Structural and mechanistic insights into the interaction between Rho and mammalian Dia. Nature 435:513-518.

Rozelle AL, Machesky LM, Yamamoto M, Driessens MH, Insall RH, Roth MG, Luby-Phelps K, Marriott G, Hall A, Yin HL (2000) Phosphatidylinositol 4,5-bisphosphate induces actin-based movement of raft-enriched vesicles through WASP-Arp2/3. Current biology : CB 10:311-320.

Sabatier C, Plump AS, Le M, Brose K, Tamada A, Murakami F, Lee EY, Tessier-Lavigne M (2004) The divergent Robo family protein rig-1/Robo3 is a negative regulator of slit responsiveness required for midline crossing by commissural axons. Cell 117:157-169.

Sakurai T, Gil OD, Whittard JD, Gazdoiu M, Joseph T, Wu J, Waksman A, Benson DL, Salton SR, Felsenfeld DP (2008) Interactions between the L1 cell adhesion molecule and ezrin support traction-force generation and can be regulated by tyrosine phosphorylation. Journal of neuroscience research 86:2602-2614.

Sanes JR, Lichtman JW (1999) Development of the vertebrate neuromuscular junction. Annual review of neuroscience 22:389-442.

Santiago-Medina M, Gregus KA, Gomez TM (2013) PAK-PIX interactions regulate adhesion dynamics and membrane protrusion to control neurite outgrowth. Journal of cell science 126:1122-1133.

Sawa M, Suetsugu S, Sugimoto A, Miki H, Yamamoto M, Takenawa T (2003) Essential role of the C. elegans Arp2/3 complex in cell migration during ventral enclosure. Journal of cell science 116:1505-1518.

Schmid RS, Pruitt WM, Maness PF (2000) A MAP kinase-signaling pathway mediates neurite outgrowth on L1 and requires Src-dependent endocytosis. The Journal of neuroscience : the official journal of the Society for Neuroscience 20:4177-4188.

Serafini T, Colamarino SA, Leonardo ED, Wang H, Beddington R, Skarnes WC, Tessier-Lavigne M (1996) Netrin-1 is required for commissural axon guidance in the developing vertebrate nervous system. Cell 87:1001-1014.

Serrels B, Serrels A, Brunton VG, Holt M, McLean GW, Gray CH, Jones GE, Frame MC (2007) Focal adhesion kinase controls actin assembly via a FERM-mediated interaction with the Arp2/3 complex. Nature cell biology 9:1046-1056.

Shakir MA, Jiang K, Struckhoff EC, Demarco RS, Patel FB, Soto MC, Lundquist EA (2008) The Arp2/3 activators WAVE and WASP have distinct genetic interactions with Rac GTPases in Caenorhabditis elegans axon guidance. Genetics 179:1957-1971.

Shamah SM, Lin MZ, Goldberg JL, Estrach S, Sahin M, Hu L, Bazalakova M, Neve RL, Corfas G, Debant A, Greenberg ME (2001) EphA receptors regulate growth cone dynamics through the novel guanine nucleotide exchange factor ephexin. Cell 105:233-244.

Shapiro L, Weis WI (2009) Structure and biochemistry of cadherins and catenins. Cold Spring Harbor perspectives in biology 1:a003053.

Shekarabi M, Moore SW, Tritsch NX, Morris SJ, Bouchard JF, Kennedy TE (2005) Deleted in colorectal cancer binding netrin-1 mediates cell substrate adhesion and recruits Cdc42, Rac1, Pak1, and N-WASP into an intracellular signaling complex that promotes growth cone expansion. The Journal of neuroscience : the official journal of the Society for Neuroscience 25:3132-3141.

Shewan D, Dwivedy A, Anderson R, Holt CE (2002) Age-related changes underlie switch in netrin-1 responsiveness as growth cones advance along visual pathway. Nature neuroscience 5:955-962.

Shimada T, Toriyama M, Uemura K, Kamiguchi H, Sugiura T, Watanabe N, Inagaki N (2008) Shootin1 interacts with actin retrograde flow and L1-CAM to promote axon outgrowth. The Journal of cell biology 181:817-829.

Shirasaki R, Katsumata R, Murakami F (1998) Change in chemoattractant responsiveness of developing axons at an intermediate target. Science 279:105-107.

Sigal YJ, Quintero OA, Cheney RE, Morris AJ (2007) Cdc42 and ARP2/3-independent regulation of filopodia by an integral membrane lipid-phosphatase-related protein. Journal of cell science 120:340-352.

Sit ST, Manser E (2011) Rho GTPases and their role in organizing the actin cytoskeleton. Journal of cell science 124:679-683.

Snider WD (1988) Nerve growth factor enhances dendritic arborization of sympathetic ganglion cells in developing mammals. The Journal of neuroscience : the official journal of the Society for Neuroscience 8:2628-2634.

Snow DM, Letourneau PC (1992) Neurite outgrowth on a step gradient of chondroitin sulfate proteoglycan (CS-PG). Journal of neurobiology 23:322-336.

Sofroniew MV, Howe CL, Mobley WC (2001) Nerve growth factor signaling, neuroprotection, and neural repair. Annual review of neuroscience 24:1217-1281.

Spillane M, Ketschek A, Jones SL, Korobova F, Marsick B, Lanier L, Svitkina T, Gallo G (2011) The actin nucleating Arp2/3 complex contributes to the formation of axonal filopodia and branches through the regulation of actin patch precursors to filopodia. Developmental neurobiology 71:747-758.

Steketee MB, Tosney KW (2002) Three functionally distinct adhesions in filopodia: shaft adhesions control lamellar extension. The Journal of neuroscience : the official journal of the Society for Neuroscience 22:8071-8083.

Strasser GA, Rahim NA, VanderWaal KE, Gertler FB, Lanier LM (2004) Arp2/3 is a negative regulator of growth cone translocation. Neuron 43:81-94.

Suh LH, Oster SF, Soehrman SS, Grenningloh G, Sretavan DW (2004) L1/Laminin modulation of growth cone response to EphB triggers growth pauses and regulates the microtubule destabilizing protein SCG10. The Journal of neuroscience : the official journal of the Society for Neuroscience 24:1976-1986.

Suraneni P, Rubinstein B, Unruh JR, Durnin M, Hanein D, Li R (2012) The Arp2/3 complex is required for lamellipodia extension and directional fibroblast cell migration. The Journal of cell biology 197:239-251.

Suter DM, Forscher P (2000) Substrate-cytoskeletal coupling as a mechanism for the regulation of growth cone motility and guidance. Journal of neurobiology 44:97-113.

Suter DM, Forscher P (2001) Transmission of growth cone traction force through apCAM-cytoskeletal linkages is regulated by Src family tyrosine kinase activity. The Journal of cell biology 155:427-438.

Suter DM, Errante LD, Belotserkovsky V, Forscher P (1998) The Ig superfamily cell adhesion molecule, apCAM, mediates growth cone steering by substrate-cytoskeletal coupling. The Journal of cell biology 141:227-240.

Svitkina TM, Bulanova EA, Chaga OY, Vignjevic DM, Kojima S, Vasiliev JM, Borisy GG (2003) Mechanism of filopodia initiation by reorganization of a dendritic network. The Journal of cell biology 160:409-421.

Tanaka E, Ho T, Kirschner MW (1995) The role of microtubule dynamics in growth cone motility and axonal growth. The Journal of cell biology 128:139-155.

Tang P, Cao C, Xu M, Zhang L (2007) Cytoskeletal protein radixin activates integrin alpha(M)beta(2) by binding to its cytoplasmic tail. FEBS letters 581:1103-1108.

Taunton J, Rowning BA, Coughlin ML, Wu M, Moon RT, Mitchison TJ, Larabell CA (2000) Actin-dependent propulsion of endosomes and lysosomes by recruitment of N-WASP. The Journal of cell biology 148:519-530.

Thanos S, Mey J (2001) Development of the visual system of the chick. II. Mechanisms of axonal guidance. Brain research Brain research reviews 35:205-245.

Thievessen I, Thompson PM, Berlemont S, Plevock KM, Plotnikov SV, Zemljic-Harpf A, Ross RS, Davidson MW, Danuser G, Campbell SL, Waterman CM (2013) Vinculin-actin interaction couples actin retrograde flow to focal adhesions, but is dispensable for focal adhesion growth. The Journal of cell biology 202:163-177.

Tojima T, Itofusa R, Kamiguchi H (2009) The nitric oxide-cGMP pathway controls the directional polarity of growth cone guidance via modulating cytosolic Ca2+ signals. The Journal of neuroscience : the official journal of the Society for Neuroscience 29:7886-7897.

Tsukita S, Hieda Y, Tsukita S (1989) A new 82-kD barbed end-capping protein (radixin) localized in the cell-to-cell adherens junction: purification and characterization. The Journal of cell biology 108:2369-2382.

Tsukita S, Yonemura S, Tsukita S (1997) ERM proteins: head-to-tail regulation of actin-plasma membrane interaction. Trends in biochemical sciences 22:53-58.

van der Gucht J, Paluch E, Plastino J, Sykes C (2005) Stress release drives symmetry breaking for actin-based movement. Proceedings of the National Academy of Sciences of the United States of America 102:7847-7852.

Vergara MN, Canto-Soler MV (2012) Rediscovering the chick embryo as a model to study retinal development. Neural development 7:22.

Wahl S, Barth H, Ciossek T, Aktories K, Mueller BK (2000) Ephrin-A5 induces collapse of growth cones by activating Rho and Rho kinase. The Journal of cell biology 149:263-270.

Waites CL, Craig AM, Garner CC (2005) Mechanisms of vertebrate synaptogenesis. Annual review of neuroscience 28:251-274.

Walter J, Kern-Veits B, Huf J, Stolze B, Bonhoeffer F (1987) Recognition of position-specific properties of tectal cell membranes by retinal axons in vitro. Development 101:685-696.

Wang Q, Wadsworth WG (2002) The C domain of netrin UNC-6 silences calcium/calmodulin-dependent protein kinase- and diacylglycerol-dependent axon branching in Caenorhabditis elegans. The Journal of neuroscience : the official journal of the Society for Neuroscience 22:2274-2282.

Wang X, Kweon J, Larson S, Chen L (2005) A role for the C. elegans L1CAM homologue lad-1/sax-7 in maintaining tissue attachment. Developmental biology 284:273-291.

Wang X, Zhang W, Cheever T, Schwarz V, Opperman K, Hutter H, Koepp D, Chen L (2008) The C. elegans L1CAM homologue LAD-2 functions as a coreceptor in MAB-20/Sema2 mediated axon guidance. The Journal of cell biology 180:233-246.

Wegner AM, Nebhan CA, Hu L, Majumdar D, Meier KM, Weaver AM, Webb DJ (2008) N-wasp and the arp2/3 complex are critical regulators of actin in the development of dendritic spines and synapses. The Journal of biological chemistry 283:15912-15920.

Weinl C, Drescher U, Lang S, Bonhoeffer F, Loschinger J (2003) On the turning of Xenopus retinal axons induced by ephrin-A5. Development 130:1635-1643.

Wellington A, Emmons S, James B, Calley J, Grover M, Tolias P, Manseau L (1999) Spire contains actin binding domains and is related to ascidian posterior end mark-5. Development 126:5267-5274.

Wiencken-Barger AE, Mavity-Hudson J, Bartsch U, Schachner M, Casagrande VA (2004) The role of L1 in axon pathfinding and fasciculation. Cerebral cortex 14:121-131.

Wolfenson H, Bershadsky A, Henis YI, Geiger B (2011) Actomyosin-generated tension controls the molecular kinetics of focal adhesions. Journal of cell science 124:1425-1432.

Woo S, Gomez TM (2006) Rac1 and RhoA promote neurite outgrowth through formation and stabilization of growth cone point contacts. The Journal of neuroscience : the official journal of the Society for Neuroscience 26:1418-1428.

Wu C, Asokan SB, Berginski ME, Haynes EM, Sharpless NE, Griffith JD, Gomez SM, Bear JE (2012) Arp2/3 is critical for lamellipodia and response to extracellular matrix cues but is dispensable for chemotaxis. Cell 148:973-987.

Yamada T, Okafuji T, Ohta K, Handwerker C, Drescher U, Tanaka H (2001) Analysis of ephrin-A2 in the chick retinotectal projection using a function-blocking monoclonal antibody. Journal of neurobiology 47:245-254.

Yang N, Higuchi O, Ohashi K, Nagata K, Wada A, Kangawa K, Nishida E, Mizuno K (1998) Cofilin phosphorylation by LIM-kinase 1 and its role in Rac-mediated actin reorganization. Nature 393:809-812.

Yang Q, Zhang XF, Pollard TD, Forscher P (2012) Arp2/3 complex-dependent actin networks constrain myosin II function in driving retrograde actin flow. The Journal of cell biology 197:939-956.

Yonemura S, Matsui T, Tsukita S, Tsukita S (2002) Rho-dependent and -independent activation mechanisms of ezrin/radixin/moesin proteins: an essential role for polyphosphoinositides in vivo. Journal of cell science 115:2569-2580.

Yonezawa N, Nishida E, Sakai H (1985) pH control of actin polymerization by cofilin. The Journal of biological chemistry 260:14410-14412.

Zalevsky J, Lempert L, Kranitz H, Mullins RD (2001) Different WASP family proteins stimulate different Arp2/3 complex-dependent actin-nucleating activities. Current biology : CB 11:1903-1913.

Zallen JA, Cohen Y, Hudson AM, Cooley L, Wieschaus E, Schejter ED (2002) SCAR is a primary regulator of Arp2/3-dependent morphological events in Drosophila. The Journal of cell biology 156:689-701.

Zhang X, Jiang G, Cai Y, Monkley SJ, Critchley DR, Sheetz MP (2008) Talin depletion reveals independence of initial cell spreading from integrin activation and traction. Nature cell biology 10:1062-1068.

Zigmond SH (2004) Formin-induced nucleation of actin filaments. Current opinion in cell biology 16:99-105.